



**Mario Alejandro  
Heredia Salgado**

## **SEWAGE SLUDGE DRYING AND COMBUSTION**



**Mario Alejandro  
Heredia Salgado**

## **SECAGEM E COMBUSTAO DE LAMAS BIOLÓGICAS**

Dissertação apresentada à Universidade de Aveiro para cumprimento dos requisitos necessários à obtenção do grau de Mestre em Sistemas Energéticos Sustentáveis, realizada sob a orientação científica do Doutor Luís António da Cruz Tarelho, Professor Auxiliar do Departamento de Ambiente e Ordenamento da Universidade de Aveiro, e co-orientação científica do Doutor Fernando José Neto da Silva, Professor Auxiliar do Departamento de Engenharia Mecânica da Universidade de Aveiro.

This work was carried out within the Convocatoria Abierta 2011 by a scholarship granted by the Secretaria de Educacion Superior, Ciencia Tecnologia e Innovacion SENESCYT, funded by the Government of the Republic of Ecuador.

This work was done in the scope of research project "BiomAshTech – Ash impacts during thermochemical conversion of biomass", PTDC/AACAMB/116568/2010 - FCOMP-01-0124-FEDER-019346, with financial support from FEDER funds through the Operational Competitiveness Programme - COMPETE and by National Funds through FCT – Fundação para a Ciência e a Tecnologia, Portugal



## **o júri**

### **Presidente**

**Professor Doutor Nelson Amadeu Dias Martins**

Professor Auxiliar do Departamento de Engenharia Mecânica da Universidade de Aveiro

### **Vogais**

**Professor Doutor Luís António da Cruz Tarelho**

Professor Auxiliar do Departamento de Ambiente e Ordenamento da Universidade de Aveiro  
(Orientador)

**Professor Doutor Mário Manuel Gonçalves da Costa**

Professor Associado com Agregação do Departamento de Engenharia Mecânica do Instituto Superior Técnico (Arguente)



**acknowledgement**

I thank all anonymous Ecuadorian citizens that through the figure of SENESCYT made possible the realization of this work. I also thank the teaching staff of the University of Aveiro in particular Professor Luís Tarelho by the passion with which he works day after day; passion is contagious.

To my parents for freedom as heritage. To my brother Adrian and my sister Estefania by infinity and selfless love. To Carolina for the patience. To my Brazilian friends for the warm welcome and contributions to the heart. To leaders of the HortUA project through which I met wonderful people. From the depths of me, many thanks.



**keywords**

Sewage sludge, co-combustion, artificial neural networks, sludge drying kinetics.

**abstract**

A brief review of the paper pulp production process in order to understand the origin of the sewage sludge was performed. Then a general revision of the current treatment options for this type of waste was addressed. The thermal treatment by combustion was focused and a review of the state of the art of this process was performed. The high moisture content of sludge was identified as a major concern. Thus a revision of the state of the art regarding thermal drying of sewage sludge was performed. The drying behavior of sewage sludge from the pulp and paper industry was evaluated by experiment in a drying tunnel. Strong shrinkage, cracks and a weak crust phenomenon were identified. A drying kinetic model was developed by the use of Artificial Neural Networks achieving a high Pearson correlation coefficient in the validation tests. Additionally a theoretical assessment of the co-combustion process was performed having into account a 50 MWth combustion facility. The inclusion of different portions of sewage sludge in a fuel mixture and the influence of the sludge moisture content was studied. It was found that burning sewage sludge with more than 50 wt% moisture content is not possible. Furthermore the inclusion of sewage sludge in a biomass fuel mixture causes an increase in the fuel consumption, solids production and heat losses in the flue gas. Based on general thermodynamic considerations the thermal power of a sludge dryer was calculated. The use of waste heat to supply the energy needs of the drying process was addressed by the waste heat availability estimation as sensible heat and latent heat at the stack of the facility. A set of combustion experiments were done in a pilot scale bubbling fluidized bed combustor to assess the combustion efficiency by monitoring the CO<sub>2</sub>, CO, H<sub>2</sub>O and O<sub>2</sub> levels in conjunction with the temperature profile along the reactor height. Two different types of fuel samples were prepared. One composed by 100 wt% sewage sludge (fuel sample 1) and other composed by 50 wt% sewage sludge and 50 wt% residual forest biomass (particle size <1mm) (fuel sample 2). Low CO levels were observed especially for the fuel sample 2 which indicates a very efficient combustion process. The CO emission level established by the Portuguese law for this type of reactor was never exceeded under typical operating conditions. The temperature profile along the reactor confirms that the combustion of the fuel samples prepared occurs mainly in the freeboard zone. It was not observed agglomeration problems and the fluidization conditions were kept constant during all the experimental tests. After the combustion experiments a considerable ashes quantity were found and its particle size distribution was estimated.

## palavras-chave

Lamas secundarias, co-combustão, redes neuronais artificiais, cinética de secagem.

## resumo

Foi realizada uma revisão sucinta do processo de produção de pasta de papel, a fim de compreender a origem da lama biológica. Uma revisão geral das opções atuais de tratamento para este tipo de resíduo foi abordada. O tratamento térmico por combustão foi focalizado e uma avaliação do estado da arte deste processo foi realizada. Foi verificado que o elevado teor de humidade da lama representa uma grande preocupação. Por tanto, realizou-se uma revisão do estado da arte em relação à secagem térmica das lamas. O comportamento da lama secundaria da indústria de pasta e papel foi estudado experimentalmente em um túnel de secagem. Foram observados os fenómenos de encolhimento e rachaduras além do fenómeno de crosta, embora este último não seja muito pronunciado. Foi desenvolvido um modelo de cinética de secagem com recurso ao uso de Redes Neurais Artificiais, sendo observado um elevado coeficiente de correlação nas experiências de validação. Foi realizada uma análise teórica ao processo de co-combustão de lama com biomassa florestal numa instalação de combustão de 50MW<sub>th</sub>. Estudou-se a inclusão de diferentes fracções de lama numa mistura de combustível contendo biomassa florestal, assim como também a influência do teor de humidade da lama. Verificou-se que a combustão de lamas biológicas com mais do que 50 wt% em teor de humidade não é possível. Além disso, a inclusão destas lamas na mistura de combustível provoca um aumento do consumo de combustível na instalação, da produção de sólidos e das perdas de calor no efluente gasoso da instalação. Com base em considerações termodinâmicas foi determinada a potência térmica de um secador de lamas. A utilização do calor residual para suprir as necessidades energéticas do processo de secagem foi abordada a través da estimativa da disponibilidade de calor residual na forma de calor sensível e calor latente no efluente gasoso da instalação de combustão. Foi realizado um conjunto de experiências de combustão de lamas e sua mistura com biomassa florestal num reactor de leito fluidizado borbulhante á escala piloto para avaliar a eficiência de combustão através da concentração de CO<sub>2</sub>, CO, O<sub>2</sub> e H<sub>2</sub>O, em conjunto com o perfil de temperaturas ao longo do reactor. Foram utilizados dois tipos diferentes de amostras de combustível, uma composta por 100 wt% de lama biológica (combustível 1), e outra composta por 50 wt% de lama biológica e 50 wt% de biomassa florestal residual (tamanho de partícula <1mm) (combustível 2). Foram observados baixos níveis de CO no efluente gasoso, em particular para a amostra de combustível 2, o qual indica um processo de combustão muito eficiente. Para condições de operação (temperatura e estequiometria) típicas, verificou-se que o limite de emissão de CO estabelecido pela lei Portuguesa para este tipo de fornalhas não foi excedido. O perfil de temperatura ao longo do reactor confirma que a combustão das amostras de combustível preparadas ocorre principalmente na zona do *freeboard*. Não foram verificados problemas de aglomeração e as condições de fluidização foram mantidas constantes durante todos os ensaios experimentais. Após os ensaios de combustão foi observada uma quantidade considerável de cinzas na fornalha, tendo sido avaliada a sua distribuição granulométrica.





# Contents

<b>1</b>	<b>Introduction .....</b>	<b>1</b>
1.1	PULP AND PAPER INDUSTRY .....	1
1.1.1	<i>Paper pulp production process .....</i>	<i>2</i>
1.1.1.1	Chemical digestion .....	3
1.1.1.1.1	Sewage sludge produced by the pulp and paper industry .....	3
1.2	MAIN OBJECTIVES .....	5
<b>2</b>	<b>Sewage sludge treatment in the pulp and paper industry .....</b>	<b>7</b>
2.1	OPTIONS FOR SEWAGE SLUDGE TREATMENT .....	8
2.1.1	<i>Vitrification .....</i>	<i>8</i>
2.1.2	<i>Recycling in agriculture .....</i>	<i>9</i>
2.1.3	<i>Landfill disposal .....</i>	<i>9</i>
2.1.4	<i>Waste to energy .....</i>	<i>10</i>
2.1.4.1	Co – combustion of sewage sludge in fluidized bed reactor .....	11
2.2	SEWAGE SLUDGE DRYING .....	13
2.2.1	<i>Sludge drying processes .....</i>	<i>14</i>
2.2.2	<i>Drying insights .....</i>	<i>16</i>
2.2.2.1	Sludge drying kinetics .....	18
2.2.2.2	Artificial neural networks .....	20
2.2.2.2.1	ANN architecture .....	21
2.3	HEAT RECOVERY .....	23
2.3.1	<i>Heat recovery asses .....</i>	<i>24</i>
2.3.1.1	Heat quantity .....	24
2.3.1.2	Waste heat temperature: quality .....	24
2.3.1.3	Waste stream composition .....	25
2.3.1.4	Minimum allowable temperature .....	25
2.3.1.5	Economies of scale, accessibility and other factors .....	26
2.3.2	<i>Heat recovery technologies .....</i>	<i>26</i>
2.3.3	<i>Barriers for promoting waste heat recovery practices .....</i>	<i>27</i>
<b>3</b>	<b>Combustion of biomass and sludge for heat and power production: theoretical approach .....</b>	<b>28</b>
3.1	MASS BALANCE .....	28
3.1.1	<i>Proximate and elemental fuel analysis .....</i>	<i>28</i>
3.1.2	<i>Calorific value of the fuel .....</i>	<i>28</i>
3.1.3	<i>Air consumption .....</i>	<i>29</i>
3.1.4	<i>Flue gas composition .....</i>	<i>30</i>
3.2	ENERGY BALANCE .....	31
3.3	INDUSTRIAL FACILITY OF 50 MW <sub>th</sub> .....	33
3.3.1	<i>Drying approach .....</i>	<i>33</i>
3.4	MODEL OUTPUTS .....	34
3.4.1	<i>Useful energy analysis .....</i>	<i>34</i>
3.4.2	<i>Flue gas composition .....</i>	<i>35</i>
3.4.3	<i>Analysis of a 50MW<sub>th</sub> facility .....</i>	<i>38</i>
3.4.3.1	Waste heat assess .....	39
3.4.3.1.1	Energy content in the flue gas .....	40
3.4.3.1.2	Heat requirements for the drying process .....	41
<b>4</b>	<b>Drying experiments .....</b>	<b>43</b>
4.1	PROBLEM DEFINITION .....	43
4.2	DATABASE ACQUISITION .....	43
4.2.1	<i>The Taguchi method .....</i>	<i>43</i>
4.2.2	<i>Convective drying experimental station .....</i>	<i>45</i>
4.2.2.1	Ventilation system .....	46
4.2.2.2	Heating system .....	46
4.2.2.3	Humidification system .....	46
4.2.2.4	Cooling/dehumidification system .....	46
4.2.2.5	Hardware and software platforms .....	47
4.2.2.6	Auxiliary equipments .....	48

4.2.2.6.1	Oven .....	48
4.2.2.6.2	Metallic containers .....	48
4.2.2.6.3	Aluminium container .....	49
4.2.2.6.4	Desiccator .....	49
4.2.2.6.5	Mass scale .....	49
4.2.3	<i>Experimental proceedings</i> .....	49
4.2.3.1	Sewage sludge behavior during drying experiments .....	50
4.3	EXPERIMENTAL RESULTS: DATA PREPROCESSING .....	52
4.4	NETWORK ARCHITECTURE DEFINITION .....	54
4.5	TESTING AND VALIDATION .....	55
<b>5</b>	<b>Combustion experiments</b> .....	<b>58</b>
5.1	FUEL SAMPLE 1 .....	58
5.2	FUEL SAMPLE 2 .....	59
5.3	MOISTURE, ORGANIC MATTER AND ASH CONTENT OF THE FUEL SAMPLES .....	60
5.4	EXPERIMENTAL FACILITY: PILOT-SCALE BUBBLING FLUIDIZED BED COMBUSTOR .....	62
5.4.1	<i>Reactor setup</i> .....	64
5.5	COMBUSTION EXPERIMENTS .....	65
5.5.1	<i>Temperature profiles</i> .....	74
5.5.2	<i>Solid products of combustion</i> .....	76
<b>6</b>	<b>Concluding remarks</b> .....	<b>81</b>
<b>7</b>	<b>Bibliography</b> .....	<b>85</b>
<b>8</b>	<b>Appendix</b> .....	<b>89</b>
8.1	APPENDIX 1: MATLAB SOURCE CODE OF THE MASS AND ENERGY BALANCE .....	89
8.2	APPENDIX 2: RESULTS OF THE DRYING EXPERIMENTS AT THE TUNNEL UNDER THE TAGUCHI METHODS .....	98
8.3	APPENDIX 3: MATLAB SOURCE CODE OF THE ARTIFICIAL NEURAL NETWORK MODEL .....	103



# Index of figures

FIGURE 2.1 - UP: DIRECT SLUDGE DRYING SYSTEM. DOWN: INDIRECT SLUDGE DRYING SYSTEM. SOURCE: (SIEMENS WATER TECHNOLOGIES CORP, 2008).	15
FIGURE 2.2 - TYPICAL DRYING CURVES. SOURCE (PARK, 2007).	17
FIGURE 3.1 - USEFUL ENERGY [ $\text{MJ} \cdot \text{KG FUEL}_{\text{DB}}^{-1}$ ] VS. BIOMASS PERCENTAGE [WT%] IN THE FUEL MIXTURE (BIOMASS + SLUDGE). COMBUSTION GASES TEMPERATURE IN THE FURNACE IS $800^{\circ}\text{C}$ , AND EXHAUST GASES TEMPERATURE AFTER HEAT RECOVERING IS $150^{\circ}\text{C}$ .	35
FIGURE 3.2 - FLUE GAS COMPOSITION (WET GASES) [ $\text{NM}^3 \cdot \text{KG FUEL}_{\text{DB}}^{-1}$ ] VS. BIOMASS FRACTION PERCENTAGE [WT%] IN THE FUEL MIXTURE. THE MOISTURE CONTENT WAS FIXED IN 40 WT% FOR THE BIOMASS AND 75 WT% FOR THE SLUDGE.	36
FIGURE 3.3 - FLUE GAS COMPOSITION (WET GASES) [ $\text{NM}^3 \cdot \text{KG}^{-1} \text{FUEL}_{\text{DB}}$ ] VS. BIOMASS FRACTION IN THE FINAL FUEL [WT%] (THE MOISTURE CONTENT WAS FIXED IN 40 WT% FOR THE BIOMASS AND 35 WT% FOR THE SLUDGE).	37
FIGURE 3.4 - SOLIDS PRODUCTION RATE (BOTTOM AND FLY ASH) [ $\text{KG ASH} \cdot \text{KG FUEL}_{\text{DB}}^{-1}$ ] VS. BIOMASS PERCENTAGE [WT%] IN THE FUEL MIXTURE. THE MOISTURE CONTENT WAS FIXED IN 40 WT% FOR THE BIOMASS AND 75 WT% FOR THE SLUDGE.	38
FIGURE 3.5 - FUEL MIXTURE FEED RATE [ $T_{\text{ARB}}/H$ ] VS. BIOMASS PERCENTAGE [WT%] IN THE FUEL MIXTURE FOR DIFFERENT SLUDGE MOISTURE CONTENTS (10, 30, 50 WT%). THE BIOMASS MOISTURE CONTENT WAS CONSIDERED AS 40 WT%.	39
FIGURE 3.6 - SENSIBLE AND LATENT HEAT IN THE FLUE GAS [MW] VS. BIOMASS PERCENTAGE [WT%] IN THE FUEL MIXTURE. FLUE GAS TEMPERATURE CONSIDERED EQUAL TO $150^{\circ}\text{C}$ .	40
FIGURE 3.7 - SLUDGE DRYER THERMAL POWER [MW] VS. SLUDGE MOISTURE CONTENT [WT%] FOR DIFFERENT CO-COMBUSTION CASES, THAT IS, DISTINCT PERCENTAGES OF RESIDUAL FOREST BIOMASS AND SEWAGE SLUDGE IN THE FUEL MIXTURE.	42
FIGURE 4.1 - VIEW OF THE DRYING STATION USED TO PERFORM THE DRYING EXPERIMENTS. SOURCE: (PINHO, 2012).	46
FIGURE 4.2 - SCHEMATIC OF THE DRYING STATION USED TO PERFORM THE DRYING EXPERIMENTS. SOURCE: ADAPTED FROM (BOERI, 2012).	47
FIGURE 4.3 - SCHEMATIC OF THE INSTRUMENTATION AT DRYING TUNNEL. SOURCE: ADAPTED FROM (BOERI, 2012).	48
FIGURE 4.4 - CRACK FORMATION AND CURVE UPWARD OF THE SLUDGE SAMPLE (4 HOURS AT $60^{\circ}\text{C}$ ).	51
FIGURE 4.5 - SHRINKAGE PHENOMENA AND VOLUME REDUCTION OF THE SLUDGE SAMPLE AFTER A DRYING EXPERIMENT (4,5 HOURS AT $60^{\circ}\text{C}$ ).	51
FIGURE 4.6 - REPRESENTATION OF THE VALIDATION EXPERIMENTS IN CONJUNCTION WITH THE FORECAST CURVE GIVEN BY THE ANN MODEL.	56
FIGURE 5.1 - MACROSCOPIC CHARACTERISTICS OF FUEL SAMPLE 1.	59
FIGURE 5.2 - MACROSCOPIC CHARACTERISTICS OF FUEL SAMPLE 2.	60
FIGURE 5.3 - SCHEMATIC REPRESENTATION OF THE PILOT SCALE INSTALLATION. DASHED LINE – ELECTRIC CIRCUIT, CONTINUOUS LINE – PNEUMATIC CIRCUIT, A – PRIMARY AIR HEATING SYSTEM, B – SAND BED, C – BED SOLIDS LEVEL CONTROL, D – BED SOLIDS DISCHARGE, E – BED SOLIDS DISCHARGE SILO, F – PROPANE BURNER SYSTEM, G – PORT FOR VISUALIZATION OF BED SURFACE, H – AIR FLOW METER (PRIMARY AND SECONDARY AIR), I – CONTROL AND COMMAND UNIT (UCC2), J – BIOMASS FEEDER, K – WATER COOLED GAS SAMPLING PROBE, L,M,P,Q – COMMAND AND GAS DISTRIBUTION UNITS (UCD0, UCD1, UCD2, UCD3), N – GAS SAMPLING PUMP, O – GAS CONDENSATION UNIT FOR MOISTURE REMOVAL, R,S,T,U,V,W – AUTOMATIC ON LINE GAS ANALYZERS (HC, NO, $\text{CO}_2$ , $\text{N}_2\text{O}$ , $\text{O}_2$ , CO), X – ELECTRONIC COMMAND UNIT (UCE1), Y – COMPUTER DATA ACQUISITION AND CONTROL SYSTEM, Z – EXHAUST DUCT TO CYCLONE AND BAG-HOUSE FILTER. SOURCE: (TARELHO, NEVES, & MATOS, 2011).	63
FIGURE 5.4 - SCHEMATIC REPRESENTATION OF THE FLUE GASES HEATED SAMPLING LINE.	63
FIGURE 5.5 - FLUE GAS COMPOSITION DURING THE COMBUSTION OF RESIDUAL FOREST BIOMASS DERIVED FROM EUCALYPTUS, UNDER TYPICAL STOICHIOMETRIC CONDITIONS.	66
FIGURE 5.6 - FLUE GAS COMPOSITION DURING THE COMBUSTION OF FUEL SAMPLE 1 UNDER TYPICAL STOICHIOMETRIC CONDITIONS.	68
FIGURE 5.7 - FLUE GAS COMPOSITION DURING COMBUSTION OF FUEL SAMPLE 1 WITH REDUCED STOICHIOMETRY.	69
FIGURE 5.8 - FLUE GAS COMPOSITION DURING COMBUSTION OF FUEL SAMPLE 2 UNDER TYPICAL STOICHIOMETRIC CONDITIONS.	71
FIGURE 5.9 - FLUE GAS COMPOSITION DURING COMBUSTION OF FUEL SAMPLE 2 WITH REDUCED STOICHIOMETRY.	72
FIGURE 5.10 - COMPARISON OF AVERAGE CO CONCENTRATION IN THE FLUE GAS [ $\text{MG} \cdot \text{NM}^{-3}$ ] CORRECTED FOR AN 11% OF $\text{O}_2$ DRY GASES VS. AVERAGE $\text{O}_2$ CONCENTRATION [%v] MEASURED FOR EACH COMBUSTION PERIOD.	73

FIGURE 5.11 - TEMPERATURE INSIDE THE REACTOR ALONG THE TIME FOR THE SET OF EXPERIMENTAL CONDITIONS ANALYSED BEFORE AND CORRESPONDING TO SOME DATA PRESENTED IN FIGURES 5.5 (PERIOD 1), 5.6 (PERIOD 2), 5.7 (PERIOD 3), 5.8 (PERIOD 4) AND 5.9 (PERIOD 5), AT SEVERAL LOCATIONS ALONG THE REACTOR HEIGHT. ....	75
FIGURE 5.12 - TEMPERATURE PROFILE (BASED ON AVERAGE OF TEMPERATURES ALONG THE TIME (FIG 5.10)) ALONG THE REACTOR HEIGHT FOR THE SET OF EXPERIMENTS ANALYSED BEFORE AND CORRESPONDING TO (PERIOD 1), 5.6 (PERIOD 2), 5.7 (PERIOD 3), 5.8 (PERIOD 4) AND 5.9 (PERIOD 5), AT SEVERAL LOCATIONS ALONG THE REACTOR HEIGHT. ....	76
FIGURE 5.13 - BED LOOK AFTER THE COMBUSTION EXPERIMENTS. ....	77
FIGURE 5.14 - FLY ASH DEPOSITION AT THE EXHAUST GAS DUCT. ....	77
FIGURE 5.15 - ASH DEPOSITION AT THE ZIRCONIA CELL TIP AND AT FLUE GAS SAMPLING PROBE TIP. ....	78
FIGURE 5.16 - LOOK AT THE TOP OF THE REACTOR AFTER THE COMBUSTION EXPERIMENTS. ....	78
FIGURE 5.17 - ASH DEPOSITION ALONG THE FUEL DISCHARGE DUCT LOCATED INSIDE THE REACTOR (FIGURE 5.3). THE TUBE SIDE LOCATED NEAR THE BED SURFACE IS AT THE TOP OF THE PICTURE. TOTAL LENGTH OF THE TUBE IS 2 M. ....	79
FIGURE 8.1 - DRYING KINETIC OF THE SLUDGE SAMPLE UNDER THE TAGUCHI METHODS (1). ....	98
FIGURE 8.2 - DRYING KINETIC OF THE SLUDGE SAMPLE UNDER THE TAGUCHI METHODS (2). ....	98
FIGURE 8.3 - DRYING KINETIC OF THE SLUDGE SAMPLE UNDER THE TAGUCHI METHODS (3). ....	99
FIGURE 8.4 - DRYING KINETIC OF THE SLUDGE SAMPLE UNDER THE TAGUCHI METHODS (4). ....	99
FIGURE 8.5 - DRYING KINETIC OF THE SLUDGE SAMPLE UNDER THE TAGUCHI METHODS (5). ....	100
FIGURE 8.6 - DRYING KINETIC OF THE SLUDGE SAMPLE UNDER THE TAGUCHI METHODS (6). ....	100
FIGURE 8.7 - DRYING KINETIC OF THE SLUDGE SAMPLE UNDER THE TAGUCHI METHODS (7). ....	101
FIGURE 8.8 - DRYING KINETIC OF THE SLUDGE SAMPLE UNDER THE TAGUCHI METHODS (8). ....	101
FIGURE 8.9 - DRYING KINETIC OF THE SLUDGE SAMPLE UNDER THE TAGUCHI METHODS (9). ....	102

# Index of tables

TABLE 2.1 - WASTES SPECIFIC PRODUCTION OF THE PULP FACTORIES IN $[\text{KG} \cdot \text{T}_{\text{AD}}^{-1}]$ . SOURCE:(BATISTA, 2013).....	7
TABLE 2.2 – MATLAB AVAILABLE TRANSFER FUNCTIONS. SOURCE:(GONÇALVES, 2012).....	22
TABLE 2.3 – MATLAB AVAILABLE TRAINING ALGORITHMS. SOURCE:(GONÇALVES, 2012).....	23
TABLE 2.4 – WASTE HEAT CATEGORIES CLASSIFIED BY TEMPERATURE. SOURCE:(ENERGY DESIGN RESOURCES, 2009). ....	25
TABLE 3.1– PROXIMATE AND ELEMENTAL ANALYSIS OF BIOMASS AND SEWAGE SLUDGE AT A PULP AND PAPER INDUSTRY. SOURCE: ADAPTED FROM (SANTOS, 2012). ....	29
TABLE 3.2 – CARBON LHV AT 25°C AND AVERAGE SPECIFIC HEAT VALUES OF COMBUSTION GASES, ASH AND SLAGS FOR A TEMPERATURE OF 423K, RELATIVE TO 298K. SOURCE: ADAPTED FROM(SPIERS, 1977).....	32
TABLE 3.3 – PARAMETERS CONSIDERED FOR THE DRYING CALCULATIONS. SOURCE: ADAPTED FROM (STASTA ET AL., 2006B). .....	34
TABLE 4.1– CONTROL FACTORS AND THEIR CORRESPONDENT LEVELS ESTABLISHED FOR THE DRYING MODEL CONSTRUCTION.....	44
TABLE 4.2 – ORTHOGONAL MATRIX DESIGN REPRESENTING THE EXPERIMENTAL CONDITIONS FOR EACH EXPERIMENT. ....	45
TABLE 4.3 – EXPERIMENTAL DESIGN FOR THE DRYING MODEL VALIDATION EXPERIMENTS.....	45
TABLE 4.4 – INITIAL AND FINAL MOISTURE CONTENT OF THE SEWAGE SLUDGE SAMPLES AFTER THE EXPERIMENTS AT THE TUNNEL. MOISTURE CONTENT EXPRESSED AS WEIGH RATIO, DRY BASIS $[\text{KGH}_2\text{O} \cdot \text{KG}_{\text{SLUDGE DB}}^{-1}]$ .....	53
TABLE 4.5– FINAL MOISTURE CONTENT OF THE SEWAGE SLUDGE SAMPLES AFTER THE EXPERIMENTS AT THE TUNNEL. MOISTURE CONTENT EXPRESSED IN WET BASIS [WT%]. ....	54
TABLE 4.6 – PEARSON CORRELATION COEFFICIENT OBTAINED FOR THE VALIDATION EXPERIMENTS. ....	57
TABLE 4.7 – FINAL MOISTURE CONTENT OF THE SLUDGE SAMPLE CALCULATED BY THE ANN MODEL AND FINAL MOISTURE CONTENT OF THE SLUDGE SAMPLE OBTAINED BY EXPERIMENTATION .....	57
TABLE 5.1 - GRANULOMETRIC DISTRIBUTION OF THE FUEL SAMPLE 1. ....	58
TABLE 5.2 – MOISTURE CONTENT OF THE FUEL SAMPLES IN AS RECEIVED BASIS AND ORGANIC MATTER AND ASH CONTENT OF THE FUEL SAMPLES IN DRY BASIS .....	61
TABLE 5.3 – PARTICLE SIZE DISTRIBUTION OF THE FIRST WITHDRAWN OF THE BOTTOM BED DURING COMBUSTION OF SEWAGE SLUDGE (FUEL SAMPLE 1). ....	79
TABLE 5.4 – PARTICLE SIZE DISTRIBUTION OF A BED SAMPLE WITHDRAWN DURING THE COMBUSTION OF FUEL MIXTURE OF BIOMASS AND SLUDGE (FUEL SAMPLE 2).....	80
TABLE 5.5 – PARTICLE SIZE DISTRIBUTION OF THE BOTTOM BED WITHDRAWN AFTER THE COMBUSTION TESTS, AND DURING THE REACTOR CLEANING.....	80

# List of abbreviations

AISI	American Iron and Steel Institute
ANN	Artificial neural network
WWTP	Waste water treatment plant
CELPA	Associação da Indústria Papeleira
BFBC	Bubbling fluidized bed combustor
CCR	Carbon conversion rate
d <sub>pb</sub>	Particle diameter
FTIR	Fourier Transform Infrared Spectroscopy analyzer
GDP	Gross domestic product
GVA	Gross value added
HHV	Higher heating value
LCA	Life cycle analysis
LHV	Lower heating value
pH	Hydrogen potential
ppm	Parts per million
PVC	Polyvinyl Chloride
RAM	Random access memory
VC's	Volatile compounds
VFA's	Volatile fatty acids
VOC's	Volatile organic compounds
WTE	Waste to energy

# Chemical nomenclature

C	Carbon
C <sub>7</sub> H <sub>16</sub>	n-Heptane
CH <sub>4</sub>	Methane
CO	Carbon monoxide
C <sub>x</sub> H <sub>y</sub>	Hydrocarbons
Fe <sup>2+</sup>	Magnetite
Fe <sup>3+</sup>	Hematite
H	Hydrogen
N	Nitrogen
NH <sub>3</sub>	Ammonia
NO	Nitrogen monoxide
NO <sub>2</sub>	Nitrogen dioxide
NO <sub>x</sub>	Nitrous oxides
O	Oxygen
S	Sulfur
SO <sub>2</sub>	Sulfur dioxide
SO <sub>x</sub>	Sulfur oxides

# Nomenclature

$\dot{Q}_f$	Power of the dryer	[kW]
$\dot{Q}_{\text{latent}}$	Heat flow to remove water from the sludge	[kW]
$\dot{Q}_{\text{lost}}$	Heat losses in the dryer	[kW]
$\dot{Q}_{\text{sensible}}$	Heat flow transferred to the sludge cake	[kW]
$\Delta H_{L,\text{products}}$	Latent heat of the products	[J·kg <sup>-1</sup> ]
$\Delta H_{L,\text{reactants}}$	Latent heat in the reactants	[J·kg <sup>-1</sup> ]
$\Delta H_p$	Energy in the products	[J·kg <sup>-1</sup> ]
$\Delta H_{R,\text{products}}$	Heat of reaction from products	[J·kg <sup>-1</sup> ]
$\Delta H_{R,\text{reactants}}$	Heat of combustion reaction	[J·kg <sup>-1</sup> ]
$\Delta H_{S,\text{reactants}}$	Sensible heat in the reactants	[J·kg <sup>-1</sup> ]
$cp_c$	Specific heat of the Carbon at reference temperature	[J·kg <sup>-1</sup> ·K <sup>-1</sup> ]
$cp_{CO_2}$	Specific heat of the Carbon dioxide at reference temperature	[J·kg <sup>-1</sup> ·K <sup>-1</sup> ]
$cp_F$	Specific heat of the fuel at reference temperature	[J·kg <sup>-1</sup> ·K <sup>-1</sup> ]
$cp_{H_2O}$	Specific heat of the water at reference temperature	[J·kg <sup>-1</sup> ·K <sup>-1</sup> ]
$cp_{H_2O(g)}$	Specific heat of water (gas) at reference temperature	[J·kg <sup>-1</sup> ·K <sup>-1</sup> ]
$cp_i$	Specific heat of the compound i at reference temperature	[J·kg <sup>-1</sup> ·K <sup>-1</sup> ]
$cp_{N_2}$	Specific heat of the Nitrogen at reference temperature	[J·kg <sup>-1</sup> ·K <sup>-1</sup> ]
$cp_{O_2}$	Specific heat of the Oxygen at reference temperature	[J·kg <sup>-1</sup> ·K <sup>-1</sup> ]
$cp_{\text{Sludge}}$	Specific heat of the sludge at reference temperature	[kJ·kg <sup>-1</sup> ·K <sup>-1</sup> ]
$cp_{SO_2}$	Specific heat of the Sulfur dioxide at reference temperature	[J·kg <sup>-1</sup> ·K <sup>-1</sup> ]
$cp_{W@25^\circ C}$	Specific heat of the water at 25°C	[J·kg <sup>-1</sup> ·K <sup>-1</sup> ]
$cp_z$	Specific heat of the ashes at reference temperature	[J·kg <sup>-1</sup> ·K <sup>-1</sup> ]
$H_f$	Final moisture content of the sample	[g <sub>H2O</sub> ·g <sub>sludge</sub> db <sup>-1</sup> ]
$H_i$	Instantaneous moisture content of the sample	[g <sub>H2O</sub> ·g <sub>sludge</sub> db <sup>-1</sup> ]
$H_{\text{lost}}$	Energy lost	[J·kg <sup>-1</sup> ]
$H_o$	Initial moisture content of the sample	[g <sub>H2O</sub> ·g <sub>sludge</sub> db <sup>-1</sup> ]
$H_{\text{products}}$	Energy of the products	[J·kg <sup>-1</sup> ]
$H_{\text{reactants}}$	Energy of the reactants	[J·kg <sup>-1</sup> ]
$H_{\text{useful}}$	Useful energy	[J·kg <sup>-1</sup> ]
$h_{wv,t^\circ}$	Enthalpy of water vaporization	[kJ·kg <sup>-1</sup> ]
$h_{wv@60^\circ C}$	Enthalpy of water vaporization at 60°C	[kJ·kg <sup>-1</sup> ]
$LHV_{C@25^\circ C}$	Low heating value of the Carbon at 25°C	[J·kg <sup>-1</sup> ]
$LHV_j$	Low heating value of the unburned compound j	[J·kg <sup>-1</sup> ]
$m_{@105^\circ C}$	Mass of the sample after the oven at 105°C	[g]

$M_A$	Air molecular mass	$[\text{kg}\cdot\text{kmol}^{-1}]$
$m_f$	Final mass of the product after oven at 105°C	$[\text{g}]$
$\dot{m}_{\text{fuel,arb}}$	Facility fuel consumption in as received basis	$[\text{kg}_{\text{fuelarb}}\cdot\text{s}^{-1}]$
$m_{\text{fueloven@550}^\circ\text{C}}$	Mass of the sample after burning in a furnace at 550°C	$[\text{g}]$
$M_i$	Molecular mass of the compound i	$[\text{kg}\cdot\text{kmol}^{-1}]$
$m_i$	Instantaneous mass of the sample during the experiments in the tunnel	$[\text{g}]$
$M_j$	Molecular mass of the element j	$[\text{kg}\cdot\text{kmol}^{-1}]$
$M_m$	Monolayer moisture	
$m_o$	Initial mass of the product	$[\text{g}]$
$M_{O_2}$	Molecular mass of oxygen	$[\text{kg}\cdot\text{kmol}^{-1}]$
$m_{sf}$	Mass of the sample after the tunnel experiment	$[\text{g}]$
$m_{Sf}$	Mass of the sample after the experiment at the tunnel	$[\text{g}]$
$\dot{m}_{\text{sludge}}$	Sludge mass flow	$[\text{kg}_{\text{sludgearb}}\cdot\text{s}^{-1}]$
$m_{So}$	Mass of the sample before the experiment at the tunnel	$[\text{g}]$
$m_w$	Water mass removed from the product	$[\text{g}]$
$\dot{m}_{w,\text{sludge}}$	Weight of the corresponding fraction of water in the sludge -mass flow-	$[\text{kg}_{\text{water}}\cdot\text{s}^{-1}]$
$n_{CO_2}$	Number of moles of carbon dioxide as effluent	$[\text{kmol}_{CO_2}\cdot\text{kg}_{\text{fueldb}}^{-1}]$
$n_{H_2O}$	Number of moles of water as effluent	$[\text{kmol}_{H_2O}\cdot\text{kg}_{\text{fueldb}}^{-1}]$
$n_{iR}$	Number of moles of gas species i as effluent	$[\text{kmol}_i\cdot\text{kg}_{\text{fueldb}}^{-1}]$
$n_{jF}$	Number of moles of the unburned compound j	$[\text{kmol}_j\cdot\text{kg}_{\text{fueldb}}^{-1}]$
$n_{N_2}$	Number of moles of Nitrogen as effluent	$[\text{kmol}_{N_2}\cdot\text{kg}_{\text{fueldb}}^{-1}]$
$n_{O_2}$	Number of moles of Oxygen as effluent	$[\text{kmol}_{O_2}\cdot\text{kg}_{\text{fueldb}}^{-1}]$
$n_{SO_2}$	Number of moles of Sulfur dioxide as effluent	$[\text{kmol}_{SO_2}\cdot\text{kg}_{\text{fueldb}}^{-1}]$
OM	Organic matter content in dry basis	$[\%]$
$T_A$	Temperature of the air	$[\text{K}]$
$T_F$	Temperature of the fuel	$[\text{K}]$
$T_G$	Temperature of the exhaust gases	$[\text{K}]$
$T^o$	Room temperature	$[\text{K}]$
$T_{\text{sludge},f}$	Sludge temperature at the exit of the dryer	$[\text{°C}]$
$T_{\text{sludge},o}$	Sludge temperature at the inlet of the dryer	$[\text{°C}]$
$T_Z$	Temperature of the ashes	$[\text{K}]$
$W_{a,F}$	Current ratio of Oxygen	$[\text{kg}_{O_2\text{actual}}\cdot\text{kg}_F^{-1}]$
$W_{A,F}$	Current ratio of combustion air	$[\text{kg}_{\text{air}}\cdot\text{kg}_F^{-1}]$
$W_{CE}$	Unburned Carbon fraction in the bottom ash	$[\text{kg}_C\cdot\text{kg}_{\text{bottomash}}^{-1}]$
$W_{CF}$	Carbon content in the fuel in dry basis	$[\text{kg}_C\cdot\text{kg}_F^{-1}]$
$W_{CV}$	Unburned Carbon fraction in the fly ash	$[\text{kg}_C\cdot\text{kg}_{\text{flyash}}^{-1}]$
$W_{EF}$	Fraction of bottom ash in the fuel	$[\text{kg}_{\text{bottomash}}\cdot\text{kg}_F^{-1}]$
$W_{HF}$	Hydrogen content in the fuel dry basis	$[\text{kg}_H\cdot\text{kg}_F^{-1}]$
$W_{jF}$	Fraction of the element j in the fuel	$[\text{kg}_j\cdot\text{kg}_F^{-1}]$
$W_{NF}$	Nitrogen content in the fuel dry basis	$[\text{kg}_N\cdot\text{kg}_F^{-1}]$
$W_{OF}$	Oxygen fraction in the fuel dry basis	$[\text{kg}_{O_2}\cdot\text{kg}_F^{-1}]$

$w_{OF}$	Oxygen content in the fuel dry basis	$[kg_O \cdot kg_F^{-1}]$
$W_{s,F}$	Stoichiometric consumption of oxidizer	$[kg_{O_2\text{stoich}} \cdot kg_F^{-1}]$
$w_{SF}$	Sulfur content in the fuel dry basis	$[kg_S \cdot kg_F^{-1}]$
$wt$	Weight percent	$[\%]$
$W_{VA}$	Weight ratio of the water vapor in the combustion air	$[kg_{H_2O} \cdot kg_{\text{dry air}}^{-1}]$
$W_{VF}$	Fraction of fly ash in the fuel	$[kg_{\text{flyash}} \cdot kg_F^{-1}]$
$W_{WF}$	Weight ratio of the moisture content in the fuel in dry basis	$[kg_{\text{water}} \cdot kg_{\text{fueldb}}^{-1}]$
$w_{ZE}$	Ash fraction as bottom ash	$[kg_{\text{ash}} \cdot kg_{\text{bottomash}}^{-1}]$
$w_{ZF}$	Inorganic byproducts of combustion	$[kg_{\text{ash}} \cdot kg_{\text{fueldb}}^{-1}]$
$w_{ZV}$	Ash fraction as fly ash	$[kg_{\text{ash}} \cdot kg_{\text{flyash}}^{-1}]$
$Y_{O_2,A}$	Molar fraction of Oxygen in the combustion air	$[kmol_{O_2} \cdot kmol_{\text{dry air}}^{-1}]$
$Y_{s,C}$	Stoichiometric coefficient for Carbon	$[kmol_{O_2} \cdot kmol_C^{-1}]$
$Y_{s,H}$	Stoichiometric coefficient for Hydrogen	$[kmol_{O_2} \cdot kmol_H^{-1}]$
$Y_{s,j}$	Stoichiometric consumption of element j	$[mol \cdot mol^{-1}]$
$Y_{s,S}$	Stoichiometric coefficient for Sulfur	$[kmol_{O_2} \cdot kmol_S^{-1}]$
$z$	Excess of air	$[\%]$



## Subscripts

<b>Arb</b>	-	As received basis
<b>Db</b>	-	Dry basis
<b>E</b>	-	Bottom ash
<b>F</b>	-	Fuel
<b>V</b>	-	Fly ash
<b>AD</b>	-	Air dry tones



## **1 Introduction**

All the human activities have impacts on the environment no matter how well-designed they are thus, regardless the amount of control and technology involved, consequences are always expected. Industrial activities are one of those human activities where waste generation appears as an unavoidable fact. Our economy and accordingly our industrial processes were designed as open streams where huge customer's consumption rates feed and keep the system working. This structure has a maniac tendency to produce wastes that nobody wants; therefore, a safe final destination for these wastes appears as a major concern. Landfill disposal was popular in the past years, but nowadays due to many reasons (e.g. government regulation, high environmental control standards), too many strategies and techniques were developed to manage and treat wastes. Nonetheless still exists some specific constraints that limit their application as well there is an open discussion about the best treatment technique for each case of waste.

Framed in this problematic this thesis will focus a specific type of waste that comes from the pulp and paper industry, namely sewage sludge. There are several options to treat and dispose this type of wastes as well there are several constraints. In general the main issue is related with its high moisture content, because of that it will be explored the main features of the paper sludge drying phenomena to achieve a better understanding of this physic process.

The next main subject of this document is related with the sewage sludge co-combustion process in a pilot scale bubbling fluidized bed reactor. The combustion efficiency of two different types of fuels based on dried sewage sludge in the first case and dried sewage sludge plus residual forest biomass for the second case will be assessed in terms of reactor temperature profiles and flue gas composition.

Additionally a case study will be used to realize and asses the main concerns as well the energy fluxes involved in a hypothetical closed loop process in a pulp and paper industry where using waste heat to drive the drying stage, the sewage sludge will be enabled as fuel to be burned in a fluidized bed reactor. The installed power established for the energy production facility was 50 MW<sub>th</sub>.

### **1.1 Pulp and Paper industry**

The pulp and paper sector is a very particular case of industry because the associated companies handle all the production chain (raw materials growth, harvest, processing, sales and including the product end of life disposal).

In Portugal the pulp and paper sector is the largest forest owner, manages 2% of the national territory, 4,5% of the national forest area and 20% of the eucalyptus total area. In terms of macroeconomic indicators the pulp and paper sector represents a turnover higher than 2 million of euros by 2011 with a 1% growth in relation with the

past year. In 2009 this sector represented 2% of the national gross value added (GVA), 8% of the industrial GVA, 4% of the national gross domestic product (GDP) and 7% of the national industrial production (CELPA, 2011).

Energy is one of the big concerns of this industry. Energy consumption grew 4,5% and for 2011 was fixed in 65.888 TJ due to production increases. The sector shows a big bet on bio-fuels, biomass represents 68% of the fuels consumed. The principal biofuel consumed at this sector is the black liquor (which is a sub product of the pulp production process) that represents 86% of the bio fuels consumed. As well the pulp and paper sector is one of the few in the Portuguese industry scenario which is self-sufficient in terms of electric energy; the production exceeds consumption in 34%. Another important fact is the growth of 15% in the electricity production by cogeneration (combined production of electricity and heat for industrial purposes) which is one of the most efficient ways to use primary sources of energy. The electricity production of this sector in 2011 was 3,44 TWh and the consumption was 2,56 TWh, therefore, there was a liquid electricity injection to the grid of 880 GWh. The cogeneration sector in 2010 was responsible for 13% of the total electricity production in the country. Inside this 13% the pulp and paper sector has a share of 5,4%. In Portugal, the pulp and paper is the sector that uses more biomass to produce electricity (73,1%) when compared with other thermoelectric power stations (1,2%) and the rest of the cogeneration sector (1,9%). A direct consequence of this and due to the high efficiency of the cogeneration systems is the emission factor per kWh produced when compared with other sectors and technologies. The average emission factor in Portugal for 2010 was 436 g CO<sub>2</sub>/kWh which includes all the renewable energy sources. On the other side in the pulp and paper sector the emission factor was 133 g CO<sub>2</sub>/kWh, 69% less than the national average (CELPA, 2011).

Clearly it is noticed a healthy industry with a strong tendency to growth in terms of production and turnover but not only this; it can be noticed an increasing interest of this sector to invest in new business areas not directly associated with the pulp and paper segment like energy production for instance.

#### 1.1.1 *Paper pulp production process*

In order to understand the source where the sewage sludge is produced it is important to have a consistent idea about the pulp production process. A brief review is presented below.

Basically, the wood consists of lignin, cellulosic fibers and also fatty acids and resins. The fibers typically have a size of 1-5 mm and a thickness of 0,02-0,04 mm. Its use in paper manufacture requires its separation. There are two main processes to achieve this objective, namely: lignin chemical dissolution (digestion) and mechanical breakdown. Some processes are more appropriate for soft woods (long fibers e.g. pine tree) and other for hard woods (short fibers e.g. eucalyptus). Both processes have two main objectives; separate the cellulose fibers from the lignin fibers and bleach it because their natural color is brown.

The chemical dissolution process is self-sufficient in terms of energy due to the incorporation of significant parts of biomass as fuel for the process while the mechanical breakdown process requires an average of 1000 kWh to produce a ton of pulp. The wood usage rate in mechanical breakdown process is high, around 95% in contrast with 45% in the chemical dissolution. In the mechanically breakdown process broken fibers are produced, therefore the paper strength is low. In the chemical dissolution process long fibers are produced, therefore the paper strength is high. All this features implies a significant difference in costs for each process. Due to the amount of organic matter lost during the pulp production the scope of this work will be centered in the chemical dissolution process.

#### 1.1.1.1 Chemical digestion

There are two types of chemical digestion processes, the sulphate method (or kraft) and the sulfite method (acidic). The kraft method is the most popular because produces a strength pulp and involves thermal economy.

As a resume the stages of the kraft method are:

- The process starts cutting the trunk of the tree and transporting it from the forest to the factory. In the factory the tree barks are separated and the trunk is reduced to small chips. These small chips are stocked to then feed the digester.
- The digestion occurs in two stages; in the first one the chips enter to the low pressure zone of the digester to be heated by steam as they fall down. In the second stage the pressure in the digester is increased to 9 kgf·cm<sup>-2</sup> approximately; the temperature goes to 155 - 175 °C and at these conditions the chips get in contact with the digestion liquor. Then the digestion is interrupted by rapid cooling with cold liquor followed by a decompression stage. Here the pulp color is brown.
- The process continues with a washing stage with water in counterflow where the big wood pieces not digested are separated. Then follows a filtration stage under vacuum. At the end the pulp gets thickened and densified and the black liquor goes to another process to recover the chemical assets and the organic matter dissolved.
- Finally the pulp is bleached with chlorine, washed, densified again and wrapped in packs to transport it to the paper factories. The pulp still does not have the properties of the paper, namely opacity, surface finish and strength therefore, it is still necessary a refining process to convert it into paper.

##### 1.1.1.1.1 Sewage sludge produced by the pulp and paper industry

There are four types of sewage sludge generated in the pulp and paper industry during the described production process, namely:

- Primary sludge
- Biological sludge (also called secondary)
- Dregs
- Grits

As referred in section 1.1.1.1 there is a parallel process to the pulp production where by causticisation the black liquor is recovered, turning it into white liquor to refill the digesters. This process is more complex than the pulp production by itself; it involves evaporation processes and many lixiviation stages. Along this stages two types of sludge are generated, they are called dregs and grits.

As mentioned this recovering process of black liquor involves not only the chemical assets recovery, it also involves organic matter recovery that is used as fuel with an important contribution to the pulp production energy needs, due to this fact the sludge generated in this phase only contain a residual amount of organic matter in consequence the heating value of it are extremely low.

Besides that, there are two extra types of sludge that basically come from the company waste water treatment plants (WWTP). A WWTP is a facility which objective is to transfer the pollutants from a liquid phase to a solid phase with lower volume and high pollutants concentration. At the exit of a WWTP two type of products are obtained, a liquid effluent with low concentration of pollutants able to discharge to the environment and a semi solid product (sludge) that generally has a high concentration of pollutants. Normally the pulp and paper factories divide the waste water treatment process between a primary clarifier and a secondary clarifier.

The degree of primary treatment is achieved by several physical processes; generally harrowing and desanding followed by a primary clarifying stage. The first two actions are known as preliminary treatment where the big solids are removed to avoid clogging, overflow problems and to prevent damages in the mechanical devices downstream. Then the rest of particles which sedimentation rate is high (mainly consisting of sands) are removed in a desanding stage.

After preliminary treatment and desanding stage, the effluent still contains organic and inorganic matter besides other suspense solids. These solids will be removed largely in the primary clarifier, where they deposit it as, primary sludge that is usually removed by pumping without microbiological intervention.

The effluent from the primary treatment still contains approximately 20% of the suspended solids present in the initial effluent and all the dissolved organic and inorganic matter. This organic matter still needs to be reduced to accomplish with the discharge policies. The organic removal is called secondary treatment and it can be accomplished by two methods; chemical - physical processes (coagulation, filtration, chemical oxidation, activated carbon adsorption, etc.) or biological processes (activated sludge, aerated lagoons, trickle bed reactors, etc.) The secondary treatment by

biological processes can remove about 85% of the organic matter present in the effluent using microorganisms.

The biological process uses activated sludge which microorganisms are kept suspended in the effluent. The reservoir is mechanically aerated from the bottom and naturally aerated (by air contact) in the upper surface. The microorganisms use the organic matter in the effluent as nutriment and convert part of it in biological cells or biomass. When the effluent has a high content of organic matter a large variety of microorganisms is needed for the treatment (mixed crops). The sludge with billions of microorganisms can be reused. Generally the used sludge is recirculated to the aerated tank mixing it with air and new effluent. At the end of secondary treatment the effluent is transferred to a clarifier to remove the excess of microorganisms. The removed matter from the secondary clarifier is called secondary sludge. The secondary sludge normally passes through a dewatering and filtering stage generally by mechanical compression. At the exit of the mechanical press the moisture content in “wet basis” is typically between 75 to 85% if a thickening table is used and 85 to 90% if not.

To complete the secondary treatment, the effluent from the clarifier is disinfected with chlorine before discharge it in the receiving medium. The chlorine removes the pathogenic bacteria and reduces the smells. This treatment can also be done by ultra – violet rays or ozone.

In many cases the sludge are obtained as mixed sludge (primary sludge mixed with secondary sludge). In other cases the sludge are separated in different clarifiers and then processed in common. Therefore the primary and secondary sludge are an unavoidable waste, coming from the WWTP as a result of the extraction of organic matter from the effluent and from the microorganism’s growth (biological matter not stabilized).

## **1.2 Main Objectives**

Knowing that the high moisture content of the sewage sludge is a major problem when considering its energetic valorization by combustion, this work is dedicated to address this issue from two different approaches, namely, theoretical and experimental. Also, recognizing the need of a better knowledge about the combustion process of sewage sludge, in a second part of the work it was evaluated the combustion process of sewage sludge, and its mixture with residual forest biomass, in a pilot-scale bubbling fluidized bed combustor. In this context, for this work the following objectives were considered:

The first one was to develop a theoretical model on MATLAB to allow the assessment of the influence of sewage sludge moisture content in a fuel mixture composed by different mass portions of sewage sludge and residual forest biomass. It was intended to use a case study based on a 50MW<sub>th</sub> combustion facility to perform an analysis in terms of useful energy, fuel consumption, flue gas composition, waste heat in the flue gas and solid products of combustion. Based on this information it was

intended to estimate the power needed to drive a drying process for the sewage sludge under several scenarios.

Knowing that a drying stage for the sewage sludge is a key factor and as a complement of the theoretical analysis, the second main objective was to identify through experimentation in a drying tunnel which of the features often reported in the literature about solids drying, namely shrinkage, cracks and specially crust phenomena are present for this type of sewage sludge from pulp and paper industries. It was intended to develop a drying kinetic model that having into account the aforementioned phenomena, be able to describe the moisture content reduction along the time for several drying conditions. The establishment of the time needed to shift the sludge moisture content to values suitable for its combustion with energy recovery using low drying temperatures (below 60°C) was the goal.

Finally, the third objective of this work was to prepare two different biomass fuel samples based on sewage sludge and its mixture with residual forest biomass, and to perform a set of combustion experiments in a pilot scale bubbling fluidized bed reactor in order to assess the combustion behavior of these fuels.



## 2 Sewage sludge treatment in the pulp and paper industry

Once defined the source of the wastes subject of this thesis, it is necessary to have a better understanding about the amounts of wastes involved. It is presented Table 2.1 which resumes the specific wastes production rate in -air dry tons- that refers the conditions in which the pulp is sold, this means that it does not suffer drying (normally the moisture content is 10%).

Table 2.1 - Wastes specific production of the pulp factories in  $[\text{kg} \cdot \text{tAD}^{-1}]$ . Source:(Batista, 2013).

Wastes	Specific production $[\text{kg} \cdot \text{tAD}^{-1}]$
Woods park	8
Tailings of sieving (uncooked/nodes + tailings of end sieving)	10
Grits + Dregs	15
Ash from electric filters and slag's	20
Primary sludge	10
Secondary sludge	7
TOTAL	70

As mentioned despite the increase of technology and electronic communications, paper demand is still growing. The wastes generated during its production follow this trend; accordingly recycling has gained prominence as a subject matter that serves as orientation to discuss about how this considerable amount of wastes can be managed.

A meaningful discussion of recycling requires a common vocabulary, based on clear and consistent definitions. *Reduce* can refer as using or discarding less of a product or decreasing its toxicity during production or in waste stream. *Reuse* occurs when the original function is maintained. On the other hand adapting an item for new use without changing its essential form or nature (e.g. use of a coffee can as a container for nuts and bolts) is called *repurposing*. If a product requires some cleaning or repair before it can be used again, it is *remanufactured* or *refurbished*. There is another interesting concept called *down cycling* which consider the conversion of waste materials into new materials or products of lesser value and reduced functionality compared to the original. Unlike *up cycling*, concept that considers the conversion of a waste material into something of greater value.

Several additional options are available especially for organic waste which is the case of *refuse-derived fuel* where wastes can be used as fuel to be burned for energy recovery in a waste-to-energy (WTE) plant or other industrial facility. Organic matter can also be partially decomposed to gas by digestion or to a humus-like material by composting (Gaines, 2012).

Summarizing, recycling can be seen as the transformation of waste (items that are unwanted or perceived as unusable and would otherwise be thrown away) into usable products or materials, which is sometimes referred as resource recovery.

## 2.1 Options for sewage sludge treatment

Due to the physical and chemical processes involved during its treatment, the sludge is contaminated with a wide range of pollutants. The sewage sludge has the tendency to accumulate heavy metals and hardly biodegradable organic compounds as well as potentially pathogenic organisms like virus and bacteria's present in the waste water. Due to this the sludge must be conveniently treated before send it to a final destination. During these last years a very active research area dedicated to this issue arises. Taking into account the recycling definitions presented in section 2, four main treatment tendencies were identified: ceramization, incineration, agricultural application and landfill disposal.

### 2.1.1 Vitrification

The main purpose of a waste treatment technique is the inertization of the waste to control its dangerousness. To achieve this objective, one of the available options is to immobilize it in a more stable matrix that does not react with the environment; basically it is intended to transfer the hazardous pollutants to a solid matrix that ensures their efficient encapsulation. When the immobilization technique was applied to the sludge issue, according to academic publications two options were identified as very suitable, the sludge incorporation as raw material in bricks production and the sludge incorporation in expanded clay production (light weight aggregates).

Bricks production considers the addition of low percentage of sludge (no more than 20 wt%) to the red pulp; some vantages are reported. The high temperature in ceramic kilns ensures the destruction of hazardous bacteria's and microorganisms present in the sludge and the non-volatile metals are effectively fixed in the bricks. Related to the final product, less raw materials consumption was reported in conjunction with less energy consumption in the burning process due to the sludge calorific value. Moreover, the addition of sewage sludge in bricks promote a strength increase when the product is crude or green, texture and color of the final product does not present any change. On the other hand some disadvantages were reported such as an increased energy consumption in the drying process due to the high sludge moisture content, difficulty of obtaining products with specific dimensions (shrinkage), larger burning cycles to avoid the "black heart" ( $\text{Fe}^{3+}$  to  $\text{Fe}^{2+}$  hematite  $\rightarrow$  magnetite) and the technological characteristics evolve negatively with respect to porosity and mechanical strength after burning (Batista, 2013).

The sewage sludge incorporation as raw material in the production of expanded clay reports remarkable results. The aggregates were successfully obtained with spherical form, porous internal structure and a good grain size distribution. The rate in which the sewage sludge was incorporated in the clay matrix was 10 and 20 wt% of primary sludge and up to 30 wt% of incorporation in the case of biological sludge. Leaching tests were not significant, showing that this process results in an efficient inertization of wastes. The characteristics of the production process and the

product were kept unchanged. However, the high water content of the sewage sludge requires a strict initial control of the burn operation (Fernandes, 2005).

These results shows the effective implementation of cellulosic sewage sludge in stable matrixes becoming products with an increased added value being an interesting environmental solution., however the excessive moisture content of the sludge appears as an issue to overcome.

#### *2.1.2 Recycling in agriculture*

Primary and secondary sludges are rich in nutrients such as Nitrogen and Phosphorous; moreover considering their organic content they can be useful to eroded soils as an organic corrector. The application of both type of sludges are suitable for acid soils because it causes considerable increases in soil Hydrogen potential (pH) but care is required regarding the way chosen to accomplish it. It is important to take into account the seasons of the year in conjunction with the quantity of sludge to be added, weather, soil conditions and type of crops. Adding sludge with high heavy metals content to the soils can be serious due to its ability to accumulate in the vegetable and animal tissues. Regarding the type of crops many surveys indicate that accumulation effect takes place rapidly in horticultural products and big cereals crops.

Additional issues are reported regarding to the low Magnesium content of the sludge, which in soils whose Magnesium percentage of exchange is low requires the addition of this element as an additive to the fertilizer. Furthermore there is a significant increase in the values of exchangeable Sodium in the soil; this fact can became a conditioning factor in the systematic application of large amounts of primary and biological sludge due to the detrimental effect that a high percentage of exchangeable Sodium can exert on the physical characteristics of the soils structure. Furthermore the frequency and quantities of sludge that soils require is low when compared with the amount of sludge to dispose and treat (Batista, 2013).

#### *2.1.3 Landfill disposal*

According to Portuguese law (DL 239/97) a landfill is a disposal facility used for the controlled deposition of waste above or below the natural surface. The wastes are thrown neatly and covered with earth or similar material. There is a systematic control of leaching waters and gases and a controlled monitoring of the environmental impact during operation and after closure. The most common problems that a landfill brings can be described as follows: long period of land utilization and considerable surface area that a landfill requires. It also must be account the resources and raw materials lost, dependency to weather, needing of cover material, bad smells, risk of groundwater contamination and presence of mice and carrion birds. Moreover it must be taken into account that a landfill is an uncontrolled and chaotic reactor. In addition, decomposition of organic wastes in oxygen absence produces methane which has a global warming potential twenty five times greater when compared to the same mass of CO<sub>2</sub>.

During the last years by policies, governments are putting a big pressure on landfill deposition activities by increasing the costs of wastes disposal with organic content. The principal objective is to create and encourage recycling systems and establish other synergies. Some statistics shows that about 12% of the total solid wastes generated in the pulp and paper sector were destined to landfill. As shown in Table 2.1 sewage sludge is just one part of those solid wastes; being more specific other studies shows that 70% of the sewage sludge produced is directed to landfills (Batista, 2013).

When there are other options to recycle and treat wastes, by far, landfilling is the worst choice, furthermore as shown in the case of sewage sludge, deposition costs are high and another issue must be taken into account; the high moisture content of the sludge increase transportation costs; essentially the main bulk transported is water therefore the need of a drying stage gets relevance.

#### 2.1.4 *Waste to energy*

The heat treatment as a waste treatment option attempts to inertize the sludge by means of cracking the organic molecules by elevated temperature in the presence of oxygen (combustion) or in its absence (pyrolysis and gasification). Those processes are more effective as higher the temperature and time of residence in the reactor of the hazardous material to be destroyed. The considerable organic content of biological sludge makes them interesting for combustion.

Incineration in essence is a concept that comprises the wastes combustion with or without energy recovery in units built for this purpose. Nevertheless a special case was identified where using industrial plants that have not been specifically constructed for this purpose after a few modifications, wastes can be burn. This is the case, for instance; of sludge incorporation as fuel in cement production kilns. This process is known as fuels derived from wastes.

Advantages of incineration as a waste treatment technique, in general terms can be summarized as follows. Incineration ensures the effective destruction of hazardous component in the waste in conjunction with a considerable volume and weight reduction. Moreover the flue gas control can be done, using the already implemented monitoring systems in the furnaces. It is also important to mention the less land area usage when compared with other treatment options e.g. landfilling. Finally, the operational costs reduction due to energy recovery is also an important advantage to take into account. Some researchers report as disadvantages the fact that only wastes with high organic content can be burn. In addition emissions control of some metals can be hard. Regarding to financial issues some studies shows that starting an incineration plant from zero can represent a high investment, then those kind of plants can require a support fuel due to the low heating value of some types of wastes (Batista, 2013).

The case of sludge incorporation as fuel for clinker production is interesting, because the organic matter provides a significant part of the heat needed for clinquerization which is commonly known as energy intensive. At the end of the

process the sludge ashes that contain potentially hazardous heavy metals are sintered and stabilized in cement which is a very stable matrix. Furthermore, the pozzolanic (aluminosilicates) characteristics of the sludge ashes are extremely important because it can partially supply one of the main clinker active components, Calcium (Wzorek, 2012). Regarding to this appliance it is important to take into account Chlorine content in the ashes because it can attack the steel in the structures where cement is applied. Moreover it is very important to take into account the Sodium content, because it causes late expansion of cement which can cause cracks (Rajamma, 2011). Other important fact that limits the sludge incorporation in cement is its high water content because the process in the clinker kiln is endothermic until the water from the sludge is evaporated. This fact decreases the kiln temperature and also would increase the flow rate of flue gas, which could overload existing devices for flue gas cleaning and capacity of fans. The characteristic parameters suggested for sludge utilization in cement kilns are: a maximum of 20 wt% of water content, a LHV of minimum 9 MJ/kg and a granulometry between 0 and 5 mm (Stasta, Boran, Bebar, Stehlik, & Oral, 2006). Another issue to overcome is availability; practically it is needed a clinker factory close to a pulp factory. The transportation option is not suitable due to the high moisture content as mentioned in section 2.1.3. Definitely, a drying process as pre-treatment option at the place which the sludge is generated is fundamental to enable any other treatment option.

#### 2.1.4.1 Co – combustion of sewage sludge in fluidized bed reactor

As discussed in section 2.1.1 to 2.1.4 there are many interesting options for the sludge final treatment and destination, focusing the scope of this dissertation, the sludge utilization as fuel will be discussed. The burning technology chosen is the fluidized bed reactor once it has been proven as one of the best technologies available for the energetic conversion of solid fuels, especially biomass (Tarelho, 2012).

Basically, the secondary sludge due to its relative stability regarding to elemental composition and of course because its considerable heating value when compared with dregs and grits makes it suitable for incineration but the high moisture content prevents its combustion with energy recovery. To overcome this issue co-combustion regime is an option. Co-combustion is a technique where two or more different type of fuels (different elemental and proximal composition) are combusted. This combustion regime becomes an interesting option, since it allows for the use of existing infrastructures already equipped with appropriate devices for emissions control, reducing at the same time their fuel consumption. Usually a base fuel with a high heating value is used to support the process and small and controlled amount of other fuels are added; generally coal and biomass are used as base fuels.

Some previous studies shows that the maximum amount of wet sludge that can be burned in co-combustion regime is close to 50 wt%. Higher concentrations of wet sludge, prevent reach and maintain a temperature of 850 °C in the reactor (Lars-Erick Amand, Leckner Bo, Karsten Lücke, 2001).

For co-combustion of wood or coal with paper mill sludge, was found that adding a maximum amount of 25 wt% of sludge, the behavior of the main fuel prevails (Leckner, Åmand, Lücke, & Werther, 2004). It is also reported that the sludge combustion kinetic is similar to wood due to the high content of volatiles which makes this fuel very reactive. It was found that when burning sludge, volatiles combustion occurs mainly in the freeboard zone, neglect this fact can cause an increase of the carbon monoxide (CO) concentration in the stack and even the volatile organic compounds (VOC's).

Similarly that volatiles, there is a fast release of VOC's at the reactor fuel feeding port. As mentioned, sludge combustion takes place mainly in gaseous phase; consequently VOC's and CO emissions are highly dependent of this behavior. This means that an efficient combustion of volatile practically destroys VOC's therefore; there is a correlation between incomplete combustion, CO and VOC's production (Lars-Erick Åmand, Leckner Bo, n.d.)(Gulyurtlu, Abelha, Grego, & Garcı, 2004).

Another important feature of the sludge behavior to take into account is the weight difference between them and other types of fuels. Basically due to weight difference, sludge particles fall down different in the reactor and it causes important changes in the combustion process. Thus reach a sufficiently high temperature of combustion is important to an effective effluents control. Care needs to be taken when heavy metals are part of the sludge composition. Reaching temperatures above 900 °C could allow the release of heavy metals in the effluents stream in a gaseous phase. Basically the objective is to keep all dangerous components in a solid phase in the form of slags and ashes (L.-E. Åmand & Leckner, 2004).

Regarding to solid products of combustion is well known that the sludge combustion produces more quantity of ashes when compared with coal or other biomass types like wood. Biomass post combustion products are fewer than those from coal combustion but it is important to note that due to the presence of heavy metals on its elemental composition the biomass post combustion solid products are more dangerous even more in the case of sludge since it comes from WWTP. Other important feature to take into account besides the quantity and hazard is that ashes from sludge combustion are stickier than others. Therefore, the sludge usage as fuel requires the implementation of some changes in the infrastructure of the power station facilities. Basically it is needed to re size the effluents treatment systems such as cyclones and ash filters.

Additional issues were also reported when Sodium, Potassium and Chlorine content in the sludge is high. De-fluidization problems were reported because those elements cause a considerable reduction in the bed sand melting point. Temperatures higher than 900 °C can smelt the bed sand and consequently de-fluidize the reactor (Shao, 2007).

Regarding to flue gas composition some surveys shows that emissions of SO<sub>x</sub> and NO<sub>x</sub> decrease with increasing sludge feeding rate, but CO shows the reverse

tendency due to the decrease in combustion temperature caused by a large amount of moisture in the sludge (Tsai, Wu, Huang, & Lee, 2002). When assessing moisture content influence in the NO and NO<sub>2</sub> emissions it was found that emissions from wet sludge are similar or even lower than those from dried sludge (L. Åmand & Leckner, 2001). High Chlorine emissions is generally reported which can be effectively controlled by scrubbers or injecting hydrated lime in the flue gas path (Hartman, Svoboda, Pohor, & Trnka, 2005).

An efficient combustion is important to prevent undesirable effluents, when assessing the combustion performance in terms of carbon conversion rate (CCR) and the emission rates of CO, C<sub>x</sub>H<sub>y</sub> and NO<sub>x</sub> the results of the parametric study shown that a 35% water content and 60g feeding mass generated the best conditions for combustion. The total CO and NO<sub>x</sub> emission decreases as the secondary air ratio increases at the same time the CO<sub>2</sub> emission increases. It was shown that the cases in which the sludge water content was 35% and 45% emit relatively lower molecular weight C<sub>x</sub>H<sub>y</sub>, a result that reveals higher combustion efficiency thereby for general industrial burners, staged combustion with secondary air injection is one of the popular methods to reduce emissions (Shin, Jang, & Hwang, 2005).

Regarding to heavy metals emissions special attention was paid to the most volatile species Mercury and Cadmium. Some surveys show that there was no Mercury in the bed, it was found in the form of fly ashes. Some Cadmium was found in the bed, especially during operation with coal. In general terms Mercury and Cadmium were enriched in the fly ash. The typical distribution of ashes between bottom and fly ash is about 30% - 70%, but in some cases it can go to a 50% - 50% distribution. Mercury was found mostly in the bag filter, whereas Cadmium was rather evenly distributed between secondary cyclone and bag filter. The survey concludes that most of the trace elements were found in the ash and the emission of trace elements with the flue gases was small in the cases investigated; the concentrations were less than the maximum acceptable emissions established by the European Union (L.-E. Åmand & Leckner, 2004).

Regarding to stock and handling operations some issues were also reported. When the moisture content exceeds 10%, bacteria's activity causes a drop of the heating value and also produces bad smells, therefore the storage time for this type of fuels cannot be prolonged (Leckner et al., 2004).

## **2.2 Sewage sludge drying**

As discussed in section 2.1, many techniques were tested in order to treat sludge, several applications were developed but in general it was found that the high moisture content is the big constraint to overcome; definitely a dried sludge is required to enable any other treatment option. For co-combustion that is the waste treatment technique that will be discussed in this document a drying stage as a pretreatment option is extremely important.

Mechanical dewatering of sludge is a process that has been used generally as a means of solid concentration in discharged waste. For this purpose some systems are used, as decantation, centrifugation, filtration, etc. Those are able to raise the solids content in the final residue to values between 20 - 40 wt%. However after this process important moisture content still remains in the sludge; that is the reason why a thermal dewatering process is needed. There are a lot of drying systems applied in the industrial sector but adaptation to handle sludge has some difficulties, for instance the mass transport (dryer feeding), which in many drying processes can be done by simple means; in the case of sludge due to its plastic behavior is a big issue.

For sewage sludge thermal treatment, design and assessment there are three main factors that must be taken into account:

- Thermal transfer (heat and mass) which determine the heating means;
- Mass manipulation, which determine the physical transport medium;
- Vapor transport, which determine the absorption medium and the means of environment protection.

### 2.2.1 *Sludge drying processes*

Based on the aforementioned factors several devices available to manage and dry sludge were developed and they can be classified by the drying technique used to transfer heat. By this concept two types of systems can be defined: indirect and direct. The first one uses air in direct contact with the sludge mass. For the second type of systems the heat mean (water steam or heating oil for instance) is separated from the sludge mass by a wall.

In terms of infrastructure, direct systems are simpler than indirect systems because they use air to heat the sludge and to absorb its moisture. Indirect systems require more complex heat transfer systems either in the heat transfer to the heat medium or in the heat transfer to the sludge mass. In both cases the objective is to transfer heat to the core of the sludge and spread it uniformly, here the sludge physical characteristics are very important.

Direct drying is suitable for easy disaggregated products with a big drying specific surface because this facilitate heat transfer to the sludge cake and moisture absorption from the surface. It can be experienced some difficulties if is needed to handle a very amorphous, plastic and wet mass.

On the other hand, indirect drying completely separates the heat transport mean and the moisture absorption mean. The heat addition is made through a partition wall between the sludge and the heating mean, thereby depending of the shape of this wall, the heat transfer surface area can be considerably increased, thus increasing the water evaporation rate; of course the sludge mass consistency continue being a limiting factor.



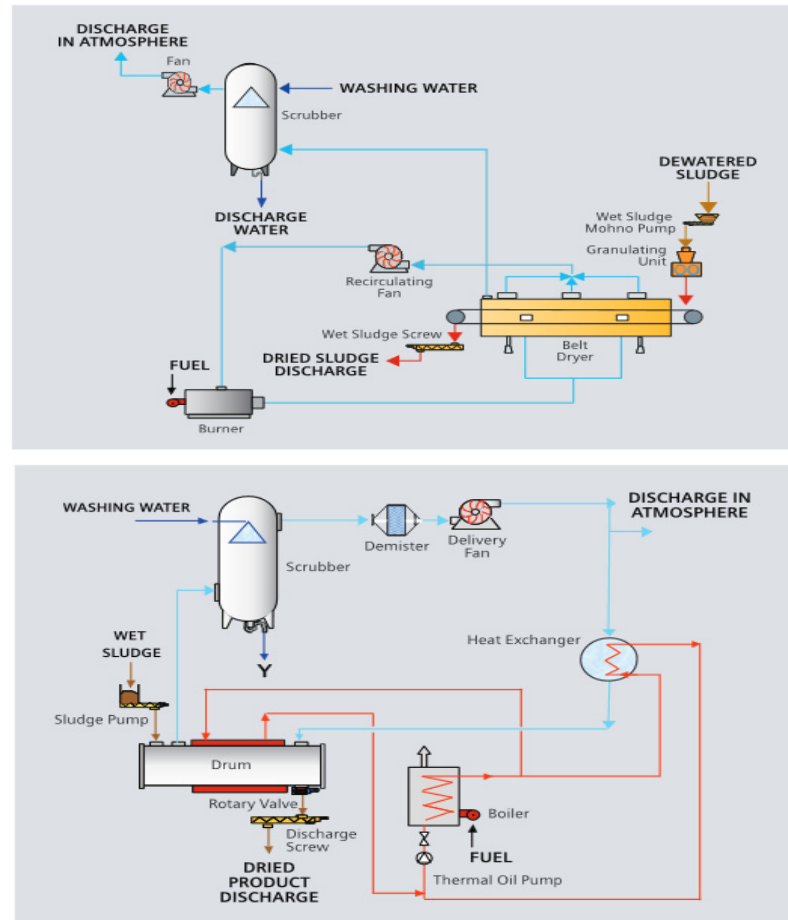


Figure 2.1 - Up: direct sludge drying system. Down: indirect sludge drying system. Source:(Siemens Water Technologies Corp, 2008).

Starting with the difficulty involved in handling a wet mass in the form of paste, it is added the effect of changing the sludge plastic mass characteristics. According to (Undebarrena, 1999) between 60% and 50% of moisture content, the sludge gets a plastic texture, fundamentally elastic, sticky and difficult to handle. Therefore the drying system must be able to keep the sludge mass moving to achieve the next stage. Below 50% of moisture content the sludge gets a texture easier to transport and handle. To avoid handling problems with sludge with a moisture content up to 50% some technologies applied a recirculation process where a small part of dried sludge is returned to the dryer feeding port or the place where the plastic problems occurs.

When the moisture reaches the surface of the sludge cake it evaporates being transported to the absorption medium. As mentioned, direct drying uses air as absorption medium which implies the need of operate with high temperatures and flows. Extremely high temperature can modify the sludge composition and trigger an important entrainment of solid particles that must be captured at the exhaust of the dryer. The solids capture can be done with bag filters. In some cases the vapors condensation is done after the solid filtration.

In indirect drying systems, air is used just for the vapor absorption, therefore, is possible to use relatively small volumes avoiding the solids entrainment. However some cases require an exhaust gases washing (wet process for capture and condensation of vapors and solids) as a safety measure due to the presence of volatile compounds. An important study was carried on, where the emission characteristics of volatile compound during paper mill sludge drying process were investigated on a lab-scale tubular drying furnace and a pilot-scale paddle dryer. The results indicates that five kinds of VCs, i.e.  $\text{CO}_2$ ,  $\text{NH}_3$ ,  $\text{C}_7\text{H}_{16}$  (n-heptane), volatile fatty acids (VFAs) and  $\text{CH}_4$  were emitted during the drying process. It was found that the VFAs and  $\text{CO}_2$  were the main compounds released. The temperature and water content of sludge had great effects on the emission rates of  $\text{NH}_3$ ,  $\text{C}_7\text{H}_{16}$ ,  $\text{CO}_2$  and VFAs (Deng et al., 2009).

Is also important to mention a relatively novel technique that is getting academic attention called fry drying which consists of immerse a moist material in a large volume of hot oil. As new ways of disposing recycled food oils have to be found, it is proposed the idea of a co-treatment of recycled food oils with sewage sludge to formulate a derived fuel. Deep fat frying, performed at  $160^\circ\text{C}$  with municipal digested sewage sludge, enables to remove 90% of the initial water content in less than 1500 s (Carlos A . Peregrina Cambero, 2004)(Ohm, Chae, Kim, Kim, & Moon, 2009). There is another important advantage to mention, which is the increase of the sludge heating value after drying. The heating values of the sludge samples prior to fry-drying were 0,91, 1,11 and 1,79 MJ/kg respectively. After drying, these values were increased to 22,26, 25,05 and 25,25 MJ/kg, respectively (Ohm et al., 2009).

In order to assess the environmental impacts of this process a life cycle analysis (LCA) was performed. LCA is a powerful tool used to foresee the environmental performance of a product, this approach has some limitations because some assumptions are needed (externalities), however in the four impact categories selected, fry drying systems have shown a good performance. An economic assessment appears as a necessary complement to determine the feasibility of fry drying as an intermediate step in the disposal of sludge by incineration (Peregrina, Lecomte, Arlabosse, & Rudolph, 2006).

This approach seems to be interesting since treats two types of problematic wastes and produces a waste derived fuel. It is important to mention that there is still no academic publications about the behavior of those derived fuels when burned on different types of reactors thus it is still unknown the flue gas composition and if it complain with international standards.

### 2.2.2 *Drying insights*

When a wet solid is dried there are two processes that take place: energy transfer (in the heat form) from the environment to the product that allows the evaporation of the moisture on its surface and internal moisture transfer from the solid core to its surface. The transport of moisture within the solid may occur by capillary action or by liquid and/or vapor diffusion, and the mechanism by which it takes place depends on the bonds between water and the solid. Water bonds physically to the

solid, and thus fills the macro- and micro-pores of the material. Humidity equilibrium is established between the moisture on the solid surface and water vapor pressure in the gas just above the solid surface, whereas free humidity is the excess humidity above the equilibrium value. Hence drying can be seen as a combined process of heat transfer (product heating) and mass transfer (moisture removal).

Convective drying as mentioned in section 2.2.1 is a process that uses the air to drive the heat and transfer the water excess from the solid to the atmosphere. This is based on the air property where increasing the temperature of the air its relative humidity decreases allowing the absorption of the product's moisture. Thus a mass loss can be verified as a result of the evaporation of a fraction of the water in the solid. The heat added allows the migration of water to the surface, therefore, the drying air must have a considerable amount of heat to yield it to the material, in addition to acceptable conditions to keep and transport a quantity of mass in the form of steam. In general terms the necessary condition to dry a product is that the partial pressure of water vapor in the product surface must be greater than the partial pressure of steam in the air.

The drying process based on mass and heat transfer can be divided in three stages although not all materials behave in the same way.

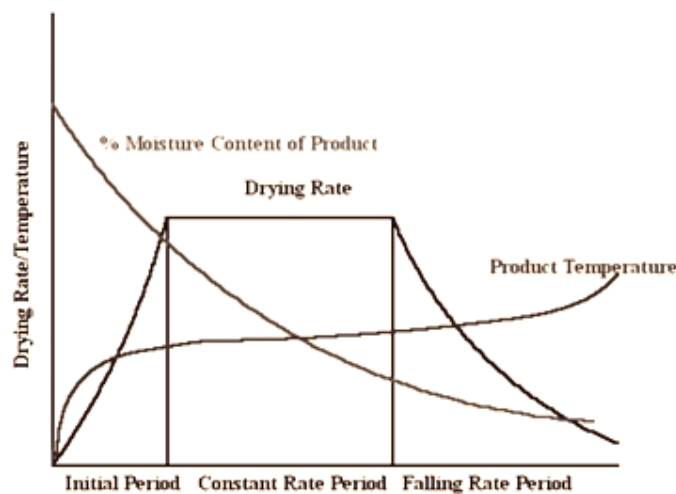


Figure 2.2 - Typical drying curves. Source(Park, 2007).

Frequently, several stages are distinguishable when a wet solid is dried under a flow of hot air. Initially, there is a short period of time when the sample is heated or cooled (evaporation can cause a cooling of the product) during which the variation of temperature depends on the heat transfer from the air to the solid. After this initial stage, sometimes follows a constant drying rate period, which is a result of the above mentioned equilibrium. Finally, there is a period where the drying rate decreases, in which the temperature of the solid increases and water diffusion from inside the solid to the surface takes place by the mechanisms described earlier. This final period has different stages depending on which mechanisms dominate the drying process as they would differ in the case of a liquid, gas or gas/liquid phase. Therefore, the drying of

moist solids is a complex process involving simultaneous and coupled heat and mass transfer. This processes can be modeled by considering mass and heat balances, and assuming that water diffuses according to kinetic laws (R. Font, M.F. Gomez-Rico, 2011).

#### 2.2.2.1 Sludge drying kinetics

There are many approaches for describing drying kinetics. (J. Vaxelaire, J.M. Bongiovanni, P. Mousques, 2000) proposed a macroscopic approach in terms of drying potential in order to assess the influence of temperature, relative humidity and air velocity in the drying process and mostly to know which set of operating conditions is better, quicker and cheaper than another. They derive an overall parameter by the difference between the chemical potential of saturated vapor at wet bulb temperature (temperature at the surface of the wet material) and the one of the vapor at dry bulb temperature. The obtained drying curves reproduce very well the drying behavior for the constant rate period but in the falling rate period some discrepancies were found.

The study also warn about the occurrence of a dry layer at the surface of the product while the center stays wet which difficult the drying process, it was found that this phenomenon in conjunction with shrinkage are important aspects of sludge drying that can strongly modify the drying kinetics. Differential shrinkage is produced due to non-uniform moisture content distribution and/or non-uniform temperature profiles. Usually shrinkage leads to crack formation then some crannies appears at the surface of the sludge cake which let the hot air to enter in the sludge core increasing the drying rates.

Diffusion models are commonly used to try to describe this complex process. Those models are applicable to solids drying for a long falling period in cases where the initial and constant rate periods are very short, or entirely absent. The use of numerical techniques for solving the heat and mass balances and the kinetic equation are not easy. The finite elements method, which solves the models for spheres, cylinders and slabs, divides these geometries into different volume elements and then applies mass and heat balances and related kinetic laws to them (Crank, 1975).

Using those strategies during the last years the sludge drying behavior was studied by many researchers. Several related documents try to establish the effects of drying conditions, the sludge behavior, and the mass and heat transfer coefficients. The researchers' uses different types of sludge as sample, due to this; some differences can be verified on their conclusions. However two main types of sludges were identified. The first one with a high granulometry that present a constant rate period during the first part of the drying process and almost do not present the crust effect and other which do not present a constant rate period and have a strong crust formation during drying; this type of sludge takes more time to dry. For both, the same global trend is observed: the mean drying flux increases with increasing air superficial velocity and temperature and decreasing air moisture content. (Léonard, Blacher, Marchot, Pirard, & Crine, 2005) conclude that the temperature has the major influence on the drying kinetics, followed by superficial velocity and air moisture content.

Regarding to the details related with handling and testing, it was found that most of the experiments were performed in experimental drying tunnels under controlled conditions. The mass lost by the samples during the drying process is monitored in continuous during the process and in some cases the temperature inside the sample is also recorded. In general terms the samples are taken from the WWTP or industrial sources. It was reported that the pressure at the samples were subjected during mechanical dewatering has no influence in the drying kinetics (R. Font, M.F. Gomez-Rico, 2011). Before the experiments the samples are normally stored at 4°C. To find the initial moisture content and the dry mass quantity, the samples generally are subjected to drying in an oven at 105°C.

For the study of the drying kinetics different types of sludge shapes were used for kinetic model development. (Reyes, Eckholt, Troncoso, & Efremov, 2004) uses a tablet shape and drying kinetics was modeled for the falling rate period using the modified quasi-stationary method and the Fick's second law. They used metal boxes filled with sludge and a drying tunnel with parallel air flow. At the beginning of drying, a thin and porous crust is formed on the surface of the samples, which remained unchanged for the first 30 min at 90 °C. From this moment a considerable shrinkage and cracking of the sludge sample was observed forming hollow cavities of different size that increase the drying rate due to the increase in the surface contact area. The effective diffusivity was also determined from the integrated Fick's equation, and correlated with temperature by an Arrhenius type equation.

(Bennamoun, Belhamri, & Léonard, 2010) uses extruded wet material (1 kilogram of cylinders with 12 millimeters diameter) in a discontinuous pilot scale convective belt dryer reproducing most of the operating conditions prevailing in a full scale continuous belt dryer. Several mathematical models, reproducing the experimental results were evaluated. The determination of the correlation coefficient was the first step and the first criterion to determine the best models. They found that the Page model and the 4th degree polynomial model describe well the obtained results; however, the coefficients of the selected models can change with the sludge type. The temperature range chosen was 120°C, 140°C and 160°C to investigate the influence of the air temperature as the most influent operating condition. In conclusion they report that drying kinetics of wastewater sludge can be affected by temperature of the heated air, but also by the type of sludge.

(J. Vaxelaire and J.R. Puiggali, 2002) proposed an analysis in terms of drying kinetics modeling a conveyor dryer belt. The set of air operating conditions (temperature, relative humidity and air velocity) were reduced to a single parameter, the drying potential. The dryer was supposed to be fed with cylindrical pellets of sludge disposed in a layer characterized by its initial porosity and thickness. The belt velocity is an operating parameter and it was fixed for each simulation. The results of the simulations show that a conveyor belt dryer is not well adapted to activated sludge (long falling rate period); and this is essentially due to a crust phenomenon. For a polyvinyl chloride (PVC) industrial sludge this kind of dryer is more efficient and allows drying with reasonable residence times. The study also established the specific heat capacity for the sludge samples, using the differential scanning calorimetry

method in the temperatures range of 50 to 90 °C. At the end was concluded that specific experiments were needed in order to better describe some particular aspects such as crusting, shrinkage, and particle size impact before industrialize the process because probably those parameters are as important as drying conditions.

(R. Font, M.F. Gomez-Rico, 2011) propose a kinetic model to account for water diffusion and internal heat transfer which considers the vaporization of humidity on the surface of the particle, diffusion effects in sewage sludge due to heat and moisture, and formation of a skin layer. They studied the thermal drying of sludge in the temperature range of 30-65 °C with two different types of sludge that present different behaviors in the formation of a skin during the drying process. Small sewage sludge spheres and cylindrical tablets were produced to develop a kinetic model and to correlate the experimental data in terms of moisture content and temperature, vs. time. At the end some important kinetic parameters were obtained (mass transfer coefficient, heat transfer coefficient, skin effect parameter, diffusion coefficient and activation energy). A general expression for the diffusivity of water inside a solid was proposed. The complexity of the system makes that the model was based in many assumptions, however it reproduces well the drying behavior and considers important effects as crust and shrinkage. It is important to mention that this very complete kinetic model can be versatile. Considering different kinetic parameters it is possible to analyze the drying kinetics of a wide variety of sludges.

#### 2.2.2.2 Artificial neural networks

As exposed in section 2.2.2.1 the drying models based on thermodynamic considerations can be very difficult to solve. In order to simplify those models, several assumptions and considerations must be taken and due to this sometimes the model outputs does not fit the reality with accuracy. Furthermore the state-of-the art revision suggests that there is enough information about theoretical models based on heat transfer, mass transfer and diffusion. Being sensible to this fact a detailed search about alternative methodologies was performed that can simplify the model construction and also that can offer a faster response about the drying consequences due to changes in the drying conditions which can be very interesting specially for developing accurate control systems for industrial applications.

An interesting approach was found. Based on progress of neurobiology some researchers are allowed to build mathematical models of neurons to simulate neural behavior. Artificial neural networks (ANN) are recognized as good tools for dynamic modeling, and have been extensively studied. The interest of these models includes the modeling without any assumptions about the nature of underlying mechanisms and their ability to take into account non-linearity and interactions between variables. It was found that ANN approach was widely used for food drying models construction; with interesting results that in most of the cases are more accurate than classical drying models (Trystram & Heyd, 1993)(Joykumar & Krishna, 2011).

At the very beginning, ANN was understood as a special regression technique, which provides a better way of finding the links between the inputs, outputs and

process variables, during the learning phase. Learning means to present, repeatedly, to an ANN a set of couples of input/output vectors, and to force it to fulfill a learning criterion: in most cases, the sum of the squared distances between real and desired output.

Matching the ANN output to the real world, passes through the neuron weights, which are modified until the learning criterion is fulfilled. But learning means nothing to anyone, except when this stage is followed by the use of the ANN. And here it seems that the ANN performs better than the classical regression, because of its generalization capacity that means its possibility to give a correct answer to a question outside the learning set. The ANN generalization relies on its capacity of finding out the hidden rules that govern the process, even if, at this time, it cannot be mathematically expressed (Lavric, 1995).

Essentially an ANN is a massive parallel-distributed information processing system that has certain performance characteristics resembling biological neural networks of human brain. ANN has been developed as a generalization of mathematical models of human cognition and neural biology. ANN's are essentially an interconnected assembly of simple processing elements, units or nodes, whose functionality is loosely based on the human's neuron. The processing ability of the network is stored in the inter-unit connection strengths, or weights. The values of the weights are obtained as mentioned by a process of training or learning from a set of training patterns. These weights are adapted by a learning rule and represent the long-term memory of the neural network.

Numerous types of the artificial neural networks exist such as multi-layer perceptron, radial basis function networks and recurrent neural networks, but each type consists of the same basic features: nodes, layers and connections. The smallest element of a network is the node. Every node receives signal from a connection, or a link. The signal is then summed together before being applied a transfer function to produce the output. The output signals are then propagated to other nodes until it reaches the output of the network. ANN models are able to describe the results of several experiments in different drying conditions. They have also the ability to accept new sets of experiments and the model can be retrained to extend the range of input parameters (Movagharnjad & Nikzad, 2007).

All the aforementioned features appear interesting to develop a model which can describe the sludge drying kinetics. Moreover once it is intended to use waste heat to drive the drying process a model that can offer a faster response under several drying conditions about the final moisture content that can be achieved in conjunction with the time needed seems a great help.

#### 2.2.2.2.1 ANN architecture

There are several features defining an ANN that must be taken into account in order to understand the mechanism used by the model in order generate the forecast.

The first parameter that defines the architecture of an ANN is the direction in which the information flows. Essentially two types of ANN were identified; the feed forward network in which the information flows only in one direction through the hidden nodes and to the output nodes and the recurrent neural networks where the information flows in cycles or loops.

Table 2.2 – MATLAB available transfer functions. Source:(Gonçalves, 2012).

<b>Code</b>	<b>Transfer function</b>
compet	Competitive transfer function
hardlim	Hard – limit transfer function
hardlims	Symmetric hard – limit transfer function
logsig	Log-sigmoid transfer function
netinv	Inverse transfer function
poslin	Positive linear transfer function
purelin	Linear transfer function
radbas	Radial basis transfer function
radbasn	Normalized radial basis transfer function
satlin	Saturating linear transfer function
satlins	Symmetric saturating linear transfer function
softmax	Softmax transfer function
tansig	Hyperbolic tangent sigmoid transfer function
tribas	Triangular basis transfer function

The term hidden layer was mentioned above, and this feature is another important detail of the ANN architecture. As mentioned there is a layer filled with the input neurons, and another layer filled with the output neurons. There is an extra layer called hidden layer that is filled with hidden neurons. They are the neurons that are neither in the input layer nor the output layer. These neurons are essentially hidden from view, and their number and organization can typically be treated as a black box to people who are interfacing with the system. Using additional layers of hidden neurons enables greater processing power and system flexibility. This additional flexibility comes at the cost of additional complexity in the training algorithm.

The neurons can reach two states, the criteria to activate or deactivate a neuron relies in a transfer function which is the third aspect of the architecture to be discussed. The sum of products of the weights and inputs is calculated in each node, and if the value is above some threshold (typically 0) the neuron fires and takes the activated value (typically 1); otherwise it takes the deactivated value (typically -1). This



threshold which is the nature of the transfer function can be defined in several ways. The MATLAB software defines several transfer functions as shown in Table 2.2.

Finally the last main feature that defines the architecture of an ANN is the training algorithm. As mentioned the objective of the ANN is to achieve the lowest possible deviation between the calculated output and the database output. A back propagation train is performed which means to compare those values until achieve a defined error value. This process lets the ANN to set the most appropriated weights for each neuron. MATLAB defines several training algorithms, which are presented below.

Table 2.3 – MATLAB available training algorithms. Source:(Gonçalves, 2012).

Code	Training algorithm
Trainlm	Levenberg-Marquardt
Trainbr	Bayesian Regularization
Trainbfg	BFGS Quasi-newton
Trainrp	Resilient Backpropagation
Trainscg	Scaled Conjugate Gradient
Traincgb	Conjugate Gradient with Powell/Beale Restarts
Traincgf	Fletcher-Powell Conjugate Gradient
Traincgp	Polak-Ribière Conjugate Gradient
Trainoss	One step secant
Trainidx	Variable Learning Rate Gradient Descent

### 2.3 Heat recovery

As exposed in section 2.1.1 to 2.1.4 a thermal treatment stage to reduce the moisture content of the sludge is extremely important because this not only enable its use as fuel but which enables any other treatment option. Thermal treatment (drying), in fact, could be energy intensive. This fact can hinder any chance of recycling. Because of that it is important to extend the analysis to possible energy sources that can drive the process in a sustainable way. Those sources must be cheap, stable and largely accessible. To accomplish it, a better understanding about the industrial waste heat sources can be the key concept.

There is worldwide concern about the best ways of using the nonrenewable sources of energy. It has encouraged research and development efforts in the re-use of the usually wasted forms of energy. Waste heat can be defined as the heat contained in a substance rejected from a process at a temperature higher than the ambient levels of the plant; for a more accurately definition it can be pointed it out that industrial waste heat refers to energy that is generated in industrial process without being put to practical use. Sources of waste heat may include gases, solids and liquids for instance: hot combustion gases discharged to the atmosphere, heated products exiting industrial

processes and heat radiated from hot equipment surfaces. Some documents refers that waste heat is any source of rejected heat having a portion which may be recovered and reused economically (Canada Department of Energy, 1988). Waste heat recovery can be also defined as a process that entails capturing and reusing the waste heat in industrial process for heating or for generating mechanical or electrical work. While some waste heat losses from industrial process are unavoidable, facilities can reduce it, improving equipment efficiency or installing waste heat recovery technologies. Understanding of the fundamentals of heat transfer mechanisms is therefore, important to establish the waste heat recovery benefits. Essentially, heat transfer occurs by three different mechanisms; radiation, conduction and convection.

The benefits of heat recovery are multiple: economic, resource saving, and environmental. The decision as to whether or not to apply a waste heat recovery and utilization system is usually economical in nature. The payback-period, net present value, internal rate of return and life-cycle cost concepts can be considered during the decision-making process. A longer payback period is generally acceptable for projects having long-life equipment, but a payback period of three to five years is generally considered reasonable (Energy design resources, 2009).

### 2.3.1 *Heat recovery asses*

Evaluating the feasibility of waste heat recovery requires characterizing the waste heat source and the stream to which the heat will be transferred. Important waste stream parameters that must be established include: heat quantity, heat quality (temperature), waste heat stream composition, minimum temperature allowed, operating schedules, availability and other logistics.

#### 2.3.1.1 Heat quantity

The quantity, or heat content, is a measure of how much energy is contained in a waste heat stream, while quality is a measure of the usefulness of the waste heat. The quantity of waste heat contained in a waste stream is a function of mass flow rate, stream composition, and temperature. It is usually evaluated based on process energy consumption, typical temperatures, and mass balances.

Although the quantity of waste heat available is an important parameter, it is not the only one effective measure of waste heat recovery opportunity. It is also important to specify the waste heat quality, which essentially is determined by its temperature.

#### 2.3.1.2 Waste heat temperature: quality

The waste heat temperature is a key factor determining waste heat recovery feasibility. Waste heat temperatures can vary significantly and can be classified by temperature range, as shown in Table 2.4.

Table 2.4 – Waste heat categories classified by temperature. Source:(Energy design resources, 2009).

Category	Temperature [°C]
High	500 to 1500
Medium	200 to 500
Low	25 to 200

In order to enable heat transfer and recovery, it is necessary that the waste heat source temperature is higher than the heat sink temperature. Moreover, the magnitude of the temperature difference between the heat source and sink is an important determinant of waste heat's utility or quality. The source and sink temperature difference influences the rate at which heat is transferred per unit surface area of heat exchanger, and the maximum theoretical efficiency of converting thermal energy from the heat source to another form of energy. Finally, the temperature range has important ramifications for the selection of materials regarding to recuperation technologies and recuperation devices.

#### 2.3.1.3 Waste stream composition

Although chemical compositions do not directly influence the quality or quantity of the available heat (unless it has some fuel value), the composition of the stream affects the recovery process and material selection. The composition and phase of waste heat streams will determine factors such as thermal conductivity and heat capacity, which will impact heat transfer effectiveness. Meanwhile, the process specific chemical makeup of off gases will have an important impact on heat exchanger designs, material constraints, and costs.

Another key consideration is the interaction between chemicals in the waste heat stream and materials of heat recovery technologies and devices. Fouling is a common problem in heat exchange, and can substantially reduce heat exchanger effectiveness or cause system failure. Methods for addressing fouling are numerous and include filtering contaminated streams, constructing the exchanger with advanced materials, increasing heat exchanger surface areas, and designing the heat exchanger for easy access and cleaning. Nevertheless, the problem of fouling remains a significant challenge in thermal science. The significant patent activity and continued antidotal reports indicate that fouling remains as an unsolved problem. Moreover, a large portion of research is reactive, involving methods for easily cleaning of fouling, rather than methods for prevent it.

#### 2.3.1.4 Minimum allowable temperature

The minimum allowable temperature for waste streams is often closely connected with material corrosion problems. Depending on the fuel used, combustion related flue gases contain varying concentrations of carbon dioxide, water vapor, NO<sub>x</sub>, SO<sub>x</sub>, unoxidized organics, and minerals. If exhaust gases are cooled below the dew

point temperature, the water vapor in the gas will condense depositing corrosive substances on the heat exchanger surface. Heat exchangers designed from low-cost materials will quickly fail due to chemical attack. Therefore, heat exchangers are generally designed to maintain exhaust temperatures above the condensation point. The minimum temperature for preventing corrosion depends on the waste stream composition that is linked to the combustion technology and type of fuel used to produce heat. The most common method for preventing chemical corrosion is designing heat exchangers with exhaust temperatures well above the dew point temperature. However, there are some cases where heat exchangers use advanced alloys and composite materials to further recover low temperature heat. These systems have not seen much commercial application due to challenges such as high material costs, large surface areas required for heat exchange, and lack of an available end use for low temperature waste heat.

#### 2.3.1.5 Economies of scale, accessibility and other factors

Several additional factors can determine whether heat recovery is feasible in a given application. For example, small scale operations are less likely to install heat recovery, since sufficient capital may not be available, and because payback periods may be longer. Operating schedules can also be a concern. If a waste heat source is only available for a limited time, the heat exchanger may be exposed to both high and low temperatures. In this case, it must be ensured that the heat exchange material does not fatigue due to thermal cycling. Additionally, it is important that the schedule for the heat source match the schedule for the heat load. If not, additional systems may be required to provide heat when the waste heat source is not available. Another concern is the ease of access to the waste heat source. In some cases, physical constraints created by equipment arrangements prevent easy access to the heat source, or prevent the installation of any additional equipment for heat recovering. Additionally constraints are presented by the transportability of heat streams. Due to this, it is expected that the application of heat recovery should be physically close to the source of waste heat for maximum benefits from recovered energy.

#### 2.3.2 Heat recovery technologies

There are four typical types of technologies used to recover waste heat. These include: direct usage, heat exchangers, heat pumps and vapor recompression. The first two technologies involve using waste heat “as is”. In such situations, the waste heat is of adequate quality for use elsewhere.

Waste heat is often available at a temperature lower than the potential load requirement. Waste heat upgrading refers to boosting the energy level of a waste heat stream so that it might perform more useful work than could otherwise be achieved. This can be accomplished through the use of heat pumps or by direct vapor compression devices.

Although waste heat recovery technologies are currently employed to varying degrees at many industrial facilities, it still faces technical and economic barriers that

impede their wider application. In order to promote waste heat recovery and process integration, efforts must be undertaken to extend the economic feasibility of conventional recovery technologies, as well as promote new technologies that can be applied to waste heat sources not typically exploited for waste heat recovery.

### *2.3.3 Barriers for promoting waste heat recovery practices*

As mentioned, numerous barriers impact the economy and effectiveness of heat recovery equipments and impede their wider installation. Many of these barriers, described earlier are interrelated, but can generally be categorized as related to cost, temperature restrictions, chemical composition, application specifics, and inaccessibility/transportability of heat sources. In general terms a long payback period is a constant constraint.

Another interesting fact that was verified is that roughly 60% of the waste heat streams available to recover are in the category of low quality. While low-temperature waste heat has less thermal and economic value than high-temperature heat, it is ubiquitous and available in large quantities. Comparison of total work potential from different waste heat sources showed that the magnitude of low-temperature waste heat is sufficiently large that it should not be neglected in pursuing opportunities for its use and recovery (U.S. Department of Energy, 2008).

In conclusion, low temperature waste heat sources appear interesting for the objective to find an energy source to drive the sludge drying process. Assess the viability of a drying process at low temperatures is important in order to enable the utilization of low grade waste heat sources traditionally not used.

### 3 Combustion of biomass and sludge for heat and power production: theoretical approach

A 50 MW<sub>th</sub> energy conversion facility will be used as a case study in order to realize the mass and energy fluxes involved and the constraints of a system where it is intended to use sewage sludge as a secondary fuel.

The facility is located in a pulp and paper industry and uses a mixture of forest biomass residues to produce electricity. The combustion technology used is a bubbling fluidized bed reactor. As the main line of business in this industry is pulp production, the sludge generation is an unavoidable fact. Because of that new ways to treat this specific waste are of major interest. One valuable option is to thermally treat the sludge to reduce its moisture content enabling them as fuel that can be feed to the fluidized bed combustor. In order to identify the main features of this alternative a first theoretical approach was performed using the mass and heat balance methodology proposed by (A. Matos, 2011). To help and support the analysis a MATLAB routine was developed which code can be found as Appendix 1.

#### 3.1 Mass Balance

In this section the mass balance model will be presented in conjunction with the equations and considerations taken into account.

##### 3.1.1 *Proximate and elemental fuel analysis*

Some academic surveys regarding the sludge composition were made before to a pulp and paper industry (Fernandes, 2005). (Santos, 2012) established the typical proximate and elemental analysis of the biomass and the sludge available as fuel in this industrial sector. Those data are presented in Table 3.1 and will be used to perform the theoretical analysis presented here.

##### 3.1.2 *Calorific value of the fuel*

Based on the elemental composition presented in Table 3.1 the higher heating value HHV and lower heating value LHV estimation were made for both fuels following the proceedings of (Channiwala & Parikh, 2002 and Parikh, Channiwala, & Ghosal, 2005). For the LHV calculation the latent heat of water vaporization was estimated as 2440 kJ/kg<sub>H<sub>2</sub>O</sub> which corresponds to a temperature of 25°C.

Table 3.1– Proximate and elemental analysis of biomass and sewage sludge at a pulp and paper industry. Source: adapted from (Santos, 2012).

	Biomass	Sewage Sludge
<b>Proximate Analysis (% arb)</b>		
Humidity	5,82	3,60
Volatile	73,01	44,24
Ash	1,33	45,62
Fixed Carbon*	19,84	6,54
<b>Elemental Analysis (%db)</b>		
C	51,70	24,40
H	6,72	4,30
N	0,29	3,54
S	0,02	0,94
O*	39,86	19,00
Ash fraction	1,41	47,82
<b>Heating Value (MJ·kg<sup>-1</sup> db)</b>		
LHV	20,34 <sup>·</sup>	10,00 <sup>·</sup>

\* By difference

<sup>·</sup> Refer to section 3.1.2

### 3.1.3 Air consumption

Using the fuel compositions presented in Table 3.1, the stoichiometric and the actual air consumption were calculated. The stoichiometric needs of oxidizer, ( $W_{s,F}$ ) was found having into account the elemental composition of the fuel mixture:

$$W_{s,F} \left[ \frac{kgO_{2stoich}}{kgF_{db}} \right] = 32 \left( \sum \left( \frac{Y_{s,j} \cdot w_{jF}}{M_j} \right) - \frac{w_{OF}}{32} \right) \quad \text{Eq. (1)}$$

where:

$$Y_{s,j} = \begin{cases} Y_{s,C} = 1 \\ Y_{s,H} = 0,25 \\ Y_{s,S} = 1 \end{cases}$$

The actual Oxygen needs can be calculated based on a given amount of excess air (z):

$$W_{a,F} \left[ \frac{kgO_{2actual}}{kgF_{db}} \right] = W_{s,F} \left( \frac{z}{100} + 1 \right) \quad \text{Eq. (2)}$$

The actual needs of air ( $W_{A,F}$ ) were calculated using the following equation:

$$W_{A,F} \left[ \frac{\text{kg actual air}}{\text{kg } F_{db}} \right] = W_{a,F} \left( \frac{M_A}{y_{O_2,A} \cdot M_{O_2}} \right) \quad \text{Eq. 3}$$

### 3.1.4 Flue gas composition

Assuming the absence of gaseous components related to incomplete combustion (e.g., CO, CH<sub>4</sub>, etc.) and having into account the elemental weighted composition of the fuel mixture, the flue gas composition can be estimated by performing a mass balance to each chemical element.

Some additional assumptions were done during the model development, which are presented below:

- The temperature of the fuels (sludge and biomass) were considered in 25°C;
- The oxidizer used is atmospheric air at 25°C and the absolute moisture content was estimated in 0.010 [kg<sub>H<sub>2</sub>O</sub>/ kg dry air]; taken from a standard psychometric diagram (at 1.013×10<sup>5</sup> Pa);
- The excess air considered (z) was 50%;
- The carbon conversion efficiency considered was 100%;
- The ratio of solids present (fly and bottom ash) was 0.2 [kg<sub>V+E</sub>/kg<sub>F</sub>];
- Was not considered the formation of gaseous products due to incomplete combustion (H<sub>2</sub>, CO, CH<sub>4</sub>, etc.);
- The air flow distribution was estimated as 80% of primary air and 20% of secondary air.

Equations 4 to 9 were used for the application of the law of mass conservation to the combustion system. These calculations establish the amount of combustion products and solid residues distribution:

$$\frac{w_{CF}}{12} = nCO_2 + \frac{w_{CV}W_{VF} \cdot w_{CE}W_{EF}}{12} \quad \text{Eq. 4}$$

$$\frac{w_{HF}}{12} + \frac{W_{WF}}{18} + \frac{W_{a,F}}{32} W_{VA} (7,66) = nH_2O \quad \text{Eq. 5}$$

$$\frac{w_{NF}}{28} + \frac{W_{a,F}}{32} (3,76) = nN_2 \quad \text{Eq. 6}$$



$$\frac{w_{SF}}{32} = nSO_2 \quad \text{Eq. 7}$$

$$\begin{aligned} \frac{w_{OF}}{32} + 0,5 \frac{W_{WF}}{18} + \frac{W_{a,F}}{32} [1 + 0.5 W_{VA}(7.66)] \\ = nCO_2 + \frac{nH_2O}{2} + nO_2 + nSO_2 \end{aligned} \quad \text{Eq. 8}$$

$$w_{ZF} = w_{ZV}W_{VF} + w_{ZE}W_{EF} \quad \text{Eq. 9}$$

### 3.2 Energy Balance

Following the mass balance, an energy balance was performed to establish the useful energy availability through equation 10.

$$\Delta H_{reactants} = \Delta H_{useful} + \Delta H_{products} + \Delta H_{lost} \quad \text{Eq. 10}$$

The reactants energy is given by equation:

$$\Delta H_{reactants} = [\Delta H_S + \Delta H_L + \Delta H_R]_{reactants} \quad \text{Eq. 11}$$

where:

$$\begin{aligned} \Delta H_{S,reactants} = [cp_F + W_{WF} \cdot cp_W](T_F - T^o) + W_{a,F} \\ [cpO_2 + (3.31) \cdot cpN_2 + (4,31) \cdot W_{VA} \cdot cpH_2O(g)] (T_A - T^o) \end{aligned} \quad \text{Eq. 12}$$

$$\Delta H_{L,reactants} = W_{WF} \cdot h_{wv,T^o} \quad \text{Eq. 13}$$

$$\Delta H_{R,reactants} = LHV_F \quad \text{Eq. 14}$$

The sensible heat of the reactants was estimated as zero because the temperature of the fuel and the ambient temperature were both considered as 25°C. The enthalpy of vaporization of water was estimated in  $-2.44 \times 10^6$  J/kg<sub>H<sub>2</sub>O</sub>.

It was considered a combustion temperature of 800°C (1073K) in steady conditions at the combustion chamber. This means that the gases at the outlet of the combustion chamber have a considerable amount of sensible heat. It was considered that most part of this energy was transferred to a proper heat recovery system (super heater and economizer), and a small part was lost, so that the exhaust gases stream achieves a temperature close to 150°C at the exhaust stack. Given these assumptions the energy content in the products was calculated through equation 15.

$$\Delta H_p = [\Delta H_S + \Delta H_L + \Delta H_R]_{products} \quad \text{Eq. 15}$$

where:

$$\Delta H_{S,products} = \sum n_{iR} \cdot M_i \cdot cp_i(T_G - T^o) + \left\{ [w_{ZV}W_{VF} + w_{ZE}W_{EF}]cp_Z \right\} (T_Z - T^o) \quad \text{Eq. 16}$$

$$\Delta H_{L,products} = 0 \quad \text{Eq. 17}$$

$$\Delta H_{R,products} = \sum n_{jF} \cdot M_j \cdot LHV_j + \{[w_{CV}W_{VF} + w_{CE}W_{EF}]cp_C\}LHV_{carbon} \quad \text{Eq. 18}$$

The average specific heat values (at constant pressure) of the combustion flue gases at the exhaust stack, used for the calculations are given in Table 3.2.

Table 3.2 – Carbon LHV at 25°C and average specific heat values of combustion gases, ash and slags for a temperature of 423K, relative to 298K. Source: adapted from(Spiers, 1977).

	<b>T@423K</b>	
<b>cp</b> <sub>CO<sub>2</sub></sub>	1093	J·kg <sup>-1</sup> CO <sub>2</sub> ·K <sup>-1</sup>
<b>cp</b> <sub>H<sub>2</sub>O</sub>	1863	J·kg <sup>-1</sup> H <sub>2</sub> O·K <sup>-1</sup>
<b>cp</b> <sub>O<sub>2</sub></sub>	921	J·kg <sup>-1</sup> O <sub>2</sub> ·K <sup>-1</sup>
<b>cp</b> <sub>N<sub>2</sub></sub>	1038	J·kg <sup>-1</sup> N <sub>2</sub> ·K <sup>-1</sup>
<b>cp</b> <sub>SO<sub>2</sub></sub>	1100	J·kg <sup>-1</sup> SO <sub>2</sub> ·K <sup>-1</sup>
<b>cp</b> <sub>c</sub>	800	J·kg <sup>-1</sup> C·K <sup>-1</sup>
<b>cp</b> <sub>z</sub>	900	J·kg <sup>-1</sup> Z·K <sup>-1</sup>
<b>LHV</b> <sub>Carbon,@25°C</sub>	3,20×10 <sup>7</sup>	J·kg <sup>-1</sup> Carbon

The energy losses ( $\Delta H_{lost}$ ) were considered as 10% of the energy content in the reactants, according equation 19.

$$H_{lost} = 0.1 \cdot H_{reactives} \quad \text{Eq. 19}$$

### 3.3 Industrial facility of 50 MW<sub>th</sub>

Through the energy balance, the amount of fuel needed to produce 50 MW<sub>th</sub> of useful thermal energy was calculated by equation 20.

$$\dot{m}_{fuel,arb} = \left( \frac{50 MW_{th}}{\Delta H_{useful}} \right) + W_{WF} \quad \text{Eq. 20}$$

In order to better assess the quantity of fuel that will be handled by the energy production facility, the water content in the final fuel mixture was also taken into account ( $W_{WF}$ ). Therefore the calculation determines the fuel consumption at the facility in “as received basis” (arb).

#### 3.3.1 Drying approach

In order to have a first approach to the thermal power needed to reduce the moisture content of the sludge, the model was extended to perform some calculations to support the design of a dryer. Two equations were used to found the power needed to shift the moisture content of the sludge from one state to another (Stasta et al., 2006). The first one takes into account the enthalpy of water vaporization at 60°C to account the power needed to evaporate the water. The second one accounts for the heat absorbed by the sludge cake.

$$\dot{Q}_{latent} = \dot{m}_{w,sludge} \cdot h_{wv@60^\circ C} \quad \text{Eq. 21}$$

$$\dot{Q}_{sensible} = \dot{m}_{sludge} \cdot cp_{sludge} \cdot (T_{sludge,f} - T_{sludge,o}) \quad \text{Eq. 22}$$

Additionally, in order to give to the model more accuracy in the calculations some heat losses were considered. Those were estimated in 4% of the total drying energy needs (Stasta et al., 2006) according equation 23.

$$\dot{Q}_{lost} = \left( \dot{Q}_{latent} + \dot{Q}_{sensible} \right) \cdot 0,04 \quad \text{Eq. 23}$$

The additional considerations for the drying calculations are presented in Table 3.3.

Table 3.3 – Parameters considered for the drying calculations. Source: adapted from (Stasta et al., 2006b).

	Quantity	Unit
$h_{wv, @60^{\circ}\text{C}}$	2354	$\text{kJ}\cdot\text{kg}^{-1}_{\text{water@60}^{\circ}\text{C}}$
$cp_{\text{Sludge}}$	1,516	$\text{kJ}\cdot\text{kg}^{-1}\cdot\text{K}^{-1}$
$T_{\text{Sludge},f}$	60	$^{\circ}\text{C}$
$T_{\text{Sludge},o}$	25	$^{\circ}\text{C}$

To estimate the thermal power needed to drive the drying process equation 24 was used.

$$\dot{Q}_f = \dot{Q}_{\text{latent}} + \dot{Q}_{\text{sensible}} + \dot{Q}_{\text{lost}} \quad \text{Eq. 24}$$

### 3.4 Model outputs

Based on the previous defined equations which were implemented in MATLAB code, several tests under different conditions were performed in order to assess the combustion behavior of sludge and biomass considering different moisture contents and final fuel ratios. The results are presented in the following sections.

#### 3.4.1 Useful energy analysis

The amount of useful energy available was estimated based on simulations considering that biomass moisture content was 40 wt%, and assuming that it is constant, and for sludge, a moisture content between 10-75 wt%. The results are shown in Figure 3.1. In the X axis it is represented the percentage of residual forest biomass on the fuel mixture (biomass+sludge).

It can be observed that when burning high percentage of sludge (low percentage of residual forest biomass) with high moisture contents there is no available energy, and the combustion process is not possible; this is observed for sewage sludge percentages in the fuel mixture higher than 95 wt% with 50 wt% moisture and higher than 70 wt% with 75 wt% moisture. For sewage sludge with lower moisture content, as for example 30 wt% and 10 wt%, it is possible to sustain an exothermic process for the operating conditions evaluated. In any case, the amount of available energy increases with decreasing the moisture content of the fuel mixture. According to these results, in theory, for the conditions analyzed, a fuel composed by sewage sludge can be burned in an exothermic process if the moisture content is below 50 wt%. Moreover it can be noticed that the amount of useful energy increases with decreasing moisture contents.

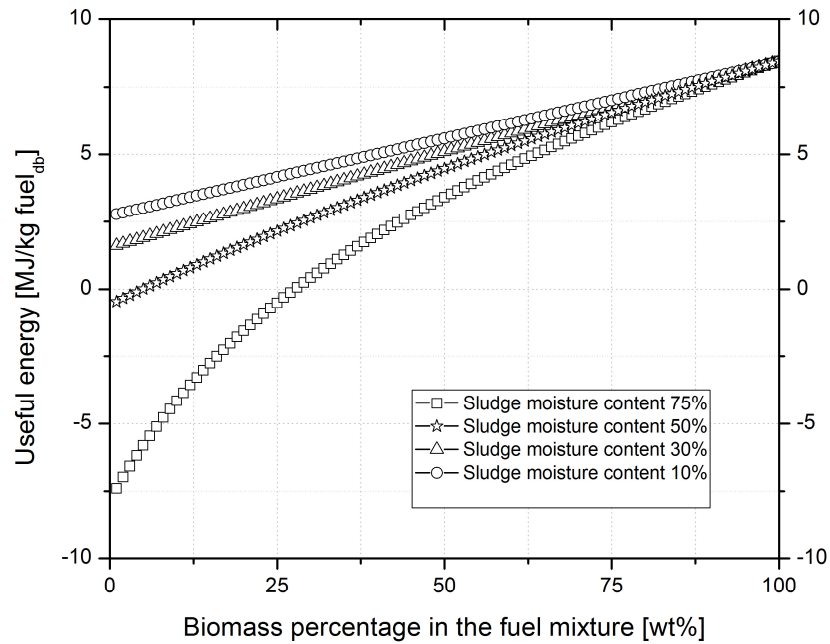


Figure 3.1 - Useful energy [ $\text{MJ} \cdot \text{kg fuel}_{\text{db}}^{-1}$ ] vs. biomass percentage [wt%] in the fuel mixture (biomass + sludge). Combustion gases temperature in the furnace is  $800^{\circ}\text{C}$ , and exhaust gases temperature after heat recovering is  $150^{\circ}\text{C}$ .

Analyzing from the standpoint of co-combustion, it can be observed that starting from a 30/70 of biomass-sludge mass ratio for the fuel mixture, the process is exothermic even for the highest moisture content (75 wt%) considered for sludge. This means that a 30/70 biomass-sludge mass ratio is the limit of a co-combustion system where it is intended to use the sewage sludge without previously thermally drying treatment.

Furthermore it can be observed that when increasing the biomass percentage in the fuel mixture the amount of useful energy increases due to the higher calorific value of the mixture.

### 3.4.2 Flue gas composition

In order to analyze the flue gas composition behavior due to changes in the fuel mixture, it was made a set of simulations for biomass and sludge moisture content fixed in 40 wt% and 75 wt% respectively. The results are shown in Figure 3.2.

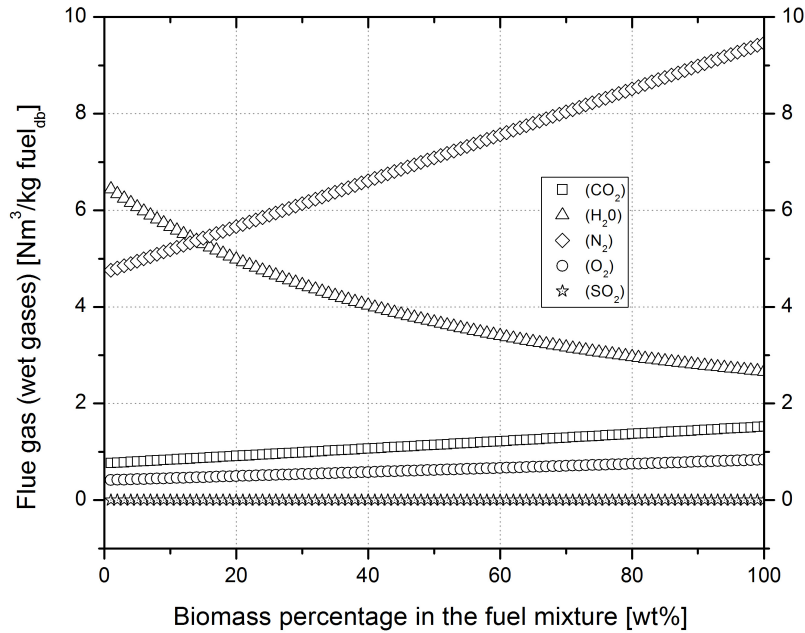


Figure 3.2 - Flue gas composition (wet gases) [ $\text{Nm}^3 \cdot \text{kg fuel}_{\text{db}}^{-1}$ ] vs. biomass fraction percentage [wt%] in the fuel mixture. The moisture content was fixed in 40 wt% for the biomass and 75 wt% for the sludge.

It can be observed a decrease on the concentration of  $\text{H}_2\text{O}$  in the flue gases with increasing the percentage of biomass, because the amount of moisture content of the fuel mixture is decreasing with increasing the amount of biomass. The concentration of  $\text{N}_2$ ,  $\text{CO}_2$ , and  $\text{O}_2$ , increases with increasing the percentage of biomass because of the decreasing in the concentration of  $\text{H}_2\text{O}$  in the flue gases, and as a consequence of decreasing the moisture content of the fuel mixture.

Since the Nitrogen content in the sludge is higher than the biomass, the high Nitrogen emission as effluent when burning just biomass would seem contradictory. This can be explained because the model take into account the stoichiometric air needs, thereby, since the biomass present a highest rate of stoichiometric air needs than sludge, and the nitrogen content in the air was estimated in 78 wt%; in the effluents balance this increase can be noticed as an increase of Nitrogen in the flue gas.

In order to assess the effect of a drying stage for the sludge to decrease its moisture content, for example 35 wt%, a simulation of this effect on the combustion flue gas composition was made. The results are shown in Figure 3.3.

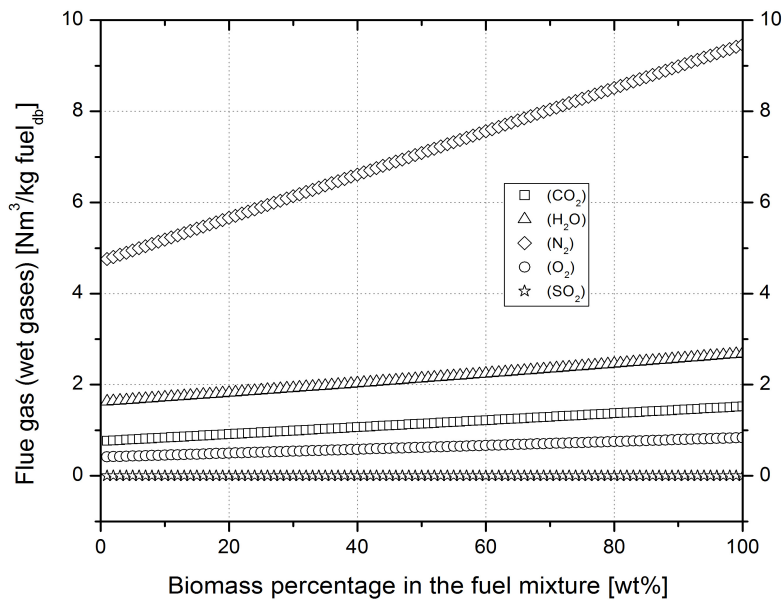


Figure 3.3 - Flue gas composition (wet gases) [ $\text{Nm}^3 \cdot \text{kg}^{-1} \text{fuel}_{\text{db}}$ ] vs. biomass fraction in the final fuel [wt%] (The moisture content was fixed in 40 wt% for the biomass and 35 wt% for the sludge).

It is observed that the amount of  $\text{H}_2\text{O}$  in the flue gas increases with increasing the percentage of residual biomass in the fuel mixture, and this can be explained in result of the higher biomass moisture content when compared to the sewage sludge moisture content. According to this theoretical analysis, in terms of flue gas composition a drying stage for the sewage sludge only has a consequent a decrease on the amount of  $\text{H}_2\text{O}$  present in gas phase.

Once the ash content in the sewage sludge is high, an exploratory analysis in order to realize about the amount of solids production involved as a consequence of sludge usage as secondary fuel was performed. The results are shown in Figure 3.4.

It is observed that the inclusion of sewage sludge in the fuel mixture produces a considerably increase in the amount of solids production, and this is explained in result of the high amount of inorganic (ash) content of the sewage sludge as shown in Table 3.1. As referred in section 2.1.4.1 this fact can be an issue that can overcharge some subsystems of the energy production facility, as the electrostatic precipitator for particulate matter emission control.

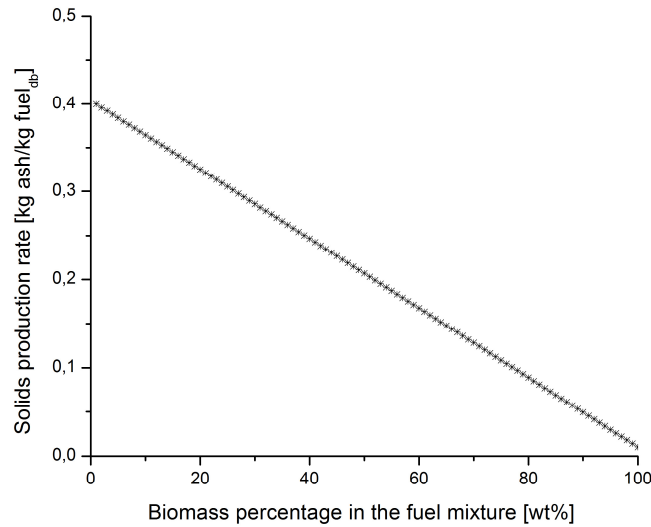


Figure 3.4 - Solids production rate (bottom and fly ash) [kg ash/kg fuel<sub>ab</sub>]<sup>-1</sup> vs. biomass percentage [wt%] in the fuel mixture. The moisture content was fixed in 40 wt% for the biomass and 75 wt% for the sludge.

All these results support the conclusion that when including sewage sludge in the fuel mixture the energy losses in the facility can be considerable. Including sludge with high moisture content shows that a considerable amount of latent heat will be available in the gaseous effluent stream. Moreover it is also important to take into account the energy content in the solid products of combustion discharged (the ashes). Because of that in the next sections it is presented some results concerning the amount of heat that can be recovered from the gaseous effluent stream in the form of sensible heat and in the form of latent heat if water steam condensation is implemented as an additional energy recovery option.

### 3.4.3 Analysis of a 50MW<sub>th</sub> facility

Based on the results of previous sections, the biomass feed rate required for a thermal power plant with 50MW<sub>th</sub> was estimated. The main objective is to know the amount of raw fuel (residual forest biomass + sewage sludge) needed to operate the facility considering distinct sludge moisture contents and distinct percentages of sewage sludge in the fuel mixture. In Figure 3.5 are shown results about the amount of raw fuel need to feed the thermal power plant. It is important to note that for all the simulations the biomass moisture content was considered as 40 wt%. The results about the fuel mixture feed rate are presented in “as received basis” (arb) to have a more accurately idea of the amounts involved.



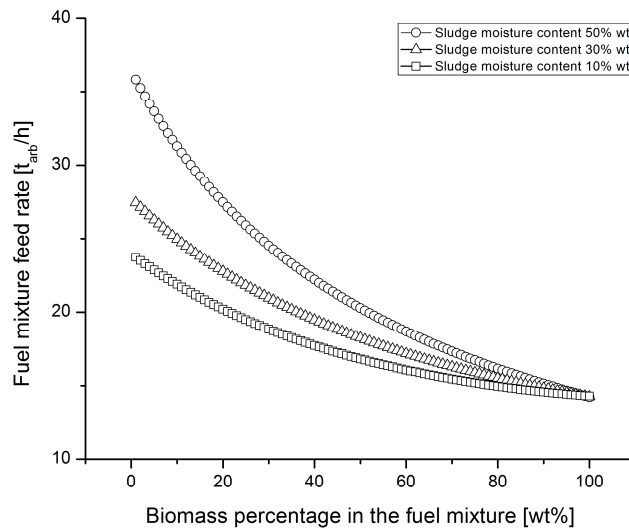


Figure 3.5 - Fuel mixture feed rate [ $t_{arb}/h$ ] vs. biomass percentage [wt%] in the fuel mixture for different sludge moisture contents (10, 30, 50 wt%). The biomass moisture content was considered as 40 wt%.

It is important to state that the situations of high moisture content (75 wt%) of sludge with low biomass share in the fuel mixture were not found of practical interest (section 3.4.1). As expected it can be noticed that the amount of fuel needed by the thermal power plant is higher when the moisture content of the sewage sludge is higher and when the percentage of residual forest biomass in the final fuel decreases. This result is explained by the high content of moisture and inorganic matter in the sewage sludge. According to the results, to produce  $50MW_{th}$ , using a fuel composed by 100% residual forest biomass the amount of fuel needed is close to  $14 t_{arb}/h$ , and when using a mixture of 50 wt% sludge (with 50 wt% moisture) and 50 wt% biomass (with 40 wt% moisture) the amount of fuel increases to around  $18 t_{arb}/h$ .

This supports the conclusion that a previous drying stage for sludge is necessary. A drying stage can considerably reduce the volume of the fuel needed improving the handling operations. However it will be important to conjugate the amount of energy needed for sludge drying with the available waste heat sources in the thermal plant. The capacity of the fuel feeders to handle a specific amount of fuel can also be a constraint.

#### 3.4.3.1 Waste heat assess

According to the previous data collected, two types of heat losses will be assessed here. The heat losses associated to the flue gas as latent heat due to water steam condensation and as sensible heat.

### 3.4.3.1.1 Energy content in the flue gas

Knowing the flue gas composition calculated in previous section 3.4.2, it was estimated the amount of heat losses related to this stream in the form of sensible heat and latent heat.

Some considerations were taken. An absolute pressure of 110 kPa and a temperature of 150°C were considered for the flue gas after economizer, in addition an ambient temperature of 25°C was considered. The heat of vaporization used for the latent heat calculation was 2123 kJ·kg<sup>-1</sup> (Incropera, DeWitt, Bergman, & Lavine, 2007). The biomass moisture content was assumed as 40 wt% and shifting on the sewage sludge moisture content between 50-10 wt% was considered. The estimated waste heat in the flue gas is shown in Figure 3.6.

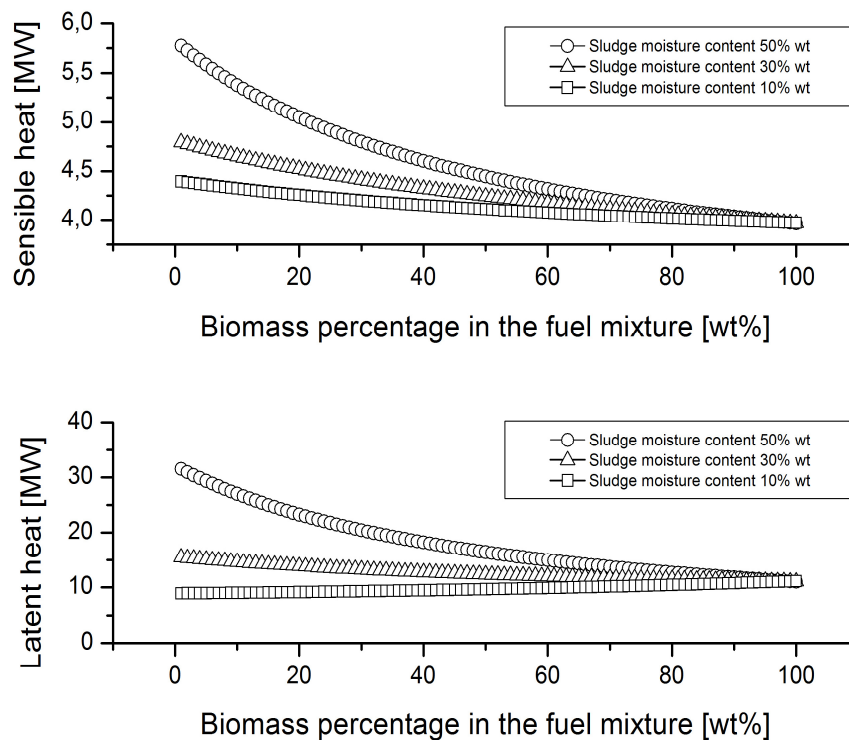


Figure 3.6 - Sensible and latent heat in the flue gas [MW] vs. biomass percentage [wt%] in the fuel mixture. Flue gas temperature considered equal to 150°C.

The heat losses related to sensible heat decrease with the sludge moisture content and with the increase in the mass percentage of residual forest biomass in the fuel (Figure 3.6). These heat losses are related to the mass rate of gaseous effluent leaving the combustion system; this in turn is related to the facility fuel consumption. As shown in Figure 3.5 high fuel consumption rates are related to high moisture content of the fuel mixture. When the moisture content of the fuel is high as it happens for high sewage sludge moisture content and high share of sewage sludge in the fuel

mixture; the loss of sensible heat increases more in result of a sudden increase in the fuel consumption of the facility.

Regarding to latent heat losses, they are related with fuel moisture content. The higher the moisture content in the fuel mixture the higher the amount of latent heat lost at the stack. The addition of sewage sludge with moisture content higher than 30 wt% to the fuel mixture causes considerable increase in the latent heat content of the flue gas when compared with the situation of residual forest biomass combustion. Effectively the emission of flue gas per unit of fuel in the case of sludge is lesser than the biomass; in counterpart the amount of fuel needed to produce the same amount of energy is higher in the case of sludge; this increased fuel consumption causes a sudden increase in the mass rate of flue gas. This explains that for the cases of sludge moisture content 30 wt% and 10 wt%, although the moisture content of the biomass is higher (40 wt%) almost the same amount of the latent heat is lost.

Summarizing, as mentioned above the inclusion of high mass percentage of sewage sludge in the fuel mixture, implies significant increase on the amount of fuel consumed by the facility in order to deliver the desired thermal output. Following this increase in the fuel consumption an increasing amount of flue gas is expected; the heat losses are closely linked to this gaseous stream. The magnitude of losses due to latent heat in all cases analyzed is in the order of megawatts.

#### 3.4.3.1.2 Heat requirements for the drying process

Based on the equations presented in section 3.3.1 in conjunction with data obtained, a first approach to estimate the thermal power involved in a hypothetical drying system to the sewage sludge was performed.

It was evaluated the thermal power needed to dry the corresponding part of sludge under different co-combustion cases. Therefore, the corresponding sludge mass rate was estimated taking into account the generation of 50 MW<sub>th</sub> of useful thermal power in the facility using the residual forest biomass + sludge mixture studied before.

The results are shown in Figure 3.7; the graphic was constructed in a way that the Y axis shows the thermal power needed to shift the moisture content from 75 wt% to another condition of the correspondent part of sludge of a total amount of fuel needed to produce 50MW<sub>th</sub>. Additionally each curve of the graph represents different co-combustion cases.

As expected, it can be noticed an increasing demand of heat to dry the sludge with increasing the sludge percentage in the fuel mixture and also with decreasing the sludge moisture content.

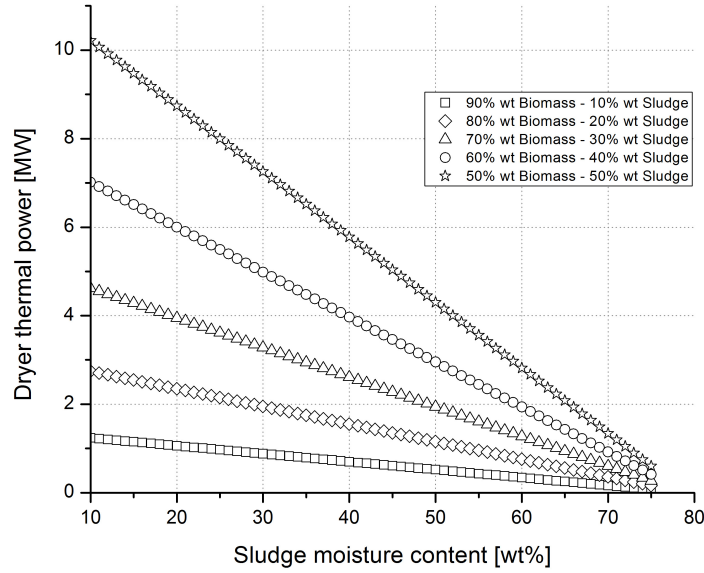


Figure 3.7 - Sludge dryer thermal power [MW] vs. sludge moisture content [wt%] for different co-combustion cases, that is, distinct percentages of residual forest biomass and sewage sludge in the fuel mixture.

It is important to mention that this is a rough analysis of the problem, based only in general thermodynamic considerations. However, it can be considered for orientation purposes about the energy fluxes involved. This information is important because it can be compared with the heat availability calculated for the gaseous effluent at the stack (section 3.4.3.1.1).

As mentioned in section 2.2.2.1 the drying process is a very complex process that involves simultaneous heat and mass transfer phenomenon. More detailed considerations about the sewage sludge behavior during drying will be analyzed in Chapter 4.

## **4 Drying experiments**

The sludge drying is a complex process that involves diffusion within the sludge and heat transfer from the drying fluid to it; moreover there are other physical features that strongly influence these processes. The behavior of this particularly type of sewage sludge is unknown regarding to the described features in section 2.2.2 (crust phenomena, shrinkage, cracking). In addition the time needed to shift the moisture content from one point to another is also unknown. In this section it is intended to establish the sewage sludge behavior when submitted to a controlled hot air stream. The objective is to develop a model that having into account all the involved phenomena be able to forecast the sludge final moisture content after a period of time, under several drying conditions. The ANN was chosen as development methodology. As exposed in section 2.2.2.2 the artificial neural networks approach presents several advantages when compared to the physical models created based on thermodynamic considerations.

The development of a project based on artificial neural networks involves several stages, namely: problem definition; database acquisition, data preprocessing, network architecture definition; training, testing and validation (Karrer, D Cameira, R. Vasques, A. e Benzecry, 2005).

### **4.1 Problem definition**

The main objective is to develop a model that having into account all the phenomena's that a drying process involves be able to forecast the final moisture content of the sewage sludge after a certain time interval, in a process where the initial conditions (air temperature, air moisture content and air velocity) are known.

### **4.2 Database acquisition**

One of the principal deficiencies with current neural network research is associated with the design of the neural networks. The design of a neural network involves the selection of an optimal set of design parameters to achieve fast convergence speed during training and the required accuracy during recall (Khaw, Lim, & Lim, 1995). The state-of-the art revision shows that there is no parameter or formula that can be followed in order to define the number of experimental tests that must be run in order to train the network that guarantees a good error percentage in the forecasted values. All the academic publications shows a quite non uniformity in the size of the databases used for training achieving extra-large databases in most of the cases. The approach chosen to address this issue relies in an experimental design methodology, the Taguchi method.

#### **4.2.1 The Taguchi method**

This method developed by Genichi Taguchi, has been widely used for product and process design in many manufacturing companies. The Taguchi method provides a mathematical tool called the orthogonal array which allows the analysis of the

relationships between a large number of design parameters within the smallest number of possible experiments. A key concept of the Taguchi method for quality is to quantify the losses which occur because of poor quality, using loss functions (Roy, 1990).

According to the Taguchi method in order to achieve a strong and reliable product is necessary to recognize the factors that have direct influence on the quality and then assign them criteriously selected levels. Taguchi classifies the quality factors between control factors and noise factors. Control factors are those able to be supervised and modified. For this work the control factors considered were the air temperature, the air moisture content and the air velocity. Noise factors are those that cannot be controlled for instance the environment conditions, pollutants, etc.

As exposed in section 2.3 the validation of low grade waste heat sources is a major concern; because of that the levels of each factor were chosen having into account a drying process at low temperatures and considering the operational limits of the drying tunnel. Additionally according to (Deng et al., 2009), high drying temperatures will lead to release VOCs, VFAs and CH<sub>4</sub>. The Table 4.1 shows the control factors considered in conjunction with their levels.

Table 4.1– Control factors and their correspondent levels established for the drying model construction.

Levels	Temperature [°C]	Absolute Moisture [g H <sub>2</sub> O·kg <sub>air</sub> <sup>-1</sup> ]	Velocity [m·s <sup>-1</sup> ]
1	60	15	2,5
2	45	12	2
3	35	9	1,5

Applying the factorial method the number of experiments to perform will be twenty seven (3<sup>3</sup>) due to the number of possible combinations. According to the Taguchi method this number can be improved to nine experiments using the fractional factorial method by an orthogonal matrix. Taguchi proposes several normalized orthogonal matrixes; essentially at the end of the experiments each factor must use each level the same number of times. The Table 4.2 shows the orthogonal matrix used, adapted with the levels and factors chosen for the drying model development. Nine different types of experiments were established, that constitute the database that will be used to train the network.

Furthermore three additional experiments were established in order to validate the drying model. The levels of each factor for the validation experiments 1 and 2 were chosen randomly inside the limits shown in Table 4.2. The temperature value for the validation test 3 was chosen out of the limits of the Table 4.2 in order to assess the extrapolation capability of the ANN model. The summary of the levels chosen for the validation tests are presented in Table 4.3.

Table 4.2 – Orthogonal matrix design representing the experimental conditions for each experiment.

	Temperature [°C]	Absolute Moisture [g H <sub>2</sub> O·kg <sub>air</sub> <sup>-1</sup> ]	Relative humidity [%]	Velocity [m·s <sup>-1</sup> ]
Taguchi 1	45	15	25	2,5
Taguchi 2	45	12	20	2
Taguchi 3	45	9	15	1,5
Taguchi 4	60	15	12	2
Taguchi 5	60	12	10	1,5
Taguchi 6	60	9	7	2,5
Taguchi 7	35	15	42	1,5
Taguchi 8	35	12	34	2,5
Taguchi 9	35	9	26	2

Table 4.3 – Experimental design for the drying model validation experiments.

	Temperature [°C]	Absolute moisture [g H <sub>2</sub> O·kg <sub>air</sub> <sup>-1</sup> ]	Relative humidity [%]	Velocity [m·s <sup>-1</sup> ]
1	50	9	12	2,5
2	40	12	26	1,5
3	30	15	56	2

#### 4.2.2 Convective drying experimental station

In general terms the operation mode of the drying station is as follows: the air is forced inside the drying chamber by a fan with controlled speed. Then it is heated by electric resistances to achieve the desired temperature. A spray system is used for humidification and a dehumidifier is used to chill and dehumidify the air when it is needed. Several sensors were installed in order to monitor the control factors defined in Table 4.1.

As can be observed in Figure 4.1, the air circulates in a closed loop. The mass loss of the sewage sludge sample during the experiments was registered by a load cell. The sewage sludge sample was placed in a special base that minimizes the horizontal aerodynamic drag caused by the air stream.



Figure 4.1 - View of the drying station used to perform the drying experiments. Source: (Pinho, 2012).

#### 4.2.2.1 Ventilation system

Ventilation was performed by a centrifugal fan, driven by an AC motor which controls the speed of the drying air. The fan reaches a maximum flow rate of  $0,27 \text{ m}^3\cdot\text{s}^{-1}$ , equivalent to a velocity of  $3 \text{ m}\cdot\text{s}^{-1}$ . The air speed was measured by an air speed transducer manufactured by Omega, model FMA 1000, inserted into the drying tunnel next to the drying chamber.

#### 4.2.2.2 Heating system

The heating process is divided into two stages. The first stage or pre-heating stage which uses two electric resistances (1 kW each) positioned after the fan. The second stage or super heating stage which uses two additional electric resistances (0,5 kW each) located after the cooling system. The maximum temperature that the air reaches is  $60^\circ\text{C}$ . The temperature was measured by a thermo hygrometer, manufactured by the brand Vaisala, model HMT 100 introduced into the drying tunnel next to the drying chamber.

#### 4.2.2.3 Humidification system

The humidification was performed by a pneumatic nozzle which introduces a water spray into the tunnel between the preheating zone and the cooling /dehumidification zone by Venturi effect. The pneumatic system was set up at 4 bars and a water reservoir was used for storing purposes. The relative humidity of the air was measured by the same device that measures the air temperature.

#### 4.2.2.4 Cooling/dehumidification system

The air dehumidification is intended for cool the air to reach saturation and condense the water vapor contained therein, thereby reducing the absolute humidity of the drying air when needed. The cooling was performed by an evaporator enclosed in a refrigeration system comprising: a compressor, a condenser, an expansion valve and



an evaporator (the working fluid was R134a). The evaporator was positioned into the tunnel between the humidification zone and super heating zone. A schematic of the facility is shown in Figure 4.2.

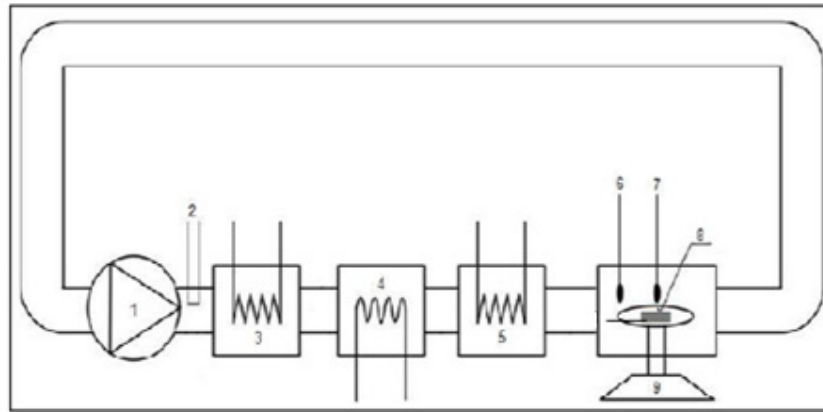


Figure 4.2 - Schematic of the drying station used to perform the drying experiments. Source: adapted from (Boeri, 2012).

1. Centrifugal fan;
2. Humidifier;
3. Electric resistances (2 kW);
4. Dehumidifier / chiller;
5. Electric resistances (1 kW);
6. Speed transducer;
7. Thermo hygrometer;
8. Sludge sample;
9. Load cell.

#### 4.2.2.5 Hardware and software platforms

The drying process was controlled by a MATLAB/SIMULINK® platform in conjunction with a PCI-6025E data acquisition board of National Instruments. Four analog inputs of 12 bits were used for monitor the real temperature, relative humidity, air speed inside the drying chamber and the weight loss of the sewage sludge sample. Two analog outputs of 12 bits were used to control the chiller and the centrifugal fan; furthermore three input/output digital gates were used to control the electric resistances and the pneumatic nozzle. The computer used was a Pentium dual core of 2,25 GHz and 2GB of RAM. A schematic of the hardware instrumentation is presented in Figure 4.3.

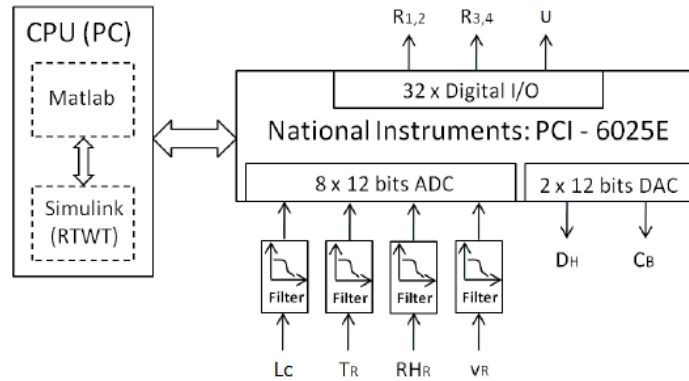


Figure 4.3 - Schematic of the instrumentation at drying tunnel. Source: adapted from (Boeri, 2012).

where:

- $C_B$  Centrifugal fan;
- $D_H$  Dehumidifier;
- $R_{1,2}$  Electric resistances 1 and 2 of 1 kW each one;
- $R_{3,4}$  Electric resistances 3 and 4 of 0,5 kW each one;
- $RH_R$  Real relative humidity;
- $L_c$  Load cell;
- $T_R$  Real temperature;
- $U$  Humidifier;
- $V_R$  Real speed.

The software allows programming various stages of drying. Each stage is defined by its duration, time interval for data acquisition in conjunction with the desired levels of temperature, humidity and velocity of the drying air. The signals received by the computer control board are stored in a MATLAB file.

#### 4.2.2.6 Auxiliary equipments

The auxiliary equipments used during the experiments, and that are not part of the drying tunnel will be described in the following sections.

##### 4.2.2.6.1 Oven

An industrial oven was used to determine the initial and final moisture content of the sludge. The oven brand is P Selecta with automatic control of the internal temperature.

##### 4.2.2.6.2 Metallic containers

The metal containers are metal plates with cap, which were used to handle and transport the sewage sludge samples.

#### 4.2.2.6.3 Aluminium container

An Aluminum box was used to place the sewage sludge samples into the tunnel during the drying experiments. The dimensions of the box were: length 75 mm; width 95 mm and height 70 mm. The mass of the container was 95,99 g.

#### 4.2.2.6.4 Desiccator

The desiccator is a device that inhibits moisture gains of the sludge sample when placed inside. It was used to cool the metal containers when they leave the oven, in an environment of low humidity. At the bottom there is a drying agent, typically silica gel, along with a humidity indicator which contains cobalt salts. That salts bluish pink when they become saturated with moisture.

#### 4.2.2.6.5 Mass scale

A digital scale was used to measure the mass of the sludge samples before and after its passage through the oven, and before and after every drying experiment in the tunnel. The scale brand is Kern 434-33 and supports a load of 510 g with an accuracy of 0,001 g.

### 4.2.3 *Experimental proceedings*

The sewage sludge samples were collected from a pulp and paper company. They were transported in plastic bags to the laboratory, classified, weighted and stored. The big portion of the collected sludge was intended for the combustion experiments (section 5.1 and 5.2). The samples intended for the drying experiments were stored inside sealed plastic bags in a freezer at 4°C. Each drying experiment comprises the following stages:

Two different samples were prepared at the beginning of each experiment. One sample was used for the initial moisture content determination. The second sample was used to perform the drying experiment at the tunnel. The correspondent weights were registered before and after each process.

The initial moisture content determination was performed in an oven (section 4.2.2.6.1), heating the samples to 105°C for 3 hours in average. The amount of water removed by the drying process at the oven was found by equation 25.

$$m_w = m_o - m_f \quad \text{Eq. 25}$$

The moisture content of a product generally is expressed in function of the mass of the dry matter, because it remains constant along all the drying process unlike the mass of the wet solid, that can change, hence it is not indicated to express the moisture content (Boeri, 2012).

Therefore the initial moisture content in dry basis (weight ratio) was found through equation 26.

$$H_0 = \frac{m_o - m_f}{m_f} \quad \text{Eq. 26}$$

Subsequently duration of 16200 seconds was programmed for each drying experiment. It is pretended to achieve moisture contents of the samples after the tunnel below 50 wt% moisture content as justified in section 3.4.1.

The data acquisition was programmed to record the main drying parameters every 90 seconds. At the end of the experiment, the sewage sludge sample weight was registered. The final moisture content determination was performed in an oven (section 4.2.2.6.1), heating the samples to 105°C for 3 hours approximately. The final moisture content (weight ratio) in dry basis was established by equation 27.

$$H_f = \frac{m_{sf} - m_{@105^\circ\text{C}}}{m_{@105^\circ\text{C}}} \quad \text{Eq. 27}$$

where:  $m_{sf}$  represents the mass of the sludge sample after the drying experiments in the tunnel and  $m_{@105^\circ\text{C}}$  represents the mass of the sludge sample after drying in the oven at 105 °C.

#### 4.2.3.1 Sewage sludge behavior during drying experiments

During the drying experiments a set of observations was performed. The objective was to define if the characteristics described by the bibliography (section 2.2.2.1) for municipal sewage sludge are similar to those generated at the pulp and paper factories.

Essentially, the behavior of the sewage sludge sample during drying (Taguchi 4; Taguchi 5 and Taguchi 6) can be described as follows:

- During the first hour a slight change in the color of the sample at its surface was observed. This suggests that the water at the surface of the sample was evaporated. The shrinkage phenomenon (only visually registered) at this stage is not pronounced.
- During the following thirty minutes the first cracks began to appear at the surface of the sewage sludge sample, especially in the center.
- At the end of the second hour it can be noticed a separation between the sewage sludge sample and the walls of the Aluminum case.
- During the first thirty minutes of the third hour the cracks began to be deeper and the shrinkage phenomena increases considerably.

- At the end of the third hour the shrinkage phenomena continues and the sample started to curve upward (Figure 4.4).

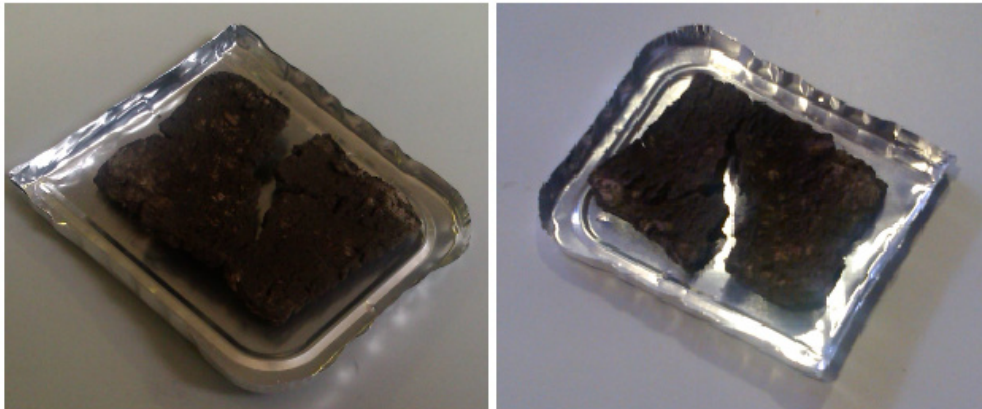


Figure 4.4 - Crack formation and curve upward of the sludge sample (4 hours at 60°C)

- During the first minutes of the fourth hour the sample seems brittle and small fragments were detached from the main cake.
- During the last twenty minutes no major changes was noticed. At the end of the drying experiment it can be observed that the core of the cake remains minimally wet while the external surface looks dry.

After the drying experiment the sewage sludge sample appears rigid and brittle in contrast with the initial, plastic paste appearance. Moreover important changes in the texture of the material were verified. The sewage sludge sample looks compact but easy to fragment. Furthermore the sewage sludge sample was completely detached of the walls of the Aluminum case and a considerable volume reduction was noticed (Figure 4.5).



Figure 4.5 - Shrinkage phenomena and volume reduction of the sludge sample after a drying experiment (4,5 hours at 60°C).

It is important to note that at the beginning the sewage sludge samples present a strong and concentrated smell. After the drying experiments a considerable reduction of the odors was noticed.

In fact all the phenomena reported by literature were verified in the sludge samples studied (shrinkage, crust phenomenon, cracks). The state-of-the-art revision suggests that the crust phenomenon strongly influences the drying time. Regarding this last, two types of sewage sludge can be differentiated, one with a strong crust phenomena which the time needed for experiments are considerably longer; 11 hours approximately (R. Font, M.F. Gomez-Rico, 2011) and the second type where the crust phenomena is present but is not a constraint for the moisture removal. The time needed for the drying experiments for the sewage sludge samples studied was in the range of the ones observed for sewage sludge samples with weak crust phenomena.

#### 4.3 Experimental results: data preprocessing

The training of a neural network requires the definition of a set of inputs that offers information about the process that is intended to simulate and also a set of targets. Five parameters were established as inputs, namely: the initial moisture content (weight ratio), the time, the air velocity, the air temperature and the air humidity. The instantaneous moisture content of the sludge sample was chosen as target. The sample weight recorded by the load cell was used to found the instantaneous moisture content of the sludge sample during the drying process. Equation 28 was used for the referred calculation.

$$H_i = \frac{H_f - H_o}{m_{sf} - m_{so}} \times (m_i - m_{so}) + H_o \quad \text{Eq. 28}$$

where:  $m_i$  is the instantaneous mass of the sludge sample measured by the load cell;  $m_{so}$  is the mass of the sewage sludge sample before the drying experiment at the tunnel;  $m_{sf}$  is the mass of the sewage sludge sample after the experiment at the tunnel;  $H_o$  is the initial moisture content (weight ratio) and  $H_f$  is the final moisture content (weight ratio).

For database construction all the parameters used as inputs with exception of the initial moisture content and the final moisture content were normalized between zero and one in order enhance the training stage. This action avoid the attribution of excessive weight to big numbers in the database (Gonçalves, 2012). The drying kinetics represented by graphs of each experiment under the Taguchi methods can be found in Appendix 2.

During the drying experiments a considerable oscillation was verified in the signal coming from the load cell. This oscillation was caused by the air flow inside the tunnel which produces an air drag in the sewage sludge sample support device. This air drag induces some noise in the recorded signal. Furthermore the weight of the sewage sludge sample also has a big influence on this issue. When the mass of the

sample was bigger, the noise signal was lesser. The mass of the Aluminum container was increased and the signal was stabilized through the use of low-pass filters. Nevertheless small deviations in the weigh lost signal can be observed. A result resume of the drying experiments in the tunnel in conjunction with the results of the validation experiments are presented in Table 4.4.

Table 4.4 – Initial and final moisture content of the sewage sludge samples after the experiments at the tunnel. Moisture content expressed as weigh ratio, dry basis [ $\text{kgH}_2\text{O} \cdot \text{kg}_{\text{sludge db}}^{-1}$ ].

	<b>Initial moisture content</b>	<b>Final moisture content</b>
	[ $\text{kgH}_2\text{O} \cdot \text{kg}_{\text{sludge db}}^{-1}$ ]	[ $\text{kgH}_2\text{O} \cdot \text{kg}_{\text{sludge db}}^{-1}$ ]
Taguchi 1	0,79	0,24
Taguchi 2	0,80	0,23
Taguchi 3	0,83	0,47
Taguchi 4	0,70	0,14
Taguchi 5	0,70	0,14
Taguchi 6	0,81	0,06
Taguchi 7	0,94	0,82
Taguchi 8	0,95	0,84
Taguchi 9	0,95	0,67
Validation 1	0,98	0,14
Validation 2	0,93	0,65
Validation 3	0,97	0,83

As mentioned in section 4.2.3 moisture content was calculated as weight ratio (dry basis). Nevertheless in industry, moisture content is commonly expressed in wet basis. Having into account that the theoretical analysis performed in section 3.4.1 considers the moisture content in wet basis, a resume of the final moisture contents achieved after the drying experiments expressed in the referred basis is presented in Table 4.5.

It can be observed that for the Taguchi experiments 1 to 6 the final moisture content achieved is suitable for combustion with energy recovery as demonstrated in section 3.4.1. For the Taguchi experiments 7 and 8 the moisture contents achieved are close to the limit where endothermic reactions were verified. An exception can be noticed for the Taguchi experiment 9 where, relatively low moisture content was achieved when compared with the same set of experiments which can be explained by the low moisture content in the drying air considered.

Table 4.5– Final moisture content of the sewage sludge samples after the experiments at the tunnel. Moisture content expressed in wet basis [wt%].

	<b>Final moisture content [wt%]</b>
Taguchi 1	15
Taguchi 2	19
Taguchi 3	31
Taguchi 4	13
Taguchi 5	12
Taguchi 6	6
Taguchi 7	45
Taguchi 8	45
Taguchi 9	33
Validation 1	12
Validation 2	38
Validation 3	43

#### 4.4 Network architecture definition

As mentioned in section 2.2.2.2.1 the creation of an ANN model requires the definition of a specific architecture. (Gonçalves, 2012) establishes that most of the problems addressing forecasting the final values of a process can be successfully modeled with just one hidden layer. A feedforward model with one hidden layer was chosen. The Pearson coefficient was used to assess the correlation between the ANN model and the validation experiments. It was observed that adding hidden layers the performance of the ANN decreases.

After the established of the number of hidden layers, the number of neurons was defined by a trial and error method. It was found that from a certain point, increasing the number of neurons the performance of the neural network decreases. At the end of this process four neurons were considered for the hidden layer.

According to (Gonçalves, 2012) the most suitable transfer functions addressing forecast problems are the hyperbolic tangent sigmoid transfer function and the log-sigmoid transfer function. Nonetheless several transfer functions were tested according to Table 2.2. At the end it was found that the hyperbolic tangent sigmoid transfer function produces the best results.

The referred document suggests two types of training algorithms to treat with forecasting issues namely Levenberg-Marquardt and Bayesian Regularization. Nonetheless several training algorithms were tested according to Table 2.3. At the end it was found that the Bayesian Regularization algorithm produces the best results. The training phase was performed by back-propagation comparing the input and output arrays until the error achieves a minimum value. An over-fitting issue was reported by

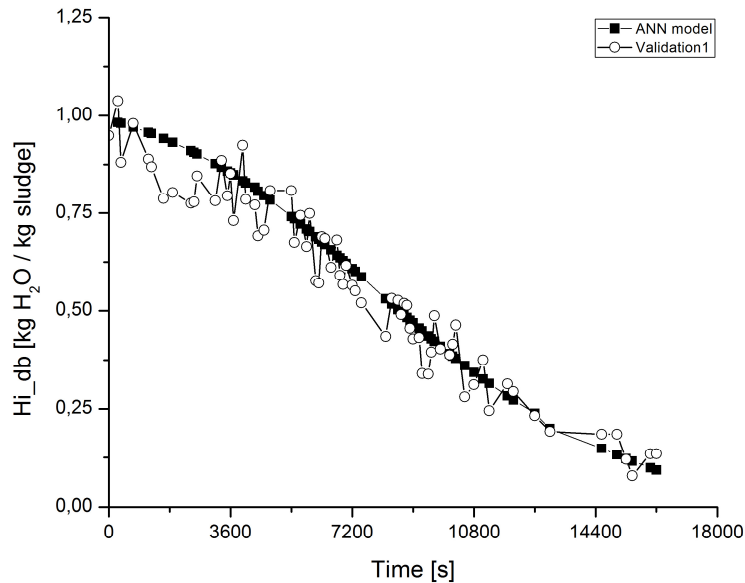


several researchers that can be verified when the error asked to achieve is too small. The mean square error was the network performance function chosen, which measures the network's performance according to the mean of squared errors. The maximum permissible error for the training phase was set up in  $10^{-5}$  and the maximum number of iterations to obtain convergence was set up in 300 epochs.

#### 4.5 Testing and validation

A validation stage was performed in order to test the generalization capabilities of the model. According to Table 4.3 three validation experiments were established. The validation experiment 1 and 2 were configured inside the limits of the database used to train the ANN. The validation experiment 3 was configured out of the database used to train the ANN, in order to assess the extrapolation ability of the network to forecast values out of the training database. A graphical representation of the results is presented in Figure 4.6.

As mentioned in section 4.3, the mass loss signal sensed by the load cell presented some oscillations. It was observed that fluctuations in the air flow produced by the variation of speed of the air blower causes vibrations on the sample support which introduces noise in the signal. It was found that this noise issue is lesser as the mass of the sample is higher.



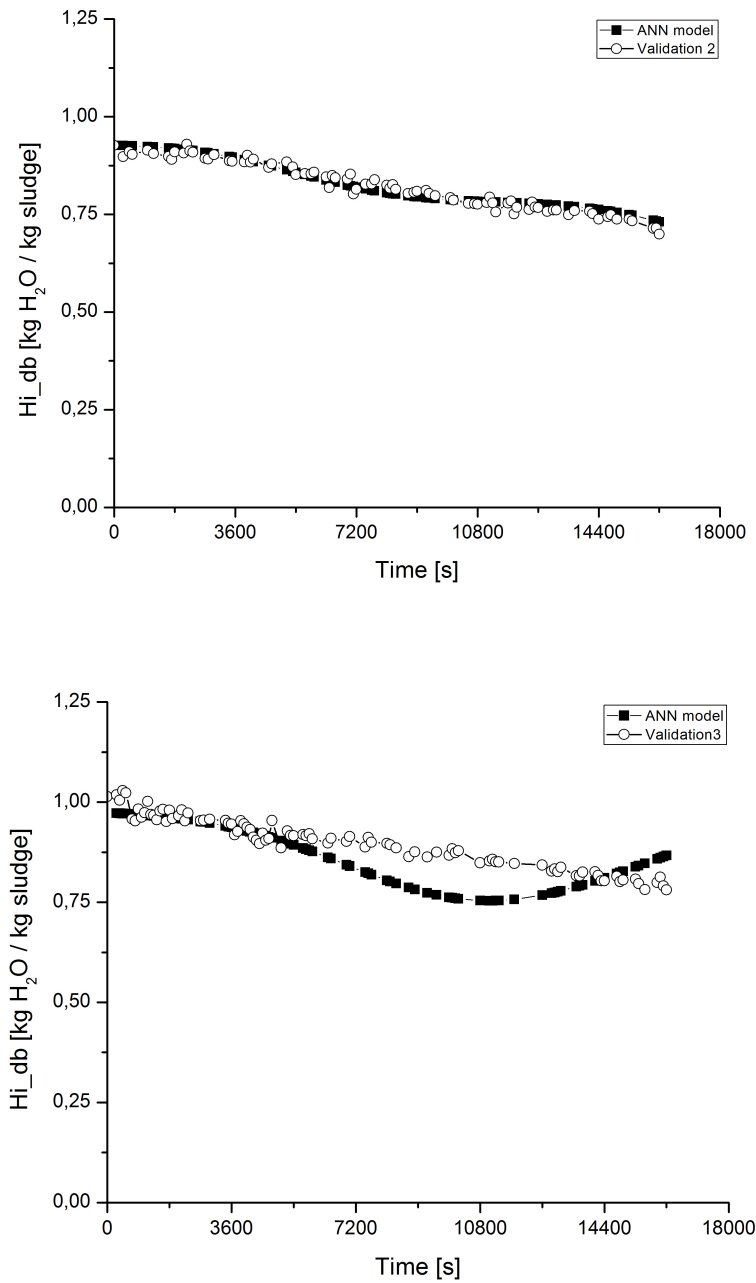


Figure 4.6 - Representation of the validation experiments in conjunction with the forecast curve given by the ANN model.

For the first case (validation1) where the initial mass is less than the other experiments and a considerable mass loss were verified, the noise introduced to the signal was higher. The Pearson correlation coefficient between the ANN model and the validation experiments are presented in Table 4.6.

Table 4.6 – Pearson correlation coefficient obtained for the validation experiments.

	<b>Pearson correlation coefficient</b>
Validation experiment 1	0,972
Validation experiment 2	0,963
Validation experiment 3	0,798

In fact the correlation between the ANN model and the validation experiments for the experiments considered inside the limits of the training database is high. For the validation experiment 3 which the temperature value is out of the training database a lesser correlation can be observed. The curve generated by the model does not follow the real behavior of the sludge sample. However the final moisture content calculated by the model is close to the final moisture content value determined by experimentation. The Table 4.6 shows the difference between the final moisture content calculated by the model and the final moisture content calculated by experimentation.

Table 4.7 – Final moisture content of the sludge sample calculated by the ANN model and final moisture content of the sludge sample obtained by experimentation

	<b>Real</b>	<b>ANN model</b>
	<b>[kgH<sub>2</sub>O·kg<sub>sludge db</sub><sup>-1</sup>]</b>	<b>[kgH<sub>2</sub>O·kg<sub>sludge db</sub><sup>-1</sup>]</b>
Validation experiment 1	0,14	0,09
Validation experiment 2	0,65	0,73
Validation experiment 3	0,83	0,86

As mentioned in section 2.3 the energy supply of the drying process should be done using waste heat sources. It was mentioned in section 2.3.3 that roughly 60% of the waste heat streams available to recover are in the category of low quality. Additionally as mentioned the use of low drying temperatures can prevent the release of dangerous gases during drying and also prevent product degradation.

There might be a wide variety of waste heat sources available to drive the drying process; accordingly the range of temperatures at which the drying process can be carried out may be diverse. It is expected that this drying kinetic model can give reliable information about the final moisture content that can be achieved considering several temperatures and drying parameters. As complement, chapter 2 offers information about the consequences of operate a combustion system under several feeding fuel moisture contents. Conjugating this information a reliable forecast of the performance of the system can be done.

## 5 Combustion experiments

In order to study the sewage sludge as fuel in a pilot scale fluidized bed combustor a set of experiments were designed. Two types of sample fuels were prepared, one was 100 wt% sludge (fuel sample 1) and the other was 50 wt% sewage sludge plus 50 wt% residual forest biomass (fuel sample 2) to perform the study in terms of reactor temperatures profile and flue gas composition.

The sewage sludge samples were collected in a pulp and paper industry and transported to the laboratory. Following the procedures established in section 4.2.3 in conjunction with equation 26, the initial moisture content of the sludge was established in  $0,70 [\text{kg H}_2\text{O} \cdot \text{kg}_{\text{sludge}}^{-1}]$ .

### 5.1 Fuel sample 1

A sample fuel (here designated by fuel sample 1) composed by 100 wt% sewage sludge was prepared. The sludge was manually shredded and extended on plastic sheets which were exposed to atmospheric conditions in order to reduce its moisture content. After several days even though weather conditions were quite unstable, with fairly frequent rainy periods a reduction in the moisture content of the fuel samples was observed.

An important shrinkage phenomenon were verified which leads to a considerable volume reduction. Furthermore the dried sludge changes its initial plastic phase appearance by a strong and consolidated solid material that looks like small stones. Some of those small stones agglomerate to others forming larger pieces; for that reason a manual crush was need. The particle size distribution of fuel sample 1 after atmospheric conditions drying is shown in Table 5.1.

Table 5.1 - Granulometric distribution of the fuel sample 1.

Particle diameter [mm]	Mass retained on the sieve [ kg ·kg fuel <sup>-1</sup> ]
dp > 4	0,104
2 > dp < 4	0,098
1 > dp < 2	0,044
0,5 > dp < 1	0,021
dp < 0,5	0,012

It is also important to note that at the beginning the sludge samples presented a strong smell that was gradually disappearing as the moisture content decreases. At the end a slightly smell still persisted. The macroscopic characteristics of fuel sample 1 after atmospheric conditions drying are shown in Figure 5.1.



Figure 5.1 - Macroscopic characteristics of fuel sample 1.

The main features of the sludge used for the preparation of the fuel sample can be characterized in terms of elemental composition according to Table 3.1. However a detailed study to find the final moisture content and the ash content of the fuel samples prepared was performed which can be found in section 5.3.

## 5.2 Fuel sample 2

The second sample (fuel sample 2) was designed in order to operate the reactor with a mixture of 50 wt% sewage sludge (70 wt% moisture) plus 50 wt% residual forest biomass (13 wt% moisture). These fine particles show some undesirable operating problems during combustion in the pilot scale fluidized bed reactor, so it was considered the evaluation of its mixture with sewage sludge in order to produce a better quality fuel.

The procedure used to mix the sludge with the fine particles from residual forest biomass shredding was as follows. Firstly the sludge was manually extruded using a sieve producing small pellets of 4 to 5 mm diameter and 7 to 8 mm length approximately. While the sludge was extruded, the eucalyptus sawdust was manually added. A 100 liters plastic bucket with cylindrical shape was used to mix the material. Then the sludge pellets and the eucalyptus sawdust were manually agitated to enhance their mixture, especially to facilitate the incorporation of the biomass fine particles into the sludge. Subsequently the plastic bucket was agitated manually, following cylindrical movements resembling a concrete mixing drum. The fuel mixture start to form spherical particles which diameter strongly depends on the bucket rotational speed. At the end the fuel sample was manually extended on plastic sheets which were exposed to atmospheric conditions in order to reduce its moisture content. After several days even though weather conditions were quite unstable, with fairly frequent short raining periods a reduction in the moisture content of the fuel samples was observed.

Unlike fuel sample 1 the volume of particles from fuel sample 2 after drying at atmospheric conditions presents a smaller volume reduction. The resultant fuel appears as a consolidated material however easily deformable under hand pressure. It is important to note that the incorporation of the sawdust was extremely effective. In fact the sawdust appears as fibers embedded in the core of each fuel particle. The macroscopic characteristics of fuel sample 2 after atmospheric conditions' drying is shown in Figure 5.2.



Figure 5.2 - Macroscopic characteristics of fuel sample 2.

Regarding the main features of the sludge and residual forest biomass used (eucalyptus sawdust), their elemental composition was considered that of Table 3.1. The moisture content and organic matter content determination is presented in section 5.3.

### **5.3 Moisture, organic matter and ash content of the fuel samples**

The moisture, organic matter and ash content of the fuel samples prepared were determined, because these features can have an important influence in the combustion efficiency. Representative samples taken from different parts of the fuel bulk were collected for analysis.

The fuel samples were properly mixed and mechanically crushed with a mill to reduce their granulometry. Then three replicas of each fuel sample were prepared.

For moisture content determination the samples were heated in an oven for three hours at 105°C. The moisture content determination was found following the proceedings described in section 4.2.3 and using equation 26.

For the organic matter and ash content determination, after the drying stage an additional gradual heating stage was performed in a muffle furnace equipped with a

ramping program (Sluiter et al., 2008). The furnace temperature ramp program was configured as follows:

- Ramp from room temperature to 105°C;
- Hold at 105°C for 12 minutes;
- Ramp to 250°C at 10°C per minute;
- Hold at 250°C for 30 minutes;
- Ramp to 550°C at 20°C per minute;
- Hold at 550°C for 180 minutes;
- Allow temperature to drop to 105°C;
- Hold at 105°C until samples are removed.

At the end the samples were placed in a desiccator until cool down, and then were weighted. The organic matter content (OM) in percentage was calculated using equation 29.

$$OM = \frac{mfuel_{oven@105^{\circ}C} - mfuel_{furnace@550^{\circ}C}}{mfuel_{oven@105^{\circ}C}} \times 100 \quad \text{Eq. 29}$$

where:

$mfuel_{oven@105^{\circ}C}$  represents the mass of the fuel sample after the drying stage in the oven at 105°C,  $mfuel_{furnace@550^{\circ}C}$  represents the fuel sample mass that remains after the end of the muffle furnace ramp program. The ash content was determined by difference to 100% relative to the organic matter content. The final results obtained are shown in Table 5.2.

Table 5.2 – Moisture content of the fuel samples in as received basis and organic matter and ash content of the fuel samples in dry basis

	<b>Moisture content<sub>wb</sub> [wt%]</b>	<b>Organic matter<sub>db</sub> [wt%]</b>	<b>Ash<sub>db</sub> [wt%]</b>
Fuel sample 1	27	50,6	49,4
Fuel sample 2	36	69,6	30,3

\*Ash determined by difference

A considerable difference in the moisture content between the fuel sample 1 and fuel sample 2 can be noticed. As mentioned the drying stage was performed under atmospheric conditions. Therefore there was no control on the sun radiation that each sample receives and the heat and mass transfer can also be affected by the changes in the convective heat transfer coefficient due to the wind. In addition the weather conditions were not the same for each sample and during the drying stage frequently short raining periods were observed.





Figure 5.3 - Schematic representation of the pilot scale installation. Dashed line – Electric circuit, Continuous line – Pneumatic circuit, A – Primary air heating system, B – Sand bed, C – Bed solids level control, D – Bed solids discharge, E – Bed solids discharge silo, F – Propane burner system, G – Port for visualization of bed surface, H – Air flow meter (primary and secondary air), I – Control and command unit (UCC2), J – Biomass feeder, K – Water cooled gas sampling probe, L,M,P,Q – Command and gas distribution units (UCD0, UCD1, UCD2, UCD3), N – Gas sampling pump, O – Gas condensation unit for moisture removal, R,S,T,U,V,W – Automatic on line gas analyzers (HC, NO, CO<sub>2</sub>, N<sub>2</sub>O, O<sub>2</sub>, CO), X – Electronic command unit (UCE1), Y – Computer data acquisition and control system, Z – Exhaust duct to cyclone and bag-house filter. Source: (Tarelho, Neves, & Matos, 2011).

Pressure, temperature and combustion flue gas can be sampled by means of eight water-cooled probes located at several heights along the reactor, two of which are immersed in the dense bed of particles and the rest located along the freeboard. Each sampling probe is equipped with an external circulating quenching water sleeve, an ice-cooled particle filter, a K-type thermocouple and a cerablanket plug at the tip for particle filtering. For the experiments only the thermocouples were used for monitoring the temperature profile along the reactor height.

A dedicated probe with the tip located inside the exhaust pipe of the reactor (Figure 5.3) was used for gas sampling using a heated line, in order to monitor the exit flue gas composition. Then the sample gas is conducted to a Fourier Transform Infrared Spectroscopy on line analyzer (FTIR). Several gases were continuously monitored, nonetheless for this case mainly the O<sub>2</sub>, CO and CO<sub>2</sub> concentration will be used in order to evaluate the performance of the combustion process. The schematic of the heated flue gas sample line is presented in Figure 5.4.

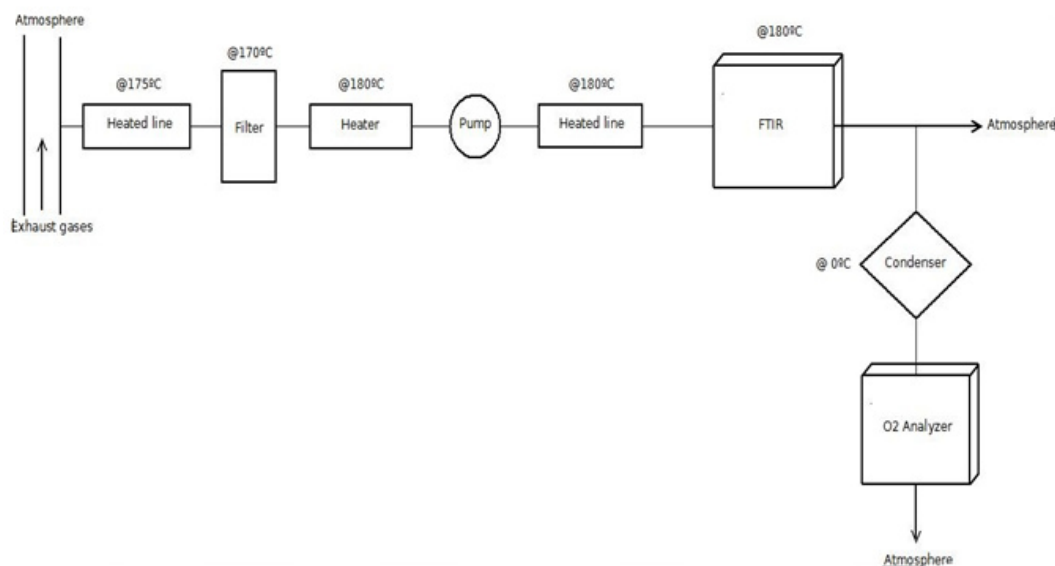


Figure 5.4 - Schematic representation of the flue gases heated sampling line.

For O<sub>2</sub> monitoring in the exit flue gas a paramagnetic analyzer was used (ADC model O<sub>2</sub>-700 with a Servomex Module); the exit gas from the FTIR was dried prior to be analyzed in the paramagnetic analyzer (Figure 5.4). Furthermore, a Zirconia cell probe located inside the BFB furnace (freeboard region) was also used for real time

monitoring of O<sub>2</sub>. Uncertainties associated with gas composition measurements in the on-line analyzers are below 2% full scale.

The operation and monitoring of the reactive system, the gas sampling system and data acquisition (temperature, pressure and gas concentration) system was performed by a computer based control and data acquisition hardware and software system (Tarelho et al., 2011).

#### 5.4.1 Reactor setup

The combustion experiments were planned so that the hydrodynamics of the reactor was kept similar during experiments. For that purpose the primary air flow rate was adjusted in order to keep the fluidizing velocity between 2,5 and 3 times the minimum fluidizing velocity, that is, between 0,28 and 0,30 ms<sup>-1</sup> depending on the bed temperature. The secondary and tertiary air was adjusted in order to each of them represent 15% of total combustion air. On following, the stoichiometry of combustion was established independently by proper adjustment of the solid biomass fuel feed rate. The bed temperature was maintained at the desired level by means of regulating the insertion of a set of eight water-cooled probes located at the bed level (Tarelho et al., 2011).

The monitoring of temperature at different heights along the reactor was made with the probes tip at half distance between the reactor wall and the axial line. The measurements (temperature and gas composition) were taken with the reactor operating at pre-set steady state conditions. At specified feeding conditions of air and biomass, the steady state condition was evaluated by monitoring the bed temperature and the exit flue gas composition (in terms of O<sub>2</sub> and CO<sub>2</sub> concentration); the Zirconium probe was helpful for this purpose because it gives reliable information about the Oxygen concentration at the core of the reactor.

For operation of the pilot scale fluidized bed reactor two different stages can be established: the pre-heating stage where the main objective is to rise the bed temperature to 500 °C to achieve fluidization conditions (simultaneously with the addition of primary air) and a second phase of combustion using solid fuel where the temperature ranges from 700 to 1000 °C, to perform the experiments.

For the pre-heating stage a mixture of propane with air is used to rise the temperature of the reactor. The propane combustion is done through a pilot burner. This burner keeps a stable flame which is independent of the fluidizing air. The flame is controlled visually through two viewports. At the same time the bed temperature was controlled through the data acquisition system using the information coming from the thermocouples. When a temperature of 500°C was achieved, the addition of solid fuel started. In this case the experiments started with solid biomass. When the reactor achieves a temperature of 750°C the preheating system was turned off and the reactor operates with solely solid fuel. When the operation was stable the addition of the fuel samples prepared was performed.

Since the fuel samples were continuously added to the bed, it was necessary to control the bed height. As shown in Table 5.2 the ash content in the fuel is considerably high, for this reason a procedure of bed discharge was implemented in order to prevent the rise up of the bed solids level. For this purpose, periodically openings of the bed discharge port permitted to withdraw a known amount of bed solids, mainly ash that accumulated at bed surfaced, in order to keep the bed height. No agglomeration neither defluidization events related to the fuel ash were observed despite several hours (around 7 to 8) of operation.

## **5.5 Combustion experiments**

The combustion experiments were performed in order to evaluate the influence of fuel characteristics (fuel sample 1 and fuel sample 2) and excess oxygen concentration on the flue gas temperature and composition; it was maintained the bubbling bed temperature between 800 to 850°C. The exhaust gases composition ( $\text{H}_2\text{O}$ ,  $\text{O}_2$ ,  $\text{CO}_2$ ,  $\text{CO}$ ) for distinct operating conditions is shown in Figure 5.5 to 5.9.

In Figure 5.5 is shown the flue gas composition, wet gases and dry gases, during shredded residual forest biomass combustion (derived from eucalyptus), with particle diameters between 1 and 10 mm. Although the flue gas composition in terms of  $\text{CO}_2$  and  $\text{H}_2\text{O}$  shows some fluctuations, the system is operating in steady state conditions; the fluctuations in the flue gas concentration are related to fluctuations in the fuel feeding and reflects the heterogeneous characteristics of the biomass fuel particles. The  $\text{CO}_2$  and  $\text{H}_2\text{O}$  behavior is very similar and reflects the moisture release and oxidation rate of the carbon and hydrogen present in the biomass fuel. The moisture content of the flue gases is the range 11 to 12 %v (wet gases). The oxygen concentration in the flue gases was in range 6 to 7%v (dry gases)

The  $\text{CO}$  shows high fluctuations and its concentration looks very sensitive to fluctuations in biomass feeding; in fact, concentration values in the range 200 to 1000 ppmv (dry gases) can be observed. These fluctuations in  $\text{CO}$  concentration are also related to the typical high volatile content of the biomass fuels, which is traduced by an intense gas phase combustion and thus very sensitive to fuel feeding conditions.

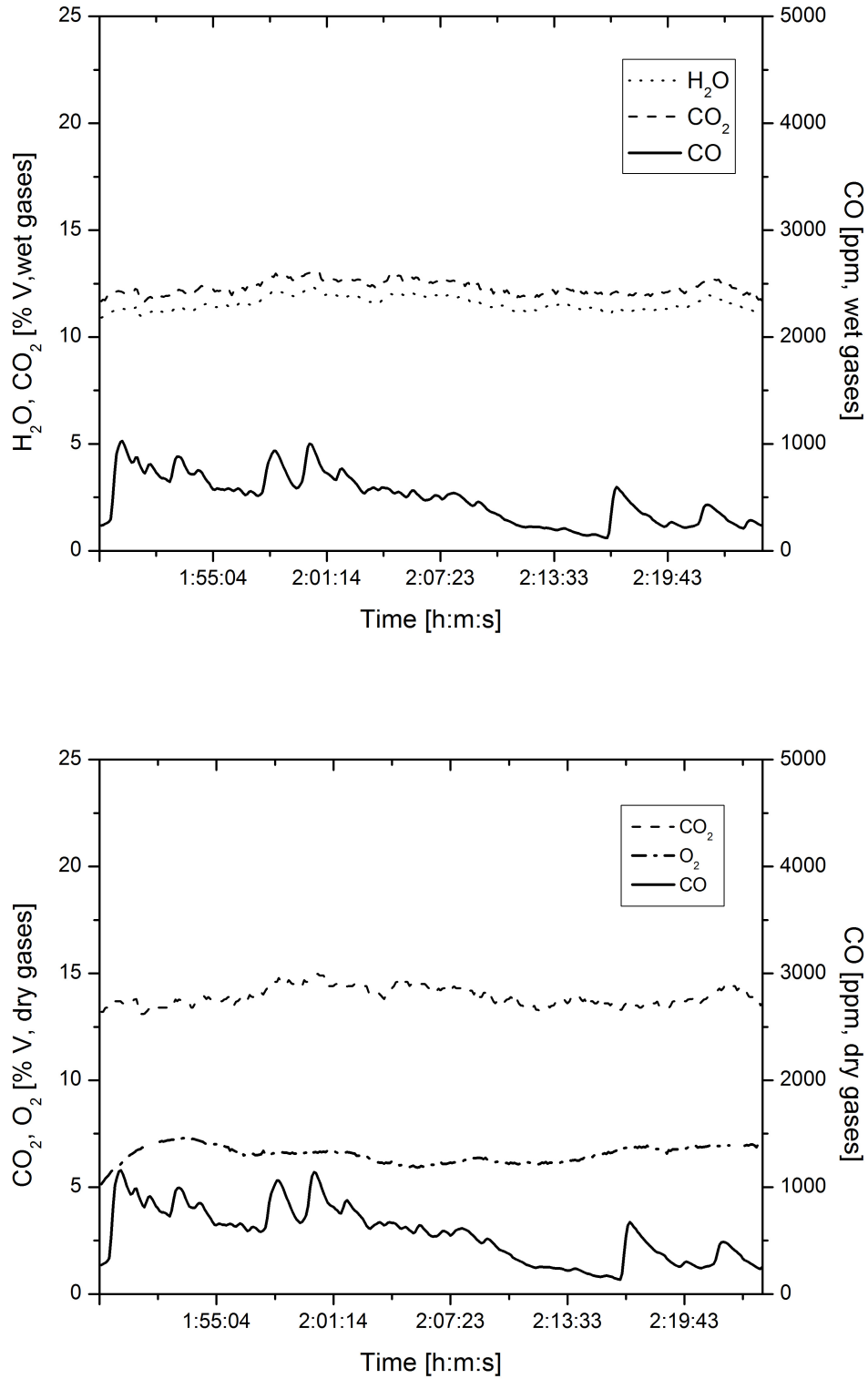


Figure 5.5 - Flue gas composition during the combustion of residual forest biomass derived from eucalyptus, under typical stoichiometric conditions.

After a period of residual forest biomass combustion, it was introduced the fuel sample 1 (sewage sludge). The screw feeders did not present problems to handle and transport the material to the reactor. After some minutes a stable bed temperature of 850°C was achieved. The flue gas composition obtained during the combustion experiments with two levels of excess oxygen are shown in Figure 5.6 and Figure 5.7; in each figure are presented information for H<sub>2</sub>O, CO<sub>2</sub> and CO on wet gases and dry gases, and for O<sub>2</sub> in dry gases.

It is observed H<sub>2</sub>O concentration is higher than that of CO<sub>2</sub> (Figure 5.6), in opposition to that observed during residual forest biomass combustion, and explained by the higher moisture content of the sewage sludge (Table 5.2). Also, it is important to refer that H<sub>2</sub>O and CO<sub>2</sub> concentration show less fluctuations when compared to that observed during residual forest biomass combustion; in part, this can be explained in result of better transportation qualities of this fuel when compared to the residual forest biomass. In average, the CO concentration is lower than that observed during combustion of residual forest biomass, despite the lower O<sub>2</sub> concentration value during sludge combustion (Figure 5.6).

Decreasing the stoichiometry, corresponding to O<sub>2</sub> concentration around 2.5%v (dry gases) in the exit flue gases during combustion of sewage sludge, it is observed that the CO<sub>2</sub> concentration in the exit flue gases is higher than that of H<sub>2</sub>O, and an increase on the average CO concentration was achieved (Figure 5.7); nevertheless, in result of a slight increase on stoichiometry, as reflected by a slight increase on the O<sub>2</sub> concentration in the exit flue gas, the CO concentration decreased to an acceptable level (considering the relatively low stoichiometry) during the second half period of the combustion test (Figure 5.7). For this lower stoichiometry condition it is observed a very regular pattern on the H<sub>2</sub>O, CO<sub>2</sub> and O<sub>2</sub> pattern along the time, reflecting good feeding conditions for this fuel.

The bed temperature achieved during this reduced stoichiometry operating condition was higher than that observed during combustion of sludge under the previous condition of higher stoichiometry. This increase in bed temperature is a consequence of the lower stoichiometry of operation, and related to the increase on fuel feed rate to the reactor, thus a higher thermal input.

It is important to state that, besides the combustion of 100% sewage sludge it were not observed neither agglomeration neither defluidization conditions. More information about the solids (bottom ash) production during these experiments will be presented in section 5.5.2.

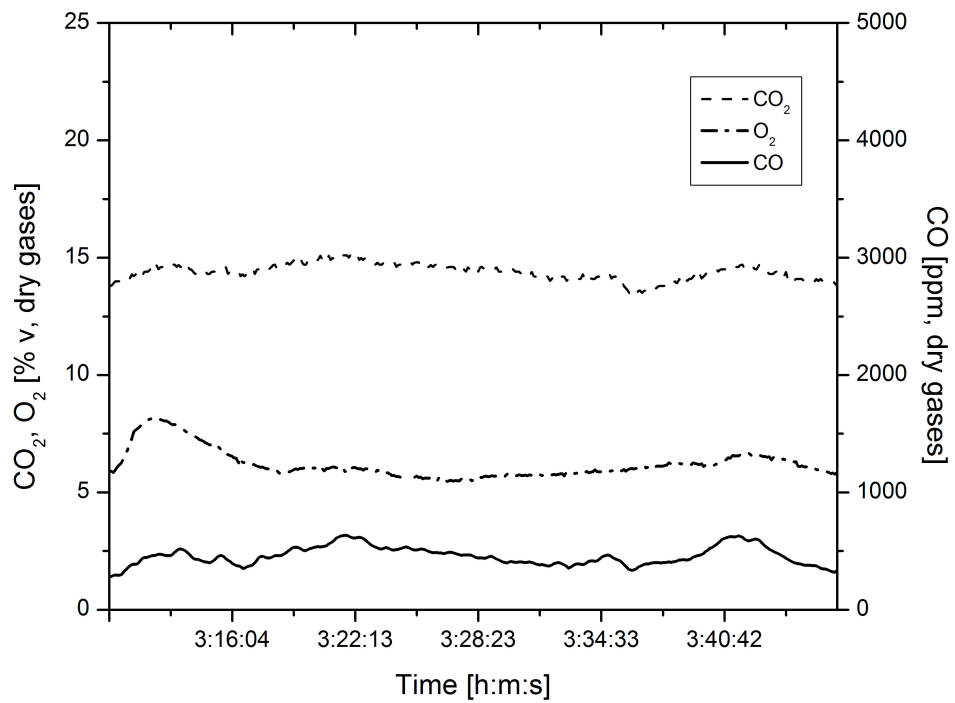
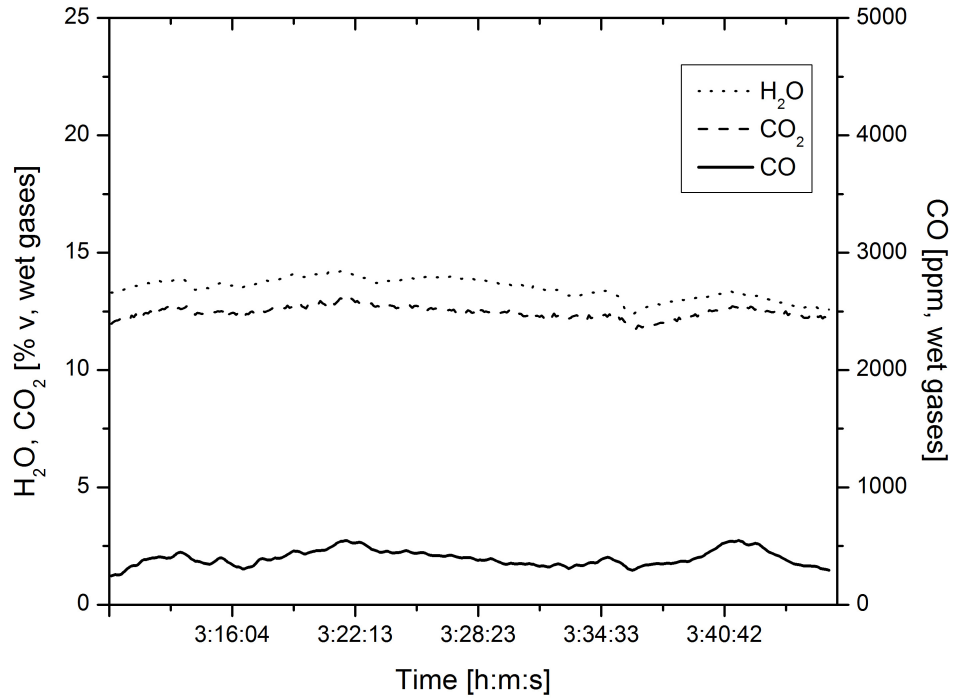


Figure 5.6 - Flue gas composition during the combustion of fuel sample 1 under typical stoichiometric conditions.

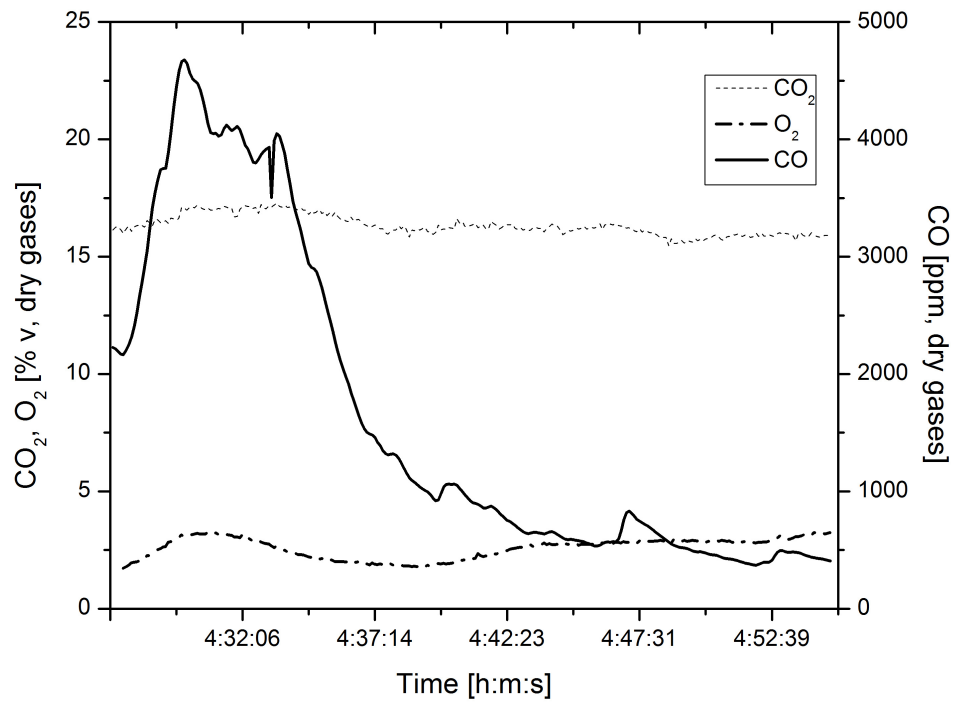
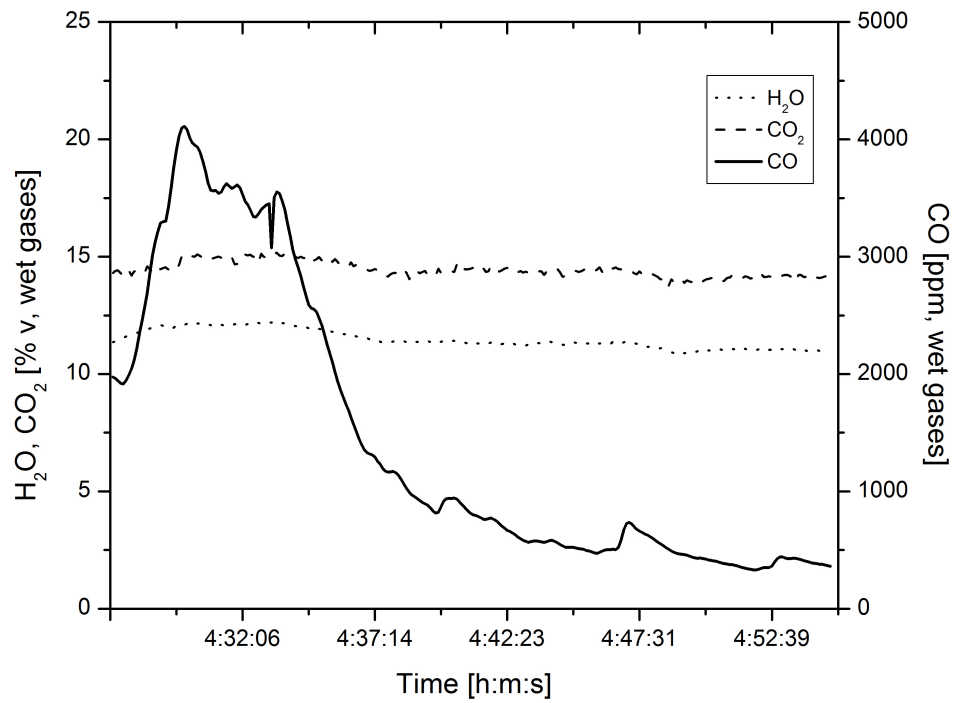


Figure 5.7 - Flue gas composition during combustion of fuel sample 1 with reduced stoichiometry.

After the combustion experiments with sewage sludge (fuel sample 1), it were performed combustion experiments with fuel sample 2 (mixture of biomass with sludge), and some results are presented in Figures 5.8 and 5.9, for two conditions of excess oxygen in the combustion flue gas.

As also observed for sewage sludge combustion, the mixture sewage sludge plus residual forest biomass (particle size <1mm) showed good transportation characteristics in the screw feeding system of the pilot scale fluidized bed reactor. Those good transportation conditions are reflected in a very steady concentration of  $H_2O$ ,  $CO_2$ , and  $O_2$  in the combustion flue gases along the time (Figure 5.8 and Figure 5.9).

For the first experimental condition (Figure 5.8) the  $O_2$  concentration in the exit flue gas (5%v, dry gases) was slight lower than that in the previous experiments with residual forest biomass or with sewage sludge, but in the range often used in industrial installations with fluidized bed combustors. It is important to state that despite a slight lower oxygen concentration in the flue gases (thus lower stoichiometry), during combustion of this mixture the  $CO$  concentration in the flue gases was significantly lower than that observed previously during residual forest biomass combustion and also during sewage sludge combustion.

By increasing the fuel mixture feed rate, the stoichiometry of operation was decreased, as reflected by the decrease on  $O_2$  concentration in the flue gases (Figure 5.9). It was noticed that this fraction of fuel mixture was wetter than the previous one (Figure 5.8) as evidenced by the increase in the moisture content (around 21%v, wet gases) in the flue gases (Figure 5.9). Nevertheless, good fuel feeding conditions were maintained, as reflected by a very uniform composition of the combustion flue gas in terms of  $H_2O$ ,  $CO_2$  and  $O_2$  concentration along the time.

The  $CO$  concentration increased when compared to the condition of higher stoichiometry (Figure 5.8), but in average was lower when compared to the observed during residual forest biomass (Teixeira, 2013) or sewage sludge combustion under similar conditions of oxygen concentrations in combustion gases (Figure 5.7)

These experiments allow concluding about the feasibility of mixing residual forest biomass with sewage sludge in order to produce a fuel mixture with appropriate characteristics to be used in fluidized bed combustors.



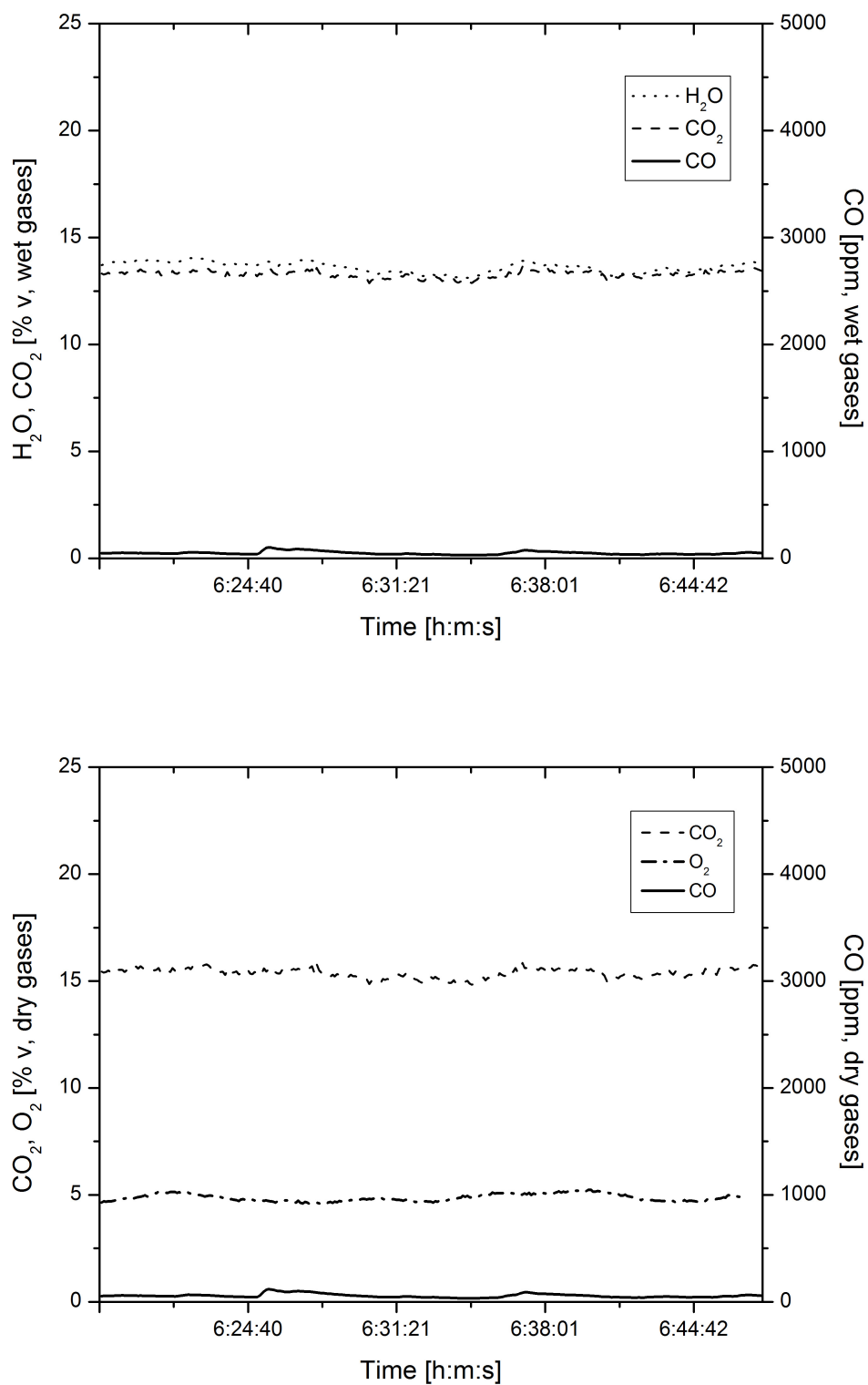


Figure 5.8 - Flue gas composition during combustion of fuel sample 2 under typical stoichiometric conditions.

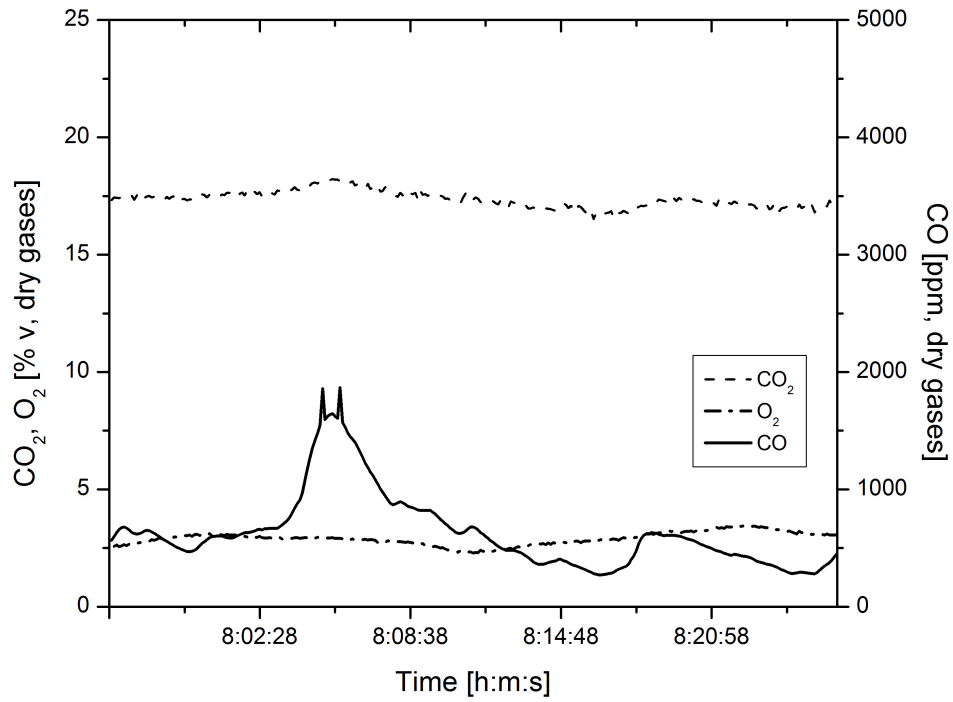
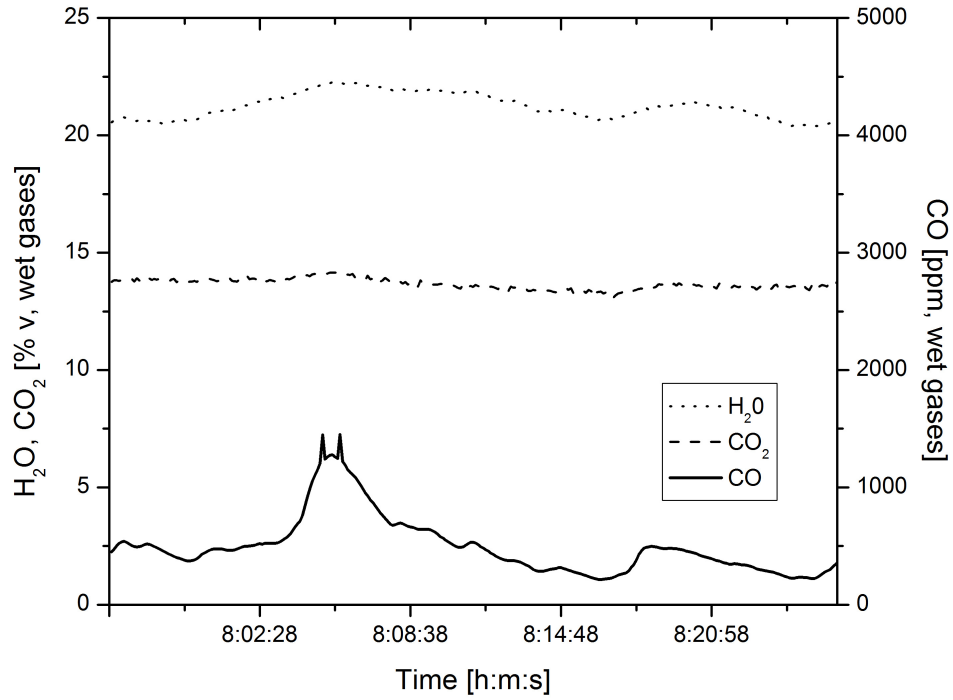


Figure 5.9 - Flue gas composition during combustion of fuel sample 2 with reduced stoichiometry.

A comparison of the average CO concentration of each experiment period and the CO emission level limits according to the Portuguese law (Portaria 677/2009) were done. Normalized conditions of pressure (101,3 kPa), temperature (273,15 K) and dry gas were considered. The average CO concentration for each stage was expressed in  $\text{mg}\cdot\text{Nm}^{-3}$  and corrected to 11% of  $\text{O}_2$  concentration in the flue gas according to the following equation:

$$G_{v0} = \frac{C_1 - C_2}{C_2 - C_0} \cdot G_{v1} \quad \text{Eq. 30}$$

where:

$G_{v0}$  represents the CO concentration in  $[\text{mg}\cdot\text{Nm}^{-3}]$  corrected for 11% of  $\text{O}_2$  concentration in the flue gas.  $C_1$  represents the  $\text{O}_2$  concentration in the air expressed in [%v].  $C_2$  represents the desired  $\text{O}_2$  concentration expressed in [%v].  $C_0$  represents the actual  $\text{O}_2$  concentration in the flue gas expressed in [%v] and  $G_{v1}$  represents the actual CO concentration in the flue gas expressed in  $[\text{mg}\cdot\text{Nm}^{-3}]$  (M. A. A. Matos & Pereira, 2010). The results are presented in Figure 5.10.

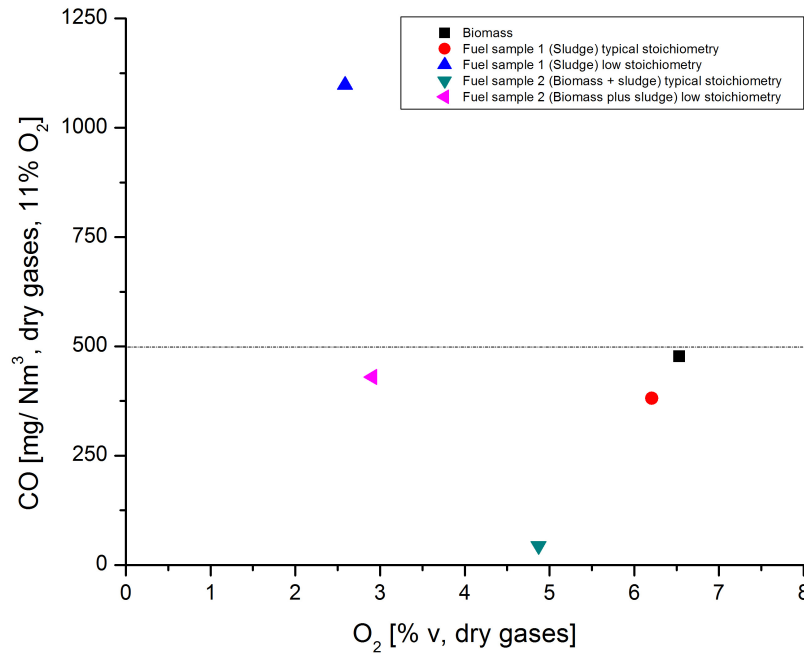


Figure 5.10 - Comparison of average CO concentration in the flue gas  $[\text{mg}\cdot\text{Nm}^{-3}]$  corrected for an 11% of  $\text{O}_2$  dry gases vs. average  $\text{O}_2$  concentration [%v] measured for each combustion period.

It was observed that the emission level of  $500 \text{ mg}\cdot\text{Nm}^{-3}$  was exceeded in the combustion period 3 (Figure 5.7). It is important to note that the stoichiometry of the first stage of this period was very low. In the second stage of this period the emission levels were stabilized to values previously observed due to a correction in the

stoichiometry value; nevertheless the high values achieved during the first stage of this period strongly influence the average value.

It also can be observed a very low CO emission level for the period 4 (Figure 5.8) which reflects high efficiency of combustion. However in all the cases analysed with the exception above mentioned the emission levels were under the limits established by the Portuguese law. Furthermore it can be noticed that CO concentration of the fuel samples prepared with the exception above mentioned are below the CO concentration observed during residual forest biomass combustion. In addition the stoichiometry used for the combustion of the fuel samples prepared was always lower than the stoichiometry used during the residual forest biomass combustion.

#### 5.5.1 *Temperature profiles*

The temperature profile along the reactor height was monitored during the combustion experiments, and the results are shown in Figure 5.11.

Five different periods are identified in Figure 5.11, and correspond to data presented before in Figures 5.5 to 5.9, and corresponding to distinct fuel compositions and excess oxygen (operating stoichiometry). The periods identified in Figure 5.11 can be described as follows:

- [1] Reactor operation with residual forest biomass; example of flue gas composition was shown in Figure 5.5.
- [2] Reactor operation with sewage sludge and typical operating stoichiometric conditions; example of flue gas composition was shown in Figure 5.6.
- [3] Reactor operation with sewage sludge and reduced stoichiometry; example of flue gas composition was shown in Figure 5.7.
- [4] Reactor operation with a mixture of residual forest biomass with sewage sludge and typical operating stoichiometric conditions; example of flue gas composition was shown in Figure 5.8.
- [5] Reactor operation with a mixture of residual forest biomass with sewage sludge and reduced stoichiometry; example of flue gas composition was shown in Figure 5.9.

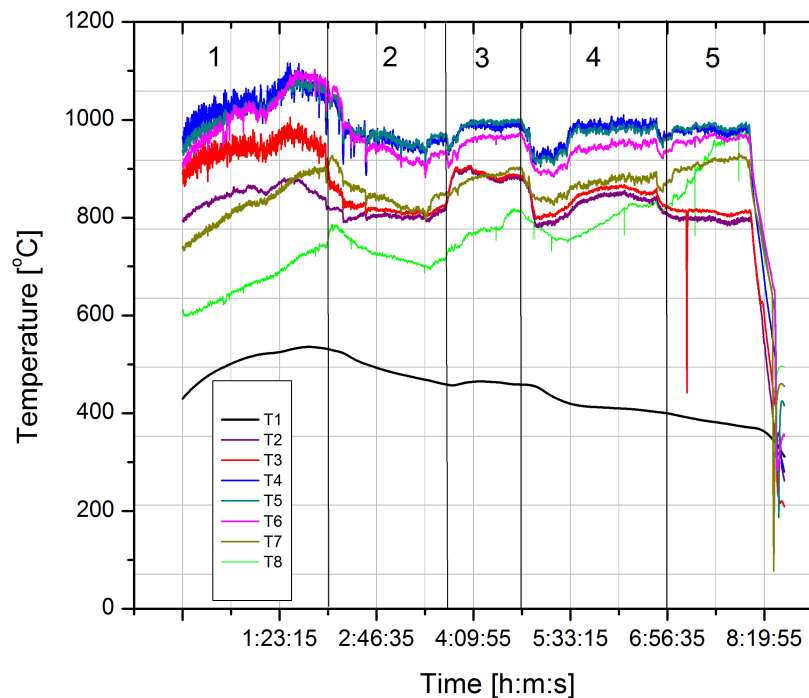


Figure 5.11 - Temperature inside the reactor along the time for the set of experimental conditions analysed before and corresponding to some data presented in Figures 5.5 (period1), 5.6 (period 2), 5.7 (period 3), 5.8 (period 4) and 5.9 (period 5), at several locations along the reactor height.

It is observed that the temperature along the reactor height shows slightly changes along the time and related to modifications in the operational conditions of the reactor, namely the characteristics of the fuel and combustion stoichiometry. Nevertheless the higher temperatures are always located in the freeboard region above the fuel discharge point (T4, T5, T6 in Figure 5.11), and are consistent with the fact that biomass fuels are characterized by a very important gas phase combustion process.

When analyzing the temperature along the time, two significant drops in the bed temperature can be noticed and are related to changes in the type of fuel used. The first one was noticed on the transition from residual forest biomass fuel, to a more wet fuel (fuel sample 1) then, during the transition from period 3 to period 4. During the initial stage of period 4 a sharp decrease on the temperature was observed and was related to the shift from fuel sample 1 to fuel sample 2; this decrease in temperature was related to the higher moisture content of fuel sample 2, that imposed the need of increase the fuel feed rate in order to rise the temperature. Nevertheless, the bed temperature was controlled within the range of 800°C to 850°C.

The temperature profiles along the reactor height for the five above-mentioned combustion periods identified in Figure 5.11 are shown in Figure 5.12. It can be seen that the higher temperatures were observed when the reactor was operating with

residual forest biomass (period 1). During combustion of sewage sludge and the mixture of sewage sludge with residual forest biomass (periods 2, 3, 4 and 5) the temperature along the reactor height is lower than that observed during combustion of biomass (period 1) and is related to the characteristics of the fuel, namely the higher amount of organic content and moisture content of the fuel when compared to the residual forest biomass. Also the stoichiometry influences the temperature along the reactor height; the conditions of lower stoichiometry (less oxygen content in the flue gases) causes increases in the temperature, as observed when comparing periods 2 and 3; this is explained by the higher energy input (fuel feed rate) during operation with lower stoichiometry. However, that tendency for the influence of stoichiometry was not observed during operation with fuel sample 2, namely periods 4 and 5, and this can be explained by the higher moisture content of the fuel mixture during period 5, as revealed by the significant higher moisture content of the combustion flue gases (Figure 5.9). In fact, period 5 showed the lower temperature profile in the reactor, and thus related to the high moisture content of the fuel.

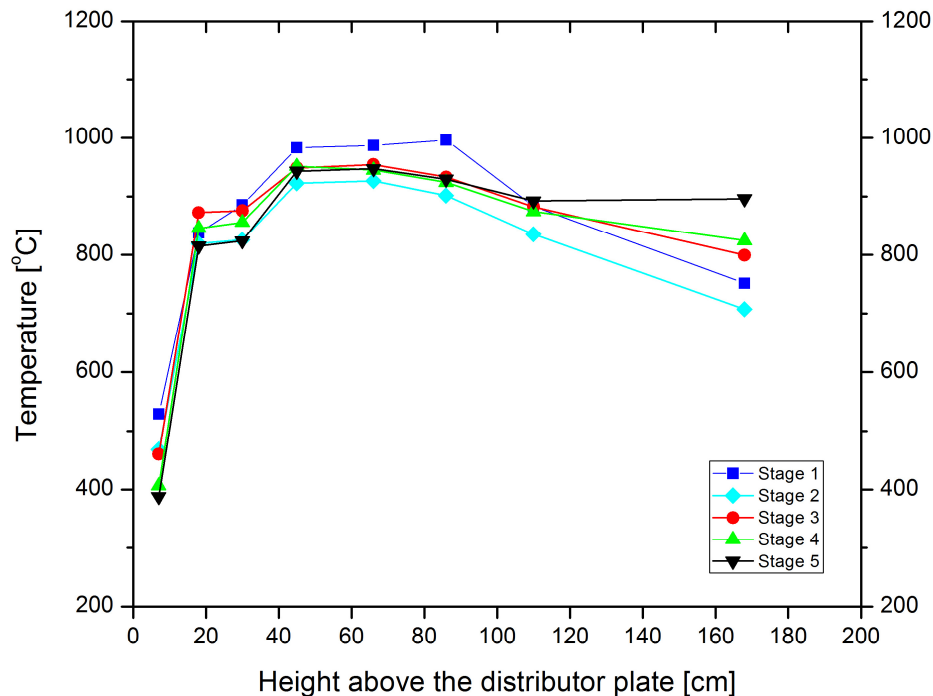


Figure 5.12 - Temperature profile (based on average of temperatures along the time (Fig 5.10)) along the reactor height for the set of experiments analysed before and corresponding to (period 1), 5.6 (period 2), 5.7 (period 3), 5.8 (period 4) and 5.9 (period 5), at several locations along the reactor height.

### 5.5.2 Solid products of combustion

During the combustion experiments an increase on the bed height was noticed and a bed withdraw was necessary. As mentioned the ash content of the fuel samples prepared is considerable (Table 5.2). The first bed withdrawn shows relatively big

particles of white/gray material mixed with the bed sand. The particles were mixed each other, not embedded. The bottom ash consistency was not so strength; through hand pressure it can be easily converted into a white/gray powder. The macroscopic look of the first bed withdrawn is shown in Figure 5.13.



Figure 5.13 - Bed look after the combustion experiments.

Regarding the fly ash, a big amount of it was found in the exhaust gas duct (Figure 5.14). Unlike the bottom ash the fly ash looks like a very fine powder.



Figure 5.14 - Fly ash deposition at the exhaust gas duct.

Furthermore an important ash deposition phenomenon was noticed in the probes located inside the combustor chamber. After the combustion experiments a crust formation on the tip of the sampling probes (Figure 5.15 right), and also in the Zirconia cell probe (Figure 5.15 left) was observed. However the crust was very friable and easily removed and cleaned.





Figure 5.15 - Ash deposition at the Zirconia cell tip and at flue gas sampling probe tip.

Also at the interior of the reactor a fine coat of ash in the inner walls was found; a picture showing the reactor inside from the top after the combustion tests is presented in Figure 5.16. It was noticed that the amount of ash adhered to the inner reactor walls was not constant along the reactor height.

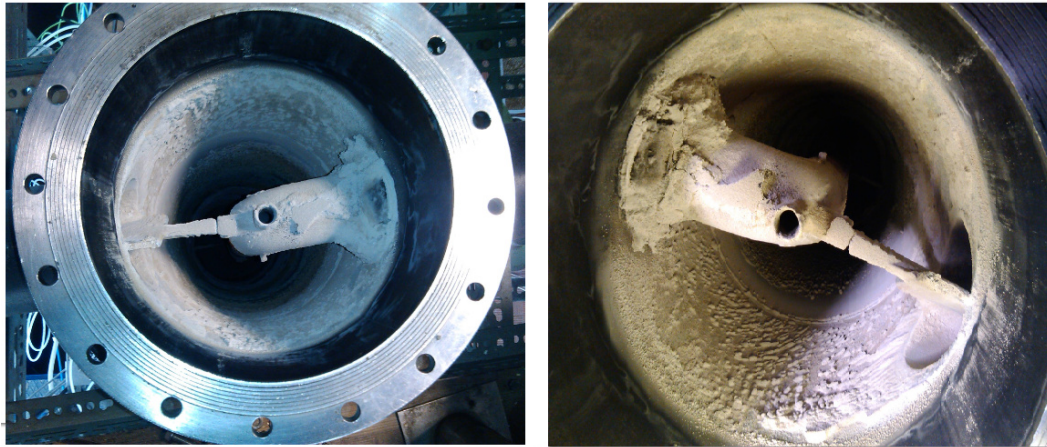


Figure 5.16 - Look at the top of the reactor after the combustion experiments.

In addition to ash deposition along the reactor inner wall, ash deposition along the fuel discharge duct located inside the reactor was observed (Figure 5.17). That Duct was removed to analyze the ash deposition, and collection of samples for further analysis. It was noticed that along the fuel discharge duct the ash deposition also varied; two regions appear cleaner than the others. The first region starts 0,50 m above the static bed and a second region is located 1,30 m above the static bed.



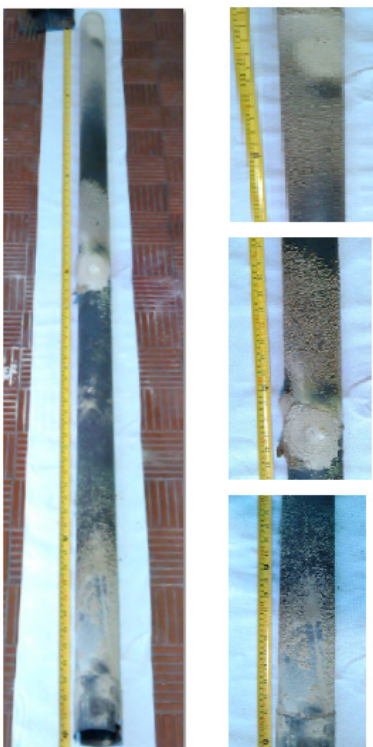


Figure 5.17 - Ash deposition along the fuel discharge duct located inside the reactor (Figure 5.3). The tube side located near the bed surface is at the top of the picture. Total length of the tube is 2 m.

Regarding the particle size distribution of the discharged bottom bed, several samples were analyzed. A sample of bottom bed withdrawn during combustion of sewage sludge is shown in Table 5.3.

Table 5.3 – Particle size distribution of the first withdrawn of the bottom bed during combustion of sewage sludge (fuel sample 1).

Particle diameter [mm]	Mass retained on the sieve [ kg · kg bed <sup>-1</sup> ]
$d_p < 250$	0,017
$250 < d_p < 710$	0,972
$710 < d_p < 1,00$	0,117
$1,00 < d_p < 2,00$	0,052
$d_p > 2.00$	0,015

A particle size distribution of a bottom bed sample withdrawn during the combustion of the fuel mixture of biomass and sludge (fuel sample 2) is presented in Table 5.4.

Table 5.4 – Particle size distribution of a bed sample withdrawn during the combustion of fuel mixture of biomass and sludge (fuel sample 2).

Particle diameter [mm]	Mass retained on the sieve [ kg · kg bed <sup>-1</sup> ]
dp < 250	0,007
250 < dp < 710	0,441
710 < dp < 1,00	0,357
1,00 < dp < 2,00	0,148
dp > 2,00	0,044

A particle size distribution of the bottom bed withdrawn after the combustion experiments, and during the reactor cleaning activities, is shown in Table 5.5.

Table 5.5 – Particle size distribution of the bottom bed withdrawn after the combustion tests, and during the reactor cleaning.

Particle diameter [mm]	Mass retained on the sieve [ kg · kg bed <sup>-1</sup> ]
dp < 250	0,057
250 > dp < 710	0,875
710 > dp < 1,00	0,026
1,00 > dp < 2,00	0,033
dp > 2,00	0,007

It can be observed that a small percent of the bottom ashes in general present particle diameters smaller than the bed particle size (around 5%). The bottom ash from the combustion of fuel sample 1 (sewage sludge) present a difference when compared with the bottom ash from combustion of fuel sample 2 (residual forest biomass plus sewage sludge). During the combustion of sewage sludge, most of the bottom ashes have the same particle size diameter of the bed sand. During the combustion of biomass plus sewage sludge a considerable percentage of the bottom ash has bigger particle sizes than the bed particles.

In fact, the analysis of all aspects related to ashes deserves a dedicated study. The establishment of the possible uses for ashes is extremely important given the considerable amount produced as a result of the combustion process. As mentioned in section 2.1.4, the pozzolanic characteristics of the ashes e.g. can be suitable for incorporation in clinker production. The definition of potential uses for ashes can be a key factor for an extended use of a fuel based on sewage sludge and based on this, interesting recycling circuits can be created. A further study of these aspects is recommended.

## **6 Concluding remarks**

The macroeconomic analysis indicates that the pulp and paper sector represents an important share in the economic activities in Portugal. Furthermore it was identified that energy production is getting relevance in the business portfolio of this sector.

Waste management is a major concern in this industry and an increasing interest to explore the incorporation of wastes into new products has been observed. For the case of sewage sludge three main trends were identified (vitrification, incorporation in agriculture, and waste to energy). The state-of-the art revision indicates that the big constraint to overcome to turn the sewage sludge into new products is its high moisture content.

A wide range of industrial equipment's dedicated for sludge drying was identified. The constraint commonly reported is the difficulty to feed the dryer due to the plastic and pasty consistency of the sewage sludge. Moreover, the intensive character regarding energy consumption of those equipment's suggest that an economically viable solution passes through the exploration of waste heat sources in order to supply the energy needs of the drying stage. Additionally, to avoid product degradation and emissions of dangerous gases during drying, the use of low temperatures are recommended, therefore low grade waste heat sources could be suitable.

The experiments performed at the tunnel allow the establishment of the main characteristics of the paper mill sewage sludge drying phenomena. The temperature of the drying air has a strong influence in moisture reduction; it was identified that moisture removal is poor using drying air temperatures below 45°C. For temperatures between 45°C and 60°C a time of 4,5 hours is enough to achieve sludge moisture contents identified as suitable for combustion (10 – 30 wt%). Moreover noticeable sewage sludge shrinkage was noticed. The formation of cracks and a thin and porous crust was also noticed.

Modeling the drying process having into account the inherent characteristics of the drying process was possible by the use of artificial neural networks approach; a high correlation coefficient was achieved. The Taguchi method used for the experimental design of the drying tests was a key factor. The ANN was trained with a relatively small database when compared with other type of drying models based also in ANN. Nevertheless the ANN architecture definition was the bottleneck due to the big amount of different features that can be tested (training algorithms, transfer functions and number of layers and neurons). However this process could be improved by the use of a second stage of the Taguchi method for the definition of a set of network architectures to test. Furthermore it was identified that forecast values, out of the training database cannot be done with enough accuracy.

In fact, there might be a wide variety of low grade industrial waste heat sources available to drive the drying process; accordingly the range of temperatures at which it can be carried out may be diverse. The presented drying kinetic model can give reliable

information about the final moisture content that can be achieved considering several temperatures and drying parameters.

The theoretical approach regarding combustion of biomass and sewage sludge allows to conclude that the combustion of sewage sludge can only be done if its moisture content is below 50 wt%, higher moisture contents produce an endothermic process. The amount of energy produced is directly related with the share of biomass and moisture content in the fuel mixture. Increasing the biomass share and decreasing the moisture content in the fuel mixture enhances the energy production. Due to this increase in the useful thermal energy, the fuel consumption of the facility decreases. In addition the fuel consumption is strongly related with the energy losses in the flue gas. A higher moisture content of the fuel mixture in conjunction with high fuel consumption rates, increases the losses of sensible and latent heat at the stack; effectively burn of wet fuels is undesirable and inefficient. This facts show the importance of a pre-treatment stage (drying) for the fuel as a key factor for the efficient operation of the energy conversion facilities.

The solid products (fly and bottom ash) resulting from combustion are also an important issue. A noticeable increase of the ashes production due to the inclusion of sewage sludge in the fuel mixture was verified; eventually maintenance and operational issues can appear especially in the flue gas filtration systems. The increased bottom ash production also can cause continuous bed withdraws to maintain a proper bed level. The bed sand taken out of the reactor can withdraw significant quantities of sensible heat; a dedicated study about this fact should be done. The final destination of the solid products (fly and bottom ash) generated is also a concern. The state-of-the art revision suggest that the pozzolanic characteristics of the ashes makes them valuable for its use in other industries; for instance clinker production; therefore interesting synergies can be established; a further study is recommended.

Regarding the combustion experiments, a uniform fuel feed to the reactor was identified as a key factor to achieve a stable operation. The results confirm that the particle size distribution of the fuel samples prepared was correct. The extrusion stage was very important to improve the handling and to achieve a correct particle size distribution.

In the case of fuel sample 2, incorporation of the fine particles of the residual forest biomass in the sewage sludge was effective. This fact suggests that handling of the fuel during drying can be improved by this way (extrusion and addition of biomass fine particles). To overcome feeding issues instead of, recirculate part of the dried material to the feeding port which is a usual practice of the driers manufacturers, the addition of biomass fine particles can cause the same effect with a significant advantage because the addition of biomass fine particles produces a significant increase in the heating value of the final product (fuel). Moreover a drum dryer-mixer powered by waste heat, with a hot air stream flowing through it appears as the most appropriate option because it allows the formation of spherical particles besides to allow control the

particle diameter through the drum rotational speed; nevertheless a deep study of such an equipment is need.

During the five periods of the combustion experiments an average temperature of 800°C was maintained at the bed level during all the experiments and despite several hours of operation the fluidization conditions were kept constant. The temperature profile shows that the highest temperatures were achieved in the freeboard zone, located above the location of biomass and secondary air addition, indicating that an important part of the combustion process of the fuel occurs mainly in gaseous phase.

For each experimental condition tested, the CO<sub>2</sub> concentration during the combustion of the fuel samples 1 and 2 was steady. The main reason to reach a steady condition is related to the uniform fuel feed conditions. Furthermore a low CO concentration was noticed when compared to the observed during residual forest biomass combustion even for very low stoichiometry's. The CO levels never exceed the emission levels established by the Portuguese law under typical stoichiometry conditions. Low CO concentration was also observed for combustion of sewage sludge with low stoichiometry which indicates that the combustion process can be improved by the use of less combustion air.

During the combustion of fuel sample 2 under typical stoichiometry conditions a very low CO concentration was observed. This indicates that the combustion efficiency (fuel oxidation) was high. The fuel sample 2 (50 wt% sewage sludge plus 50 wt% residual forest biomass) appears as a very good quality fuel, with good transportation and handling properties, acceptable heating value, and an efficient combustion. Nevertheless non uniformities in the moisture content of the fuel mixture can strongly influence the combustion efficiency as noticed during the last period of the combustion tests. The steady conditions observed for the reactor in conjunction with the fact that the fluidization conditions were maintained during all the experiments confirms that a fuel composed by sewage sludge (correctly dried) and residual forest biomass can be burned with no major problems, being an interesting option as industrial fuel.

The amounts of solid products (fly and bottom ash) generation was significant, and it was related to the high content of ash in the sewage sludge. The bottom ash particles appeared individualized regarding the sand bed particles. A detailed study about the ash chemical composition must be done in order to establish its main characteristics. The analysis of the particle size distribution shows a noticeable difference in the particle size of the bottom ashes of these two fuels (fuel sample 1 and 2). The particle size of bottom ash produced during the sewage sludge combustion is mostly within the range of the bed particles. The particle size of the bottom ash produced during the combustion of sewage sludge plus residual forest biomass is shared between sand bed-particle size diameters and greater than it.

Undoubtedly one of the main factors affecting the feasibility of this type of fuel passes through the establishment of a safe and reliable destination for the ashes. A further study of the ash composition is needed. Novel recycling processes can be

enabled by the purchase and sale of this fuel including its ashes; because of that, the potential uses for it must be investigated.

## 7 Bibliography

- Åmand, L., & Leckner, B. (2001). Co-Combustion of Sewage Sludge with Wood / Coal in a Circulating Fluidized Bed Boiler- A Study of Gaseous Emissions. Göteborg, Sweden.
- Åmand, L.-E., & Leckner, B. (2004). Metal emissions from co-combustion of sewage sludge and coal/wood in fluidized bed. *Fuel*, 83(13), 1803–1821.
- Batista, J. A. L. (2013). Resíduos celulose. In *Notes from the curricular unit: Reciclagem e novos produtos*. Universidade de Aveiro.
- Bennamoun, L., Belhamri, A., & Léonard, A. (2010). Contribution to the modelling of wastewater sludge drying kinetics: study of the operating conditions effect. *International Drying Symposium*, 828–833.
- Boeri, C. N. (2012). *Secagem convectiva de produtos alimentares: otimização e controlo*. PhD thesis. Universidade de Aveiro.
- Canada Department of Energy, M. and R. (1988). *Waste heat recovery. Energy Management Series* (pp. 7–58). Ottawa.
- Carlos A. Peregrina Cambero, P. A. and D. L. (2004). Thermal efficiency in sewage sludge fry drying. In *Proceedings of the international drying symposium* (pp. 972–978). São Paulo, Brazil.
- CELPA. (2011). *Boletim estatístico indústria papelaria Portuguesa.pdf* (p. 97). Lisboa. Retrieved from <http://www.celipa.pt/>
- Channiwala, S. A., & Parikh, P. P. (2002). A unified correlation for estimating HHV of solid, liquid and gaseous fuels. *Fuel*, 81, 1051–1063.
- Crank, J. (1975). *THE MATHEMATICS OF DIFFUSION*. (O. Clarendon Press, Ed.) (Second Edi., pp. 44–89). Oxbridge.
- Deng, W.-Y., Yan, J.-H., Li, X.-D., Wang, F., Zhu, X.-W., Lu, S.-Y., & Cen, K.-F. (2009). Emission characteristics of volatile compounds during sludges drying process. *Hazardous materials*, 162, 186–92.
- Energy design resources. (2009). *Industrial Process Heat Recovery. Design brief* (pp. 3–32). Retrieved from [http://energydesignresources.com/media/1777/EDR\\_DesignBriefs\\_processheatrecov.pdf?tracked=true](http://energydesignresources.com/media/1777/EDR_DesignBriefs_processheatrecov.pdf?tracked=true)
- Fernandes, S. (2005). *Valorização de resíduos da indústria da celulose na produção de agregados leves*. Master thesis. Universidade de Aveiro.
- Gaines, L. (2012). To recycle, or not to recycle, that is the question: Insights from life-cycle analysis. *MRS Bulletin*, 37(04), 297–458.

- Gonçalves, D. A. (2012). *Modelação da Secagem de Papel "tissue" em Ambiente Industrial*. Master thesis. Universidade de Aveiro.
- Gulyurtlu, I., Abelha, P., Grego, A., & Garci, A. (2004). The Emissions of VOC's during Co-Combustion of Coal with Different Waste Materials in a Fluidized Bed. *Energy & Fuels*, 1273(4), 605–610.
- Hartman, M., Svoboda, K., Pohor, M., & Trnka, O. (2005). Combustion of Dried Sewage Sludge in a Fluidized-Bed Reactor. *American Chemical Society*, 44(10), 3432–3441.
- Incropera, F. P., DeWitt, D. P., Bergman, T. L., & Lavine, A. S. (2007). *Fundamentals of Heat and Mass Transfer*. (F. P. Incropera & F. P. F. O. H. A. M. T. Incropera, Eds.) *Water* (Vol. 6th, p. 997). John Wiley & Sons.
- J. Vaxelaire and J.R. Puiggali. (2002). Analysis of the drying of residual sludge: from the experiment to the simulation of a belt dryer. *Drying Technology*, 20, 989–1008.
- J. Vaxelaire, J.M. Bongiovanni, P. Mousques, J. R. P. (2000). Thermal drying of residual sludge. *Water Research*, 34(17), 4318–4323.
- Joykumar, N., & Krishna, R. (2011). Neural Network Approaches for Prediction of Drying Kinetics During Drying of Sweet Potato. *CIGR*, 13(1734), 1–12.
- Karrer, D Cameira, R. Vasques, A. e Benzecry, M. (2005). Redes Neurais Artificiais Conceitos e Aplicações. In *IX Encontro de Engenharia de Produção da UFRJ*.
- Khaw, J. F. C., Lim, B. S., & Lim, L. E. N. (1995). Optimal design of neural networks using the Taguchi method. *Neurocomputing*, 7(3), 225–245.
- Lars-Erick Amand, Leckner Bo. (n.d.). Results from pre tests with fibre sludge from Stora Enso's pulp and paper mill in Skoghall.
- Lars-Erick Amand, Leckner Bo, Karsten Lücke, J. W. (2001). *Advanced air staging techniques to improve fuel flexibility, reliability and emissions in fluidized bed co- combustion* (p. 113). Stockholm.
- Lavric, G. J. V. (1995). The artificial neural networks and the drying process modeling. *Drying Technology*, 13(1579-1586), 5–7.
- Leckner, B., Åmand, L.-E., Lücke, K., & Werther, J. (2004). Gaseous emissions from co-combustion of sewage sludge and coal/wood in a fluidized bed. *Fuel*, 83(4-5), 477–486.
- Léonard, a., Blacher, S., Marchot, P., Pirard, J.-P., & Crine, M. (2005). Convective Drying of Wastewater Sludges: Influence of Air Temperature, Superficial Velocity, and Humidity on the Kinetics. *Drying Technology*, 23(8), 1667–1679.
- Matos, A. (2011). Combustão de combustíveis. In *Notes from the curricular unit: Conversão de Energias Convencionais* (pp. 5–17). Universidade de Aveiro.



- Matos, M. A. A., & Pereira, J. M. A. (2010). Propriedades e caracterização de efluentes gasosos. In *Notes from the curricular unit: Técnicas de tratamento de efluentes gasosos* (pp. 16–20). Universidade de Aveiro.
- Movagharnejad, K., & Nikzad, M. (2007). Modeling of tomato drying using artificial neural network. *Computers and Electronics in Agriculture*, 59(1-2), 78–85.
- Ohm, T.-I., Chae, J.-S., Kim, J.-E., Kim, H.-K., & Moon, S.-H. (2009). A study on the dewatering of industrial waste sludge by fry-drying technology. *Journal of hazardous materials*, 168(1), 445–50.
- Parikh, J., Channiwala, S., & Ghosal, G. (2005). A correlation for calculating HHV from proximate analysis of solid fuels. *Fuel*, 84(5), 487–494.
- Park, K. et al. (2007). *Conceitos de processo e equipamentos de secagem* (pp. 56–127). Campinas: Unicamp.
- Peregrina, C. a., Lecomte, D., Arlabosse, P., & Rudolph, V. (2006). Life Cycle Assessment (LCA) Applied to the Design of an Innovative Drying Process for Sewage Sludge. *Process Safety and Environmental Protection*, 84(4), 270–279.
- Pinho, F. (2012). *Valorização de Recursos Frutícolas Recorrendo a Desidratação*. Master Thesis. Universidade de Aveiro.
- R. Font, M.F. Gomez-Rico, A. F. (2011). Skin effect in the heat and mass transfer model for sewage sludge drying. *Separation and Purification Technology*, 77(1), 146–161.
- Rajamma, R. (2011). *Biomass fly ash incorporation in cement based materials*. PhD thesis. Universidade de Aveiro.
- Reyes, a., Eckholt, M., Troncoso, F., & Efremov, G. (2004). Drying Kinetics of Sludge from a Wastewater Treatment Plant. *Drying Technology*, 22(9), 2135–2150.
- Roy, R. K. (1990). *A Primer on the Taguchi Method* (Second Ed.). Van Nostrand Reinhold,.
- Santos, C. (2012). *Secagem e co-combustão de lamas em leito fluidizado*. Master thesis. Universidade de Aveiro.
- Shao, J. et al. (2007). Agglomeration Characteristics of Sludge Combustion in a Bench-Scale Fluidized Bed Combustor. *Energy & Fuels*, 21(10), 2608–2614.
- Shin, D., Jang, S., & Hwang, J. (2005). Combustion characteristics of paper mill sludge in a lab-scale combustor with internally cycloned circulating fluidized bed. *Waste management (New York, N.Y.)*, 25(7), 680–5.
- Siemens Water Technologies Corp. (2008). Sludge Dryers. *Siemens Water Technologies Corp.* Retrieved from [http://www.water.siemens.com/SiteCollectionDocuments/Product\\_Lines/Dewatering\\_Systems/Brochures/EPS-SLUDGEDRY-USA-BR-1008.pdf](http://www.water.siemens.com/SiteCollectionDocuments/Product_Lines/Dewatering_Systems/Brochures/EPS-SLUDGEDRY-USA-BR-1008.pdf)

- Sluiter, A., Hames, B., Ruiz, R., Scarlata, C., Sluiter, J., & Templeton, D. (2008). *Determination of Ash in Biomass*. U.S. Department of Energy.
- Spiers, H. M. (1977). *Technical data on fuel*. (Wiley, Ed.) (7th ed.). New York.
- Stasta, P., Boran, J., Bebar, L., Stehlik, P., & Oral, J. (2006). Thermal processing of sewage sludge. *Applied Thermal Engineering*, 26(13), 1420–1426.
- Tarelho, L. a. C. (2012). Tecnologia de leito fluidizado. In *Notes from the curricular unit: Conversão de Energias Renováveis* (pp. 10–45). Universidade de Aveiro.
- Tarelho, L. a. C., Neves, D. S. F., & Matos, M. a. a. (2011). Forest biomass waste combustion in a pilot-scale bubbling fluidised bed combustor. *Biomass and Bioenergy*, 35(4), 1511–1523.
- Teixeira, R. (2013). *Efeito das propriedades da biomassa na conversão em leito fluidizado*. Master thesis. Universidade de Aveiro.
- Trystram, G., & Heyd, B. (1993). *Neural networks for the heat and mass transfer prediction during drying of cassava and mango* (pp. 2–8).
- Tsai, M., Wu, K., Huang, C., & Lee, H. (2002). Co-firing of paper mill sludge and coal in an industrial circulating fluidized bed boiler. *Waste management*, 22, 439–442.
- U.S. Department of Energy. (2008). *Waste heat recovery: Technology and opportunities in U.S. industry* (pp. 6–112).
- Undebarrena, M. (1999, June). Deshidratación térmica de lodos en el ámbito industrial. *Tratamiento de Lodos*, 1–4.
- Wzorek, M. (2012). Characterisation of the properties of alternative fuels containing sewage sludge. *Fuel Processing Technology*, 104, 80–89.

## 8 Appendix

### 8.1 Appendix 1: MATLAB source code of the mass and energy balance

```
%%%%%%%%%%%%%%%%%%%%%%%%%%%%%%%%%%%%%%%%%%%%%%%%%%%%%%%%%%%%%%%%%%%%%%%%%%%%BIOMASS%%%%%%%%%%%%%%%%%%%%%%%%%%%%%%%%%%%%%%%%%%%%%%%%%%%%%%%%%%%%%%%%%%%%%%%%%%%%

%Proximate Analysis (%) AS RECEIVED BASIS

B_Humidity      = 0;
B_Volatile      = 0;
B_Ash           = 0;
B_FixedCarbon   = 0;

%Elemental Analysis in DRY BASIS
B_Carbon        = 0;
B_Hydrogen      = 0;
B_Nitrogen      = 0;
B_Sulfur        = 0;
B_Oxygen        = 0;
%Oxygen is calculated by difference

%Immediate analysis of biomass in ARB

B_Ww   = B_Humidity / 100 ;           % [kg moisture / kg biomass arb]
B_Wv   = B_Volatile /100  ;           % [kg volatile / kg biomass arb]
B_Wa   = B_Ash / 100      ;           % [kg ash / kg biomass arb]
B_Wfc  = B_FixedCarbon /100;          % [kg fixed carbon / kg biomass
arb]

% Elemental analysis of Biomass (dry basis)

B_WCr  = B_Carbon/100           ;      % [kgC / kg biomass db]
B_WHr  = B_Hydrogen/100        ;      % [kgH / kg biomass db]
B_WNr  = B_Nitrogen/100        ;      % [kgN / kg biomass db]
B_WSr  = B_Sulfur/100          ;      % [kgS / kg biomass db]
B_WOr  = B_Oxygen/100          ;      % [kgO / kg biomass db]
B_Wwr  = B_Ww / (1-B_Ww)       ;      % [kgmoisture / kg biomass db]
B_Wzr  = 1 - (B_WCr+ B_WHr+ B_WNr+ B_WSr+ B_WOr);

TotalBiomass = B_WCr+ B_WHr+ B_WNr+ B_WSr+ B_WOr + B_Wzr;    %Checking

%%%%%%%%%%%%%%%%%%%%%%%%%%%%%%%%%%%%%%%%%%%%%%%%%%%%%%%%%%%%%%%%%%%%%%%%%%%%SLUDGE%%%%%%%%%%%%%%%%%%%%%%%%%%%%%%%%%%%%%%%%%%%%%%%%%%%%%%%%%%%%%%%%%%%%%%%%%%%%

%Proximate Analysis (%) AS RECEIVED BASIS

S_Humidity      = 0;
S_Volatile      = 0;
S_Ash           = 0;
S_FixedCarbon   = 0;

%Elemental Analysis in DRY BASIS
S_Carbon        = 0;
S_Hydrogen      = 0;
S_Nitrogen      = 0;
S_Sulfur        = 0;
S_Oxygen        = 0;
%Oxygen is calculated by difference
```

```
%Immediate analysis of Sludge in ARB

S_Ww  = S_Humidity / 100      ;      % [kg moisture / kg sludge arb]
S_Wv  = S_Volatile /100      ;      % [kg volatile / kg sludge arb]
S_Wa  = S_Ash / 100          ;      % [kg ash / kg sludge arb]
S_Wfc = S_FixedCarbon /100    ;      % [kg fixed carbon / kg sludge arb]

% Elemental analysis of Sludge (dry basis)

S_WCr = S_Carbon/100          ;      % [kgC / kg sludge db]
S_WHr = S_Hydrogen/100        ;      % [kgH / kg sludge db]
S_WNr = S_Nitrogen/100        ;      % [kgN / kg sludge db]
S_WSr = S_Sulfur/100          ;      % [kgS / kg sludge db]
S_WOr = S_Oxygen/100          ;      % [kgO / kg sludge db]
S_Wwr = S_Ww / (1-S_Ww)       ;      % [kgmoisture / kg sludge db]
S_Wzr = 1 - (S_WCr + S_WHr + S_WNr + S_WSr + S_WOr);

TotalSludge = S_WCr + S_WHr + S_WNr + S_WSr + S_WOr + S_Wzr; %Checking

%%%%%%%%%%%%%%%%%%%%%%%%%%%%%%%%%%%%%%%%%%%%%%%%%%%%%%%%%%%%%%%%%%%%%%%% FUEL FRACTIONS%%%%%%%%%%%%%%%%%%%%%%%%%%%%%%%%%%%%%%%%%%%%%%%%%%%%%%%%%%%%%%%%%%%%%%%%
%%%%%%%%%%%%%%%%%%%%%%%%%%%%%%%%%%%%%%%%%%%%%%%%%%%%%%%%%%%%%%%%%%%%%%%%
%for i = 0:100                                     "only when for loop is used
to shift the fuel percentages"

%Mass_fraction_of_biomass = (i+1)/100              "only when for loop is used
to shift the fuel percentages"

%%%%%%%%%%%%%%%%%%%%%%%%%%%%%%%%%%%%%%%%%%%%%%%%%%%%%%%%%%%%%%%%%%%%%%%%
Mass_fraction_of_biomass = 0.60
Mass_fraction_of_sludge  = (1- Mass_fraction_of_biomass)

%%%%%%%%%%%%%%%%%%%%%%%%%%%%%%%%%%%%%%%%%%%%%%%%%%%%%%%%%%%%%%%%%%%%%%%%FUEL MIXTURE%%%%%%%%%%%%%%%%%%%%%%%%%%%%%%%%%%%%%%%%%%%%%%%%%%%%%%%%%%%%%%%%%%%%%%%%

%Immediate analysis of FINAL FUEL MIXTURE in ARB

F_Ww  = Mass_fraction_of_biomass * B_Ww + Mass_fraction_of_sludge *
S_Ww    ;      % [kg moisture / kg fuel arb]

F_Wv  = Mass_fraction_of_biomass * B_Wv + Mass_fraction_of_sludge *
S_Wv    ;      % [kg volatile / kg fuel arb]

F_Wa  = Mass_fraction_of_biomass * B_Wa + Mass_fraction_of_sludge *
S_Wa    ;      % [kg ash / kg fuel arb]

F_Wfc = Mass_fraction_of_biomass * B_Wfc+ Mass_fraction_of_sludge *
S_Wfc    ;      % [kg fixed carbon / kg fuel arb]

% Elemental analysis of FUEL MIXTURE (dry basis)

F_WCr = Mass_fraction_of_biomass * B_WCr + Mass_fraction_of_sludge *
S_WCr    ;      % [kgC / kg fuel db]
F_WHr = Mass_fraction_of_biomass * B_WHr + Mass_fraction_of_sludge *
S_WHr    ;      % [kgH / kg fuel db]
F_WNr = Mass_fraction_of_biomass * B_WNr + Mass_fraction_of_sludge *
S_WNr    ;      % [kgN / kg fuel db]
```

```

F_WSr = Mass_fraction_of_biomass * B_WSr + Mass_fraction_of_sludge *
S_WSr      ;          % [kgS / kg fuel db]

F_WOr = Mass_fraction_of_biomass * B_WOr + Mass_fraction_of_sludge *
S_WOr      ;          % [kgO / kg fuel db]

F_Wwr = F_Ww / (1-F_Ww);          % [kg moisture / kg fuel db]

F_Wzr = Mass_fraction_of_biomass * B_Wzr + Mass_fraction_of_sludge *
S_Wzr;

TotalFuel = F_WCr + F_WHr + F_WNr + F_WSr + F_WOr + F_Wzr
;%Checking

%%%%%%%%%%%%%%%%%%%%%%%%%%%%%%%%%%%%%%%%%%%%%%%%%%%%%%%%%%%%%%%%%%%%%%%%HIGHER HEATING VALUE%%%%%%%%%%%%%%%%%%%%%%%%%%%%%%%%%%%%%%%%%%%%%%%%%%%%%%%%%%%%%%%%%%%%%%%%

HHV = (34.91*F_WCr) + (117.83*F_WHr) + (10.05*F_WSr) - (10.34*F_WOr) -
(1.51*F_WNr) - (2.11*F_Wzr);          % [MJ / kg fuel]  "Channiwala SA,
Parikh, J Fuel 2002;81:1051"

%HHV = 10^3*((33.77*F_WCr)+(143.8*(F_WHr-(F_WOr/8)))+(9.42*F_WSr)); %
[kJ / kg fuel db] "Dulong formula"

%%%%%%%%%%%%%%%%%%%%%%%%%%%%%%%%%%%%%%%%%%%%%%%%%%%%%%%%%%%%%%%%%%%%%%%%LOWER HEATING VALUE%%%%%%%%%%%%%%%%%%%%%%%%%%%%%%%%%%%%%%%%%%%%%%%%%%%%%%%%%%%%%%%%%%%%%%%%

h_fg = 2440      ;          % [kJ / kg H2O]
                                %Latent Heat of water vaporization @25°C

mW = F_WHr * (18/2);          % [kg H2O / kg fuel db]
                                % Water mass on fuel

LHV = (HHV)-((h_fg/10^3)*mW);   % [kJ / kg fuel db]

%%%%%%%%%%%%%%%%%%%%%%%%%%%%%%%%%%%%%%%%%%%%%%%%%%%%%%%%%%%%%%%%%%%%%%%%STOICHIOMETRY CALCULATIONS%%%%%%%%%%%%%%%%%%%%%%%%%%%%%%%%%%%%%%%%%%%%%%%%%%%%%%%%%%%%%%%%%%%%%%%%

% Molecular mass of Chemical Elements

MC = 12;  % [ kg C / kmol C ]
MH = 1 ;  % [ kg H / kmol H ]
MN = 14;  % [ kg N / kmol N ]
MS = 32;  % [ kg S / kmol S ]
MO = 16;  % [ kg O / kmol O ]

% Chemicals molecular mass

MO2 = 32;  % [kg O2 / kmol O2]
MN2 = 28;  % [kg N2 / kmol N2]
MH2O= 18;  % [kg H2O / kmol H2O]
MH2 = 2 ;  % [kg H2 / kmol H2]

% Stoichiometric coefficients

YC = 1      ;  %
YH = 0.5    ;  %
YS = 1      ;  %
YN = 0      ;  %

```

```
% Stoichiometric Oxygen

Ws_kmol = YC*(F_WCr/MC) + YH*(F_WHr/MH2) + YS*(F_WSr/MS) - (F_WOr/MO2);
%[kmol O2 / kg fuel db)

Ws_kg    = MO2 * Ws_kmol ;
%[kg O2 / kg fuel db)

% Stoichiometric Air

%Air mixture ratio
Wva = 0.010;          % [kg H2O / kg dry air]
                        % from psychometric diagram

Wsa = Ws_Kg * (1+ (3.76*(MN2/MO2))+7.66*Wva*(MH2O/MO2)); % [kg
stoichiometric air / kg fuel db]

% Air excess

z = 0.5;              % percentage

% Actual Oxygen

Wa = (1+z)*Ws_kg;     % [kg O2 actual / kg fuel db]

% Actual Air

WaA = (1+z)*Wsa;      % [kg actual air / kg fuel db]

%%%%%%%%%%%%%%%%%%%%%%%%%%%%%%%%%%%%%%%%%%%%%%%%%%%%%%%%%%%%%%%%%%%%%%%%
%%%%%%%%%%%%%%%%%%%%%%%%%%%%%%%%%%%%%%%%%%%%%%%%%%%%%%%%%%%%%%%%%%%%%%%% MASS BALANCE %%%%%%%%%%%%%%%%%%%%%%%%%%%%%%%%%%%%%%%%%%%%%%%%%%%%%%%%%%%%%%%%%%%%%%%%%
%%%%%%%%%%%%%%%%%%%%%%%%%%%%%%%%%%%%%%%%%%%%%%%%%%%%%%%%%%%%%%%%%%%%%%%%

% Solid phase combustion products (fly ash + bottom ash) & unburned
carbon

%Efficiency of carbon combustion

Eff_cc = 1;           % percentage

Wc_unburned = (1- Eff_cc)* F_WCr; % [kgC unburned / kg fuel db]

%Solid Products quantity (organic + inorganic)

W_c_z = Wc_unburned + F_Wzr; % [kg solid products / kg fuel
db] bottom + fly ash

Fly_ash_fraction = 0.20; % assumed value ----> dependent
of the combustion technology

%%%%%%%%%%%%%%%%%%%%%%%%%%%%%%%%%%%%%%%%%%%%%%%%%%%%%%%%%%%%%%%%%%%%%%%% Fly Ash Production%%%%%%%%%%%%%%%%%%%%%%%%%%%%%%%%%%%%%%%%%%%%%%%%%%%%%%%%%%%%%%%%%%%%%%%%

% Estimations %
Uc_percentage = 0.10; %I will assume 10% of solid
products as unburned carbon

Ash_percentage= 1- Uc_percentage; %I will assume 90% of solid
products as ashes
```

```

Wvr = W_c_z * Fly_ash_fraction;                                % [kg of
fly ash / kg fuel db]

wcv = Wc_unburned * (Uc_percentage/Wvr);                       % [kg of
carbon / kg of combustion flying products]

wzv = 1 - wcv;                                                  % [kg of
ashes / kg of combustion flying products]

%%%%%%%%%%%%%%%%%%%%%%%%%%%%%%%%%%%%%%%%%%%%%%%%%%%%%%%%%%%%%%%%%%%%%%%% Bottom Ash Production %%%%%%%%%%

Wer = W_c_z - Wvr;                                              % [kg of
bottom ash / kg fuel db]

wce = (Wc_unburned*(1-wcv))/ Wer;                               % [kg of
carbon / kg of combustion bottom products]

wze = 1 - wce;                                                  % [kg of
ashes / kg of combustion bottom products]

%%%%%%%%%%%%%%%%%%%%%%%%%%%%%%%%%%%%%%%%%%%%%%%%%%%%%%%%%%%%%%%%%%%%%%%%
% WET GASES PRODUCTION DURING THE COMBUSTION PROCESS (PTN conditions)%
%%%%%%%%%%%%%%%%%%%%%%%%%%%%%%%%%%%%%%%%%%%%%%%%%%%%%%%%%%%%%%%%%%%%%%%%

% Complete combustion ----> absence of NO, CO, H2, NO

nCO2  = (F_WCr/MC) - (( wcv*Wvr)*(wce*Wer))/MC
;
      %[kmol CO2 /kg fuel db]

nH2O   = (F_WHr/2) + (F_Wwr/18) + (Wa/MO2)* Wva * 7.66
;
      %[kmol H2O /kg fuel db]

nN2    = F_WNr/MN2 + ((Wa/MO2)*(3.76))
;
      %[kmol N2 /kg fuel db]

nSO2   = F_WSr/MS
;
      %[kmol SO2 /kg fuel db]

nO2    = ((F_WOr/32) + ((0.5*F_Wwr)/18) + (Wa/32)*(1+0.5*Wva*7.66))-
nCO2-(nH2O/2)-nSO2
;
      %[kmol O2 /kg fuel db]

%Dry Gases
G_t_s = (nCO2 + nN2 + nSO2 + nO2) - nH2O
;
      % [kmol dry gases / kg fuel db]

% Ashes

W_Z_r = wzv*Wvr+wze*Wer
;
      % [kg ash / kg fuel db]

% end "only when for loop is used to shift the fuel percentages

```

```

%%%%%%%%%%%%%%%%%%%%%%%%%%%%%%%%%%%%%%%%%%%%%%%%%%%%%%%%%%%%%%%%%%%%%%%%
%%%%%%%%%%%%%%%%%%%%%%%%%%%%%%%%%%%%%%%%%%%%%%%%%%%%%%%%%%%%%%%%%%%%%%%% ENERGY BALANCE %%%%%%%%%
%%%%%%%%%%%%%%%%%%%%%%%%%%%%%%%%%%%%%%%%%%%%%%%%%%%%%%%%%%%%%%%%%%%%%%%%

%%%%%%%%%%%%%%%%%%%%%%%%%%%%%%%%%%%%%%%%%%%%%%%%%%%%%%%%%%%%%%%%%%%%%%%% REACTANTS %%%%%%%%%

% Sensible heat

HS_reactives = 0;      % difference between ambient temperature and
reactives temperature is 0, both at 25°C

% Latent heat

HL_reactives = F_Wwr * h_fg * -1000;      % [J / kg fuel db]

% Heat from reaction

HR_reactives = LHV * 10^6;      % [J / kg fuel db]

%Total

H_reactives = HS_reactives + HL_reactives + HR_reactives; % [J / kg
fuel db]

%%%%%%%%%%%%%%%%%%%%%%%%%%%%%%%%%%%%%%%%%%%%%%%%%%%%%%%%%%%%%%%%%%%%%%%% PRODUCTS %%%%%%%%%

%Additional data

% Specific heat of different chemicals @ 423.15 K

cp_CO2 = 1092.75;      % [J / kgCO2*K]
cp_H2O = 1863;      % [J / kgH2O*K]
cp_O2 = 921;      % [J / kgO2*K]
cp_N2 = 1038.75;      % [J / kgN2*K]
cp_SO2 = 1100;      % [J / kgSO2*K]
cp_c = 800;      % [J / kgC*K]
cp_z = 900;      % [J / kgZ*K]
PCI_carbono_25C = 3.20*10^7; % [J / kg carbon]

% Molar mass of different chemicals

MCO2 = 44;      % [kg CO2 / kmol CO2]
MSO2 = 64;      % [kg SO2 / kmol SO2]

% Temperatures

Products_temp = 423.15;      % [K]
Ambient_temp = 298.15;      % [K]

% Sensible heat from products

HS_products =
((nCO2*MCO2*cp_CO2)+(nH2O*MH2O*cp_H2O)+(nO2*MO2*cp_O2)+(nN2*MN2*cp_N2
)+(nSO2*MSO2*cp_SO2))+((wzv*Wvr+wze*Wer)*cp_z)+
((wcv*Wvr+wce*Wer)*cp_c))*(Products_temp-Ambient_temp); % [J/kg fuel
db]

```



```
% Latent heat from products

HL_products = 0; %avoid effluents condensation

% Heat from reaction

HR_products = ((wcv*Wvr + wce*Wer)*cp_c)*PCI_carbono_25C;    % [J/kg
fuel db]

% Total

H_products = HS_products + HL_products + HR_products;        % [J/kg
fuel db]

%%%%%%%%%%%%%%%%%%%%%%%%%%%%%%%%%%%%%%%%%%%%%%%%%%%%%%%%%%%%%%%%%%%%%%%% ENERGY LOST %%%%%%%%%%%%%%%%%%%%%%%%%%%%%%%%%%%%%%%%%%%%%%%%%%%%%%%%%%%%%%%%%%%%%%%%%

H_lost = 0.1 * H_reactives;                                   % [J/kg
fuel db]

%%%%%%%%%%%%%%%%%%%%%%%%%%%%%%%%%%%%%%%%%%%%%%%%%%%%%%%%%%%%%%%%%%%%%%%% USEFUL ENERGY %%%%%%%%%%%%%%%%%%%%%%%%%%%%%%%%%%%%%%%%%%%%%%%%%%%%%%%%%%%%%%%%%%%%%%%%%

H_useful = H_reactives - H_lost - H_products    ;              % [J/kg
fuel db]

%%%%%%%%%%%%%%%%%%%%%%%%%%%%%%%%%%%%%%%%%%%%%%%%%%%%%%%%%%%%%%%%%%%%%%%%
% 50 MWth FACILITY %
%%%%%%%%%%%%%%%%%%%%%%%%%%%%%%%%%%%%%%%%%%%%%%%%%%%%%%%%%%%%%%%%%%%%%%%%

% Fuel feed rate

F_frate = 50 / (H_useful/10^6)          ;          % [kg fuel db / s]

% Fuel feed rate ARB(as received basis)

F_rate_ar = F_frate + F_Wwr            ;          % [kg fuel arb / s]

%%%%%%%%%%%%%%%%%%%%%%%%%%%%%%%%%%%%%%%%%%%%%%%%%%%%%%%%%%%%%%%%%%%%%%%% POWER TO DRY SLUDGE %%%%%%%%%%%%%%%%%%%%%%%%%%%%%%%%%%%%%%%%%%%%%%%%%%%%%%%%%%%%%%%%%%%%%%%%%

%%%%%%%%%%%%%%%%%%%%%%%%%%%%%%%%%%%%%%%%%%%%%%%%%%%%%%%%%%%%%%%%%%%%%%%% DRYER THERMAL POWER %%%%%%%%%%%%%%%%%%%%%%%%%%%%%%%%%%%%%%%%%%%%%%%%%%%%%%%%%%%%%%%%%%%%%%%%%

% Enthalpy of water vaporization

H_vap = 2354 ;          % [kJ / kg water] @ 60°C / 0.042 bar

% For loop for final moisture

for j = 10:75

% Power to remove water

    M_obj = j/100;
```

```

Sludge_rate = F_rate_ar * Mass_fraction_of_sludge;      % [kg Sludge
arb / s]

Actual_moisture_content(j) = Sludge_rate * S_Ww;        % [ kg water /
s]

Final_moisture_content(j) = Sludge_rate * M_obj;        % [ kg water /
s]

Water_to_remove(j) = Actual_moisture_content(j) -
Final_moisture_content(j); % [kg water / s]

Power_1(j) = (Water_to_remove(j) * H_vap)/10^3;        % [MW]

%%%%%%%%%%%%%%%%%%%%%%%%%%%%%%%%%%%%%%%%%%%%%%%%%%%%%%%%%%%%%%%%%%%%%%%% SENSIBLE HEAT ADDED TO DRY MATTER %%%%%%%%%%

% Power added to dry matter

Process_temp = 303; % °K
Cp_dried_sludge = 1.516 ; % [kJ / kg*K] Arlabosse et al., 2005

Power_2(j) = ((Sludge_rate*(1-
M_obj))*(Cp_dried_sludge)*(Process_temp-0))/10^3; % [MW]

%%%%%%%%%%%%%%%%%%%%%%%%%%%%%%%%%%%%%%%%%%%%%%%%%%%%%%%%%%%%%%%%%%%%%%%% DRYER LOSSES %%%%%%%%%%

Losses = 0.4; % 4% of losses are assumed in the dryer

Dryer_losses(j) = (Power_1(j) + Power_2(j)) * 0.4 ; % [MW]

Power_2_dry(j) = Dryer_losses(j) + Power_1(j) + Power_2(j) % [MW]

%%%%%%%%%%%%%%%%%%%%%%%%%%%%%%%%%%%%%%%%%%%%%%%%%%%%%%%%%%%%%%%%%%%%%%%%
%Sensible Heat Availability in effluents stream%
%%%%%%%%%%%%%%%%%%%%%%%%%%%%%%%%%%%%%%%%%%%%%%%%%%%%%%%%%%%%%%%%%%%%%%%%

cp_CO2_out = 960.057; % [J / kgCO2*K] @ 150°C (A.6
interpolation Incropera)
cp_O2_out = 948.48; % [J / kgO2*K] @ 150°C
cp_N2_out = 1047.31; % [J / kgN2*K] @ 150°C
cp_SO2_out = 1100; % [J / kgSO2*K] @ 800°C

Eff_temp = 423.15 % [K] @150 °C after heat recovery devices

HS_products_dry(i) = HS_products(i) = (((nCO2(i)*(1/1-
nH2O(i)))*MCO2*cp_CO2_out)+((nO2(i)*(1/1-
nH2O(i)))*MO2*cp_O2_out)+((nN2(i)*(1/1-
nH2O(i)))*MN2*cp_N2_out)+((nSO2(i)*(1/1-
nH2O(i)))*MSO2*cp_SO2_out))*(Eff_temp-Ambient_temp); % [J/kg fuel db]

Power_effluent_drygases(i) = (HS_products_dry(i) * F_frate(i))/10^6 ;
% [MW]

```

```
%%%%%%%%%%%%%%%%%%%%%%%%%%%%%%%%%%%%%%%%%%%%%%%%%%%%%%%%%%%%%%%%%%%%%%%%
%Latent Heat Availability in effluents stream%
%%%%%%%%%%%%%%%%%%%%%%%%%%%%%%%%%%%%%%%%%%%%%%%%%%%%%%%%%%%%%%%%%%%%%%%%

% Heat of vaporization

Hfg = 2123 ;          % [kJ/kg] @ 150°C/423.15 ~ 400 K

Latent_heat_effluent(i) = (Hfg * (nH2O(i)*MH2O) * F_frate(i) )/10^3
% [MW]

end
```

## 8.2 Appendix 2: Results of the drying experiments at the tunnel under the Taguchi methods

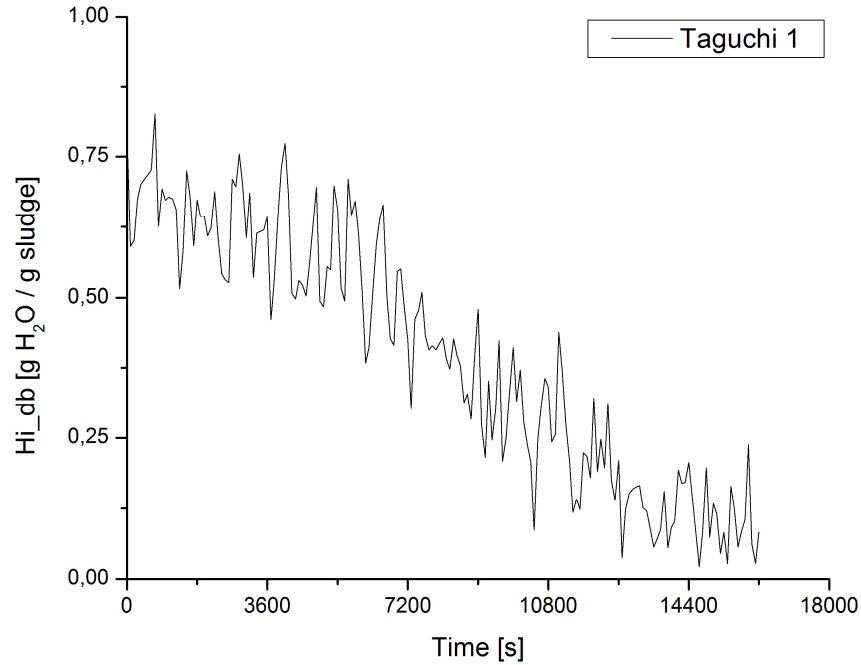


Figure 8.1 - Drying kinetic of the sludge sample under the Taguchi methods (1).

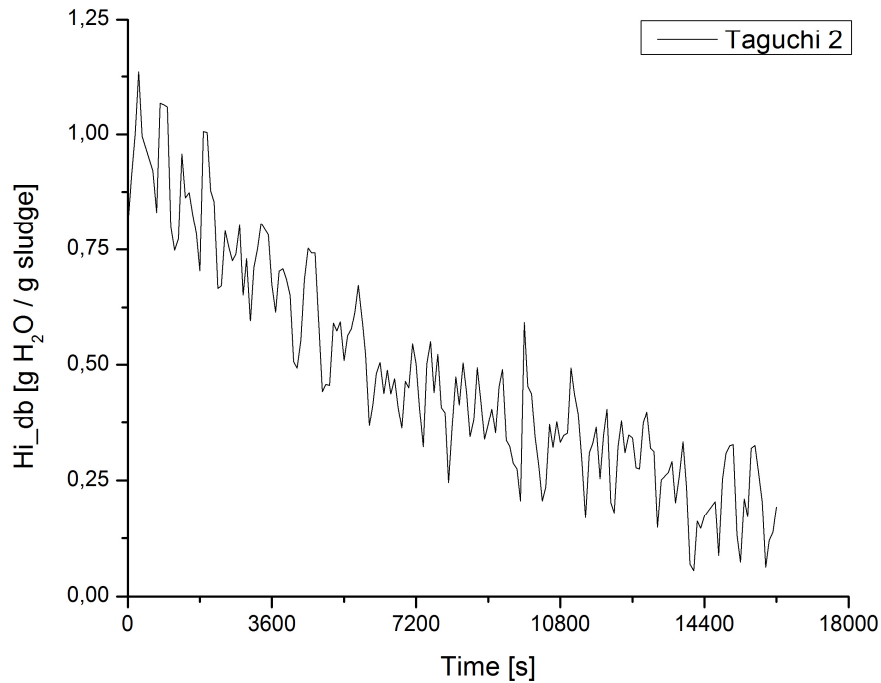


Figure 8.2 - Drying kinetic of the sludge sample under the Taguchi methods (2).

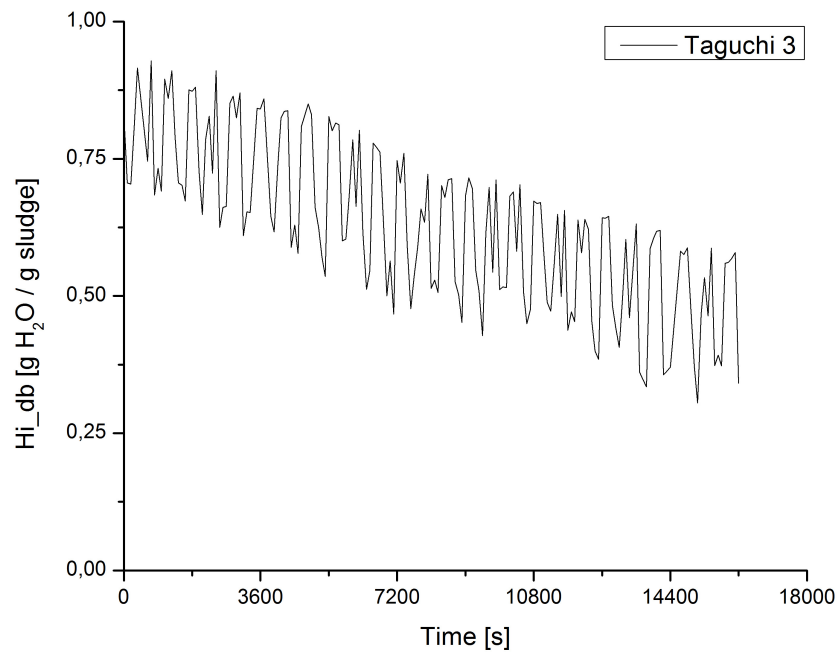


Figure 8.3 - Drying kinetic of the sludge sample under the Taguchi methods (3).

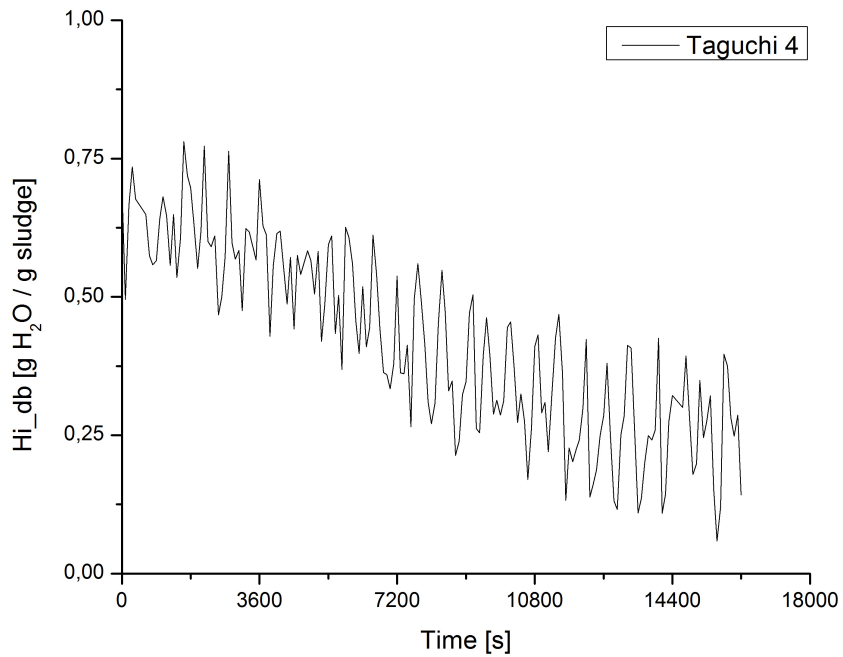


Figure 8.4 - Drying kinetic of the sludge sample under the Taguchi methods (4).

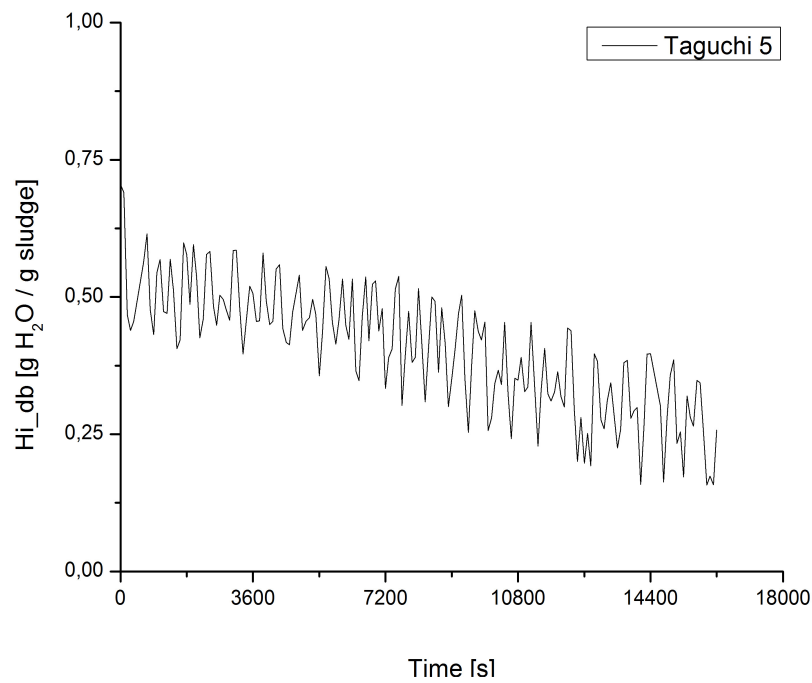


Figure 8.5 - Drying kinetic of the sludge sample under the Taguchi methods (5).

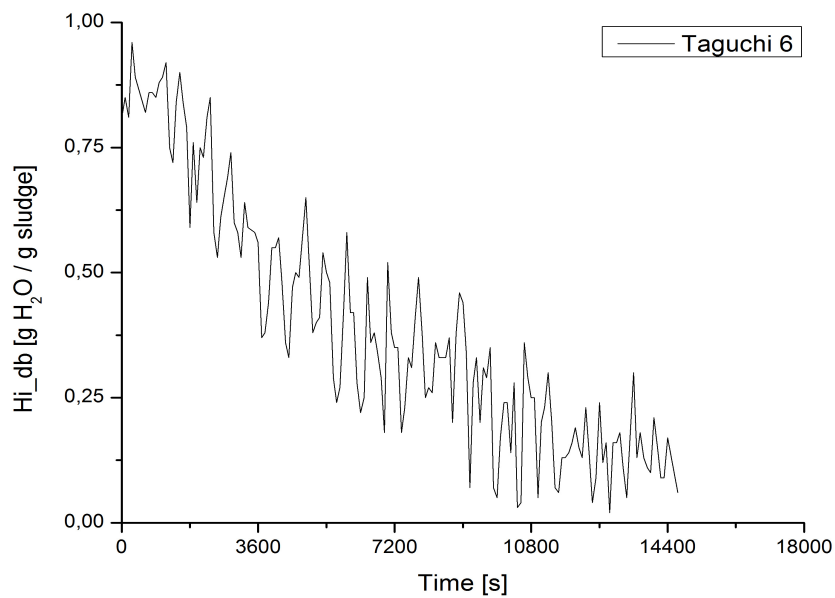


Figure 8.6 - Drying kinetic of the sludge sample under the Taguchi methods (6).

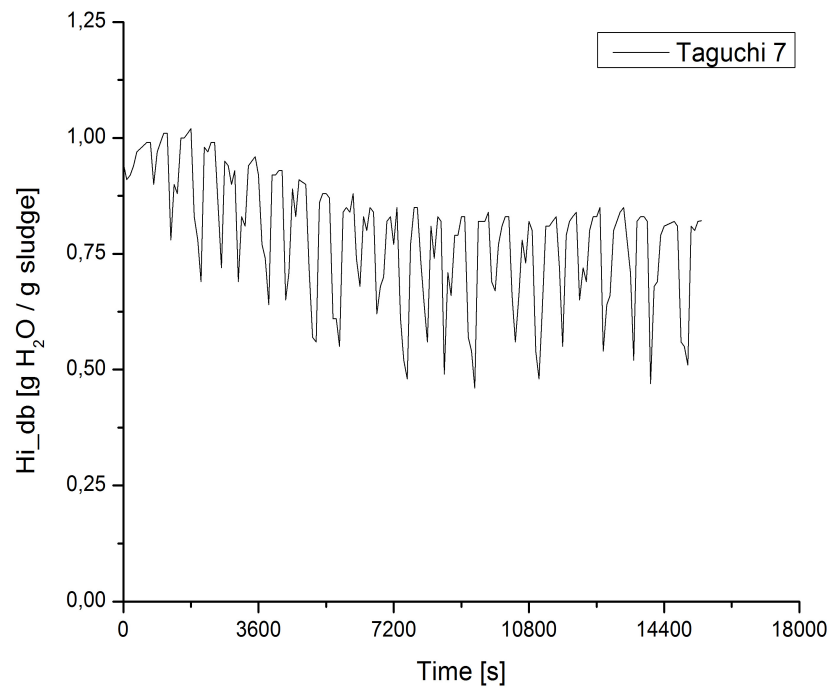


Figure 8.7 - Drying kinetic of the sludge sample under the Taguchi methods (7).

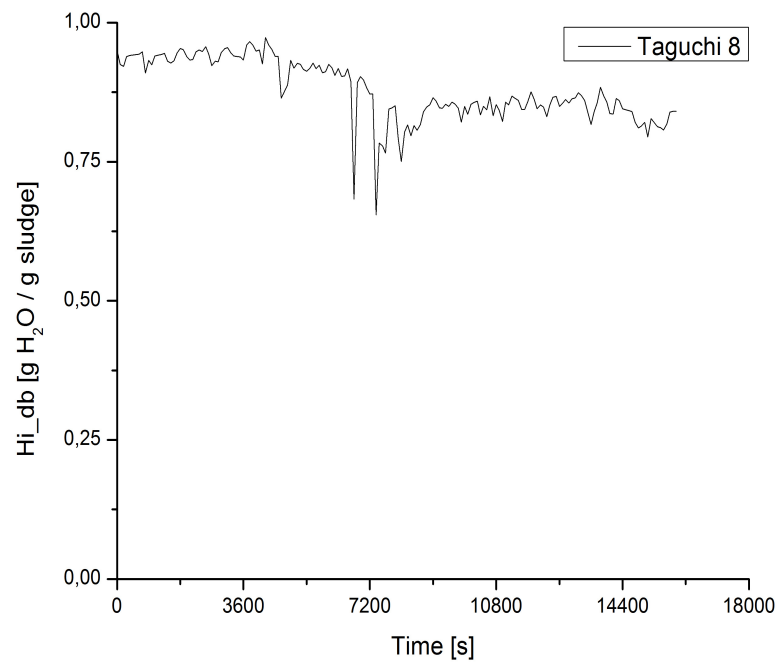


Figure 8.8 - Drying kinetic of the sludge sample under the Taguchi methods (8).

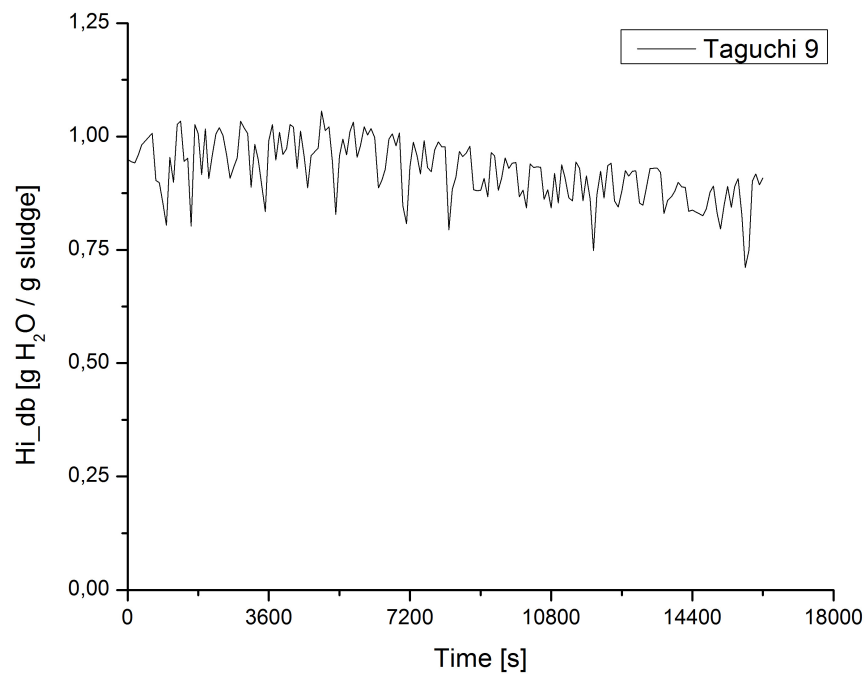


Figure 8.9 - Drying kinetic of the sludge sample under the Taguchi methods (9).



### 8.3 Appendix 3: MATLAB source code of the artificial neural network model

```
clear all

%importing data
%must have a .xls file with sheets: input and target in the same
directory

ANN=xlsread('Database1.xls','Sheet1');
input=ANN([1:5],:);
target=ANN( 6,:);
t=size(input)
to=size(target)
t=t(2);

% ANN architecture definition

rna_1=newff(input,target,[4],{'tansig'},'trainbr');
%

rna_1.inputs{1}.processFcns = {'fixunknowns','mapminmax','mapstd'};

%train network

rna_1.performFcn = 'msereg';
rna_1.performParam.ratio = 0.5;
rna_1.trainParam.show = 5;
rna_1.trainParam.epochs = 300;
rna_1.trainParam.goal = 1e-5;

[rna_1,tr]=train(rna_1,input,target);
plotperform(tr)

% For loop for generating the drying kinetic curve.

time_drying = i

Hfinal= [1:180]

j=0

for i = linspace(0,1,180)

    j= j+1

    test = [i      0.8836 0.8018 0.4320 0.9868]'; %
    vel;temp;Habs_ar;Hinicial

    G = sim(rna_1,test);
    Hfinal(j)= G;

end

plot(Hfinal)
```